

UNIVERSITY OF OKLAHOMA

GRADUATE COLLEGE

A PRODUCTION CALIBRATED RESERVOIR CHARACTERIZATION OF THE
MISSISSIPPI LIME IN A MATURE FIELD UTILIZING REPROCESSED LEGACY
3D SEISMIC DATA, KAY COUNTY, OKLAHOMA

A THESIS

SUBMITTED TO THE GRADUATE FACULTY

in partial fulfillment of the requirements for the

Degree of

MASTER OF SCIENCE

By

DANIEL BLAINE TRUMBO

Norman, Oklahoma

2014

A PRODUCTION CALIBRATED RESERVOIR CHARACTERIZATION OF THE
MISSISSIPPI LIME IN A MATURE FIELD UTILIZING REPROCESSED LEGACY
3D SEISMIC DATA, KAY COUNTY, OKLAHOMA

A THESIS APPROVED FOR THE
CONOCOPHILLIPS SCHOOL OF GEOLOGY AND GEOPHYSICS

BY

Dr. Kurt Marfurt, Chair

Dr. Matthew Pranter

Dr. Jamie Rich

© Copyright by DANIEL BLAINE TRUMBO 2014
All Rights Reserved.

ACKNOWLEDGEMENTS

I cannot adequately express my appreciation and gratitude enough to Crawley Petroleum and their leadership, namely Jim Crawley, Kim Hatfield, and Mike Drennen. Without their commitment to me and their commitment to continuing education, I would not have had the opportunity to pursue my graduate studies and thesis research. Furthermore, their commitment of time and resources to my education will forever be a gift to me that I will benefit from. I will forever be indebted to this organization of fine people for this gift.

I would also like to extend my thanks and gratitude to my committee members, Dr. Kurt Marfurt, Dr. Matthew Pranter, and Dr. Jamie Rich. Without the aid of their guidance and knowledge, I would not have been able to accomplish my goal of completing this degree. I would also like to thank a couple of my fellow students and colleagues for their help and insight they provided along the way. Mark Aisenberg, Ben Dowdell, and Sumit Verma all contributed in very helpful ways along my journey to completion of this degree.

Additionally, I would like to thank all the people of Transform Software and Services, specifically CEO Dean Witte and President Murray Roth, for providing me with access to their geoscience software for the duration of my study and Amelia Webster for support and questions. They made a very difficult task much easier to manage and ultimately complete. I also gained knowledge and experience in utilizing, what I consider to be, world class software. I am very grateful for their support and use of the software.

Lastly, certainly not in the least (but in the most), I would like to thank the love of my life, Amanda Trumbo. There is absolutely no way I would be where I am today without your continuing support, encouragement, insight, and perspective. Truly, without your help, I would not have accomplished this task. You are the rock upon which I lean, and I cannot thank you enough from the bottom of my heart for all that you have done, and will continue to do for me.

TABLE OF CONTENTS

1. List of Tables.....	vi
2. List of Figures.....	vii
3. Abstract.....	xiv
4. Chapter 1 – Introduction.....	1
5. Chapter 2 - Geologic Background.....	5
a. General Geologic Background.....	5
b. Geologic Background of the Study Area.....	16
6. Chapter 3 - Correlation of Geology to Seismic Measurements.....	26
a. Geologic Well Log Interpretation.....	26
b. Geologic Mapping.....	36
c. Seismic Expression of Geologic Features.....	49
7. Chapter 4 - Correlation of Production to Seismic Measurements.....	76
a. Correlation of Geologic Structure to Production.....	77
b. Correlation of Post-Stack Impedance Inversion Attributes to Production.....	83
c. Correlation of Prestack Impedance Inversion Attributes to Production.....	97
8. Chapter 5 - Conclusions and Limitations.....	133
9. References.....	137
10. Appendix	141
a. Legacy Seismic Data Quality and Reprocessing Techniques.....	141

LIST OF TABLES

Table 1. PE Log values with associated mineral types.....32

LIST OF FIGURES

Figure 1. Map showing Mississippi Lime tested wells within the seismic survey...	3
Figure 2. Stratigraphic column showing rock units found in Oklahoma.....	7
Figure 3. Rendition of sea level during Arbuckle deposition.....	8
Figure 4. Image of basins and geologic provinces in Oklahoma.....	13
Figure 5. Image of major fault zones and associated basins in Oklahoma.....	14
Figure 6. Image showing the Nemaha Uplift as it relates to area of study.....	15
Figure 7. Area of study as it relates to the geologic provinces of Oklahoma.....	17
Figure 8. Representation of sea level during early Mississippian time.....	18
Figure 9. Representation of sea level during late Mississippian time.....	19
Figure 10. Stratigraphic column showing the stratigraphic relationship of the Mississippi Lime in Kay County, Oklahoma.....	20
Figure 11. Types of tripolitic chert formation.....	24
Figure 12. Modern electric log suite identifying the different log information by track number.....	28
Figure 13. Cross-section through the Mississippi Lime using density logs.....	35
Figure 14. Geologic structure map on the top of the Mississippi tripolitic chert...41	
Figure 15. Geologic structure map on the top on the Mississippi Solid.....	42
Figure 16. Isopach thickness map of the Mississippi tripolitic chert.....	44
Figure 17. Isopach thickness map of the Mississippi Solid.....	48
Figure 18. Seismic synthetic.....	53

Figure 19. Map showing the wells that had digital well information used to tie to the seismic data.....	54
Figure 20. Time structure map of the Mississippi horizon.....	56
Figure 21. Outer product similarity extracted 40 ms below the Mississippi horizon.....	59
Figure 22. Diagram of thrust-fold fault model.....	60
Figure 23. Vertical slice of seismic data highlighting fault types and fault occurrence within seismic survey.....	61
Figure 24. Most positive (k_1) curvature extracted 40 ms below the Mississippi horizon.....	63
Figure 25. Most negative (k_2) curvature extracted 40 ms below the Mississippi horizon.....	64
Figure 26. Most positive (k_1) curvature co-rendered with outer product similarity extracted on the Mississippi horizon.....	67
Figure 27. Vertical slice of seismic data showing grayscale amplitude co-rendered with most positive (k_1) curvature through cross section A-A'.....	68
Figure 28. Vertical slice of seismic data showing grayscale amplitude co-rendered with most positive (k_1) curvature with most positive (k_1) curvature co-rendered with outer product similarity extracted on the Mississippi horizon through cross section A-A'.....	69
Figure 29. Most negative (k_2) curvature co-rendered with outer product similarity extracted on the Mississippi horizon.....	70

Figure 30. Vertical slice of seismic data showing grayscale amplitude co-rendered with most negative (k_2) curvature through cross section B-B'	71
Figure 31. Vertical slice of seismic data showing grayscale amplitude co-rendered with most negative (k_2) curvature with most negative (k_2) curvature co-rendered with outer product similarity extracted on the Mississippi horizon through cross section B-B'	72
Figure 32. Spectral decomposition of 22 Hz frequency extracted on the Mississippi horizon.....	74
Figure 33. Spectral decomposition of 49 Hz frequency extracted on the Mississippi horizon.....	75
Figure 34. Dip Magnitude with cumulative oil production from Mississippi Lime.....	78
Figure 35. Mississippi time structure map with cumulative oil production from the Mississippi Lime.....	79
Figure 36. Most positive (k_1) curvature with cumulative oil production from the Mississippi Lime.....	81
Figure 37. Most negative (k_2) curvature with cumulative oil production from the Mississippi Lime.....	82
Figure 38. Post-stack acoustic impedance plotted against density porosity.....	85
Figure 39. Post-stack acoustic impedance plotted against density porosity highlighting the tripolitic chert.....	86
Figure 40. Post-stack acoustic impedance plotted against photoelectric factor.....	87

Figure 41. Post-stack acoustic impedance plotted against photoelectric factor highlighting the tripolitic chert.....	88
Figure 42. Well tie of post-stack acoustic impedance seismic data with calculated acoustic impedance well log	91
Figure 43. Post-stack acoustic impedance shown with well bores and cumulative oil production from the Mississippi Lime.....	92
Figure 44. Phantom horizon slice 0-20 ms below the top Mississippi horizon through post-stack acoustic impedance with cumulative oil production from the Mississippi Lime.....	93
Figure 45. Phantom horizon slice 20-40 ms below the top Mississippi horizon through post-stack acoustic impedance with cumulative oil production from the Mississippi Lime.....	94
Figure 46. Phantom horizon slice 40-60 ms below the top Mississippi horizon through post-stack acoustic impedance with cumulative oil production from the Mississippi Lime.....	95
Figure 47. RMS post-stack acoustic impedance plotted against cumulative production from the Mississippi Lime.....	96
Figure 48. Pre-stack acoustic impedance plotted against shear impedance highlighting tripolitic chert from well log in nearby Sumner County, Ks.....	101
Figure 49. Pre-stack acoustic impedance plotted against density porosity highlighting tripolitic chert from well log in nearby Sumner County, Ks.....	102
Figure 50. Pre-stack acoustic impedance plotted against lambda-rho highlighting tripolitic chert from well log in nearby Sumner County, Ks.....	103

Figure 51. Lambda-rho plotted against mu-rho highlighting tripolitic chert from well log in nearby Sumner County, Ks.....	104
Figure 52. Pre-stack acoustic impedance plotted against lambda-rho expressing tripolitic chert seismically within the subject seismic survey.....	106
Figure 53. Pre-stack acoustic impedance plotted against lambda-rho expressing tripolitic chert seismically within the subject seismic survey.....	107
Figure 54. Pre-stack acoustic impedance plotted against lambda-rho expressing tripolitic chert seismically within the subject seismic survey.....	108
Figure 55. Pre-stack acoustic impedance plotted against lambda-rho expressing tripolitic chert seismically within the subject seismic survey as a dry hole.....	109
Figure 56. Pre-stack P-impedance extracted 40 ms below the Mississippi horizon with cumulative oil production from the Mississippi Lime.....	116
Figure 57. Phantom horizon slice 0-20 ms below the top Mississippi horizon through prestack Z_p volume with cumulative oil production from the Mississippi Lime.....	117
Figure 58. Phantom horizon slice 20-40 ms below the top Mississippi horizon through prestack Z_p volume with cumulative oil production from the Mississippi Lime.....	118
Figure 59. Phantom horizon slice 40-60 ms below the top Mississippi horizon through prestack Z_p volume with cumulative oil production from the Mississippi Lime.....	119
Figure 60. Prestack Z_p impedance extracted along the Mississippi horizon showing cross section C-C'.....	120

Figure 61. Prestack Z_P impedance extracted 20-40 ms below the Mississippi horizon shown with amplitude (grayscale) along cross section C-C'.....	121
Figure 62. Prestack Z_P impedance extracted along the Mississippi horizon showing cross section D-D'.....	122
Figure 63. Prestack Z_P impedance extracted 20-40 ms below the Mississippi horizon shown with amplitude (grayscale) along cross section D-D'.....	123
Figure 64. Prestack Z_P impedance shown with well bores and cumulative oil production from the Mississippi Lime.....	124
Figure 65. Prestack Lambda-rho values extracted 40 ms below the Mississippi Lime horizon with cumulative oil production from the Mississippi Lime.....	125
Figure 66. Lambda-rho values blended with incoherence extracted 40 ms below the Mississippi horizon with cumulative oil production from Mississippi Lime...	126
Figure 67. Pre-stack S-impedance extracted 40 ms below the Mississippi horizon with cumulative oil production from the Mississippi Lime.....	127
Figure 68. Phantom horizon slice 0-20 ms below the top Mississippi horizon through prestack Z_S volume with cumulative oil production from the Mississippi Lime.....	128
Figure 69. Phantom horizon slice 20-40 ms below the top Mississippi horizon through prestack Z_S volume with cumulative oil production from the Mississippi Lime.....	129
Figure 70. Phantom horizon slice 40-60 ms below the top Mississippi horizon through prestack Z_S volume with cumulative oil production from the Mississippi Lime.....	130

Figure 71. . Prestack Mu-rho values extracted 40 ms below the Mississippi Lime horizon with cumulative oil production from the Mississippi Lime.....	131
Figure 72. Lambda-rho plotted against Mu-rho values extracted on the Mississippi horizon at well locations colored by cumulative oil production from the Mississippi Lime.....	132
Figure 73. (a) Schematic illustration of deposition of tripolite within the study area.....	134
(b) Schematic illustration of deposition of tripolite within the study area.....	134

ABSTRACT

Production from the Mississippi Lime requires hydraulic fracturing to provide pathways for fluid flow. Current target areas in the Mississippi Lime vary between the tripolitic chert and areas of pre-existing fractures. Areas stimulated by hydraulically-induced fractures typically produce large amounts of water and vary greatly in oil and gas production. Diagenetic alteration coupled with depositional conditions gives rise to rapid lateral variation in stratigraphy. For this reason 3D seismic data are key to linking the well control to a localized picture of stratigraphy.

Reprocessing of a legacy 3D seismic data set in Kay County, Oklahoma provides significant improvements in lateral and vertical resolution of the Mississippi Lime formation. Seismic attributes illustrate the structural and stratigraphic complexity of the survey which sits along the Nemaha Ridge. Attribute analysis coupled with time structure maps show that little tripolite exists in the deeper parts of the survey. Structurally high areas favor tripolite formation but also tripolite erosion. P-wave inversion is tightly controlled to high porosity tripolite. Production correlates well with lambda-rho from prestack inversion, but does not predict several wells with poor oil production. No water production records exist. Given that today's Mississippi Lime wells produce an average of 95% water, these poor oil producers may have been excellent water producers from highly porous tripolite connected to an aquifer by faults and fractures.

CHAPTER 1

INTRODUCTION

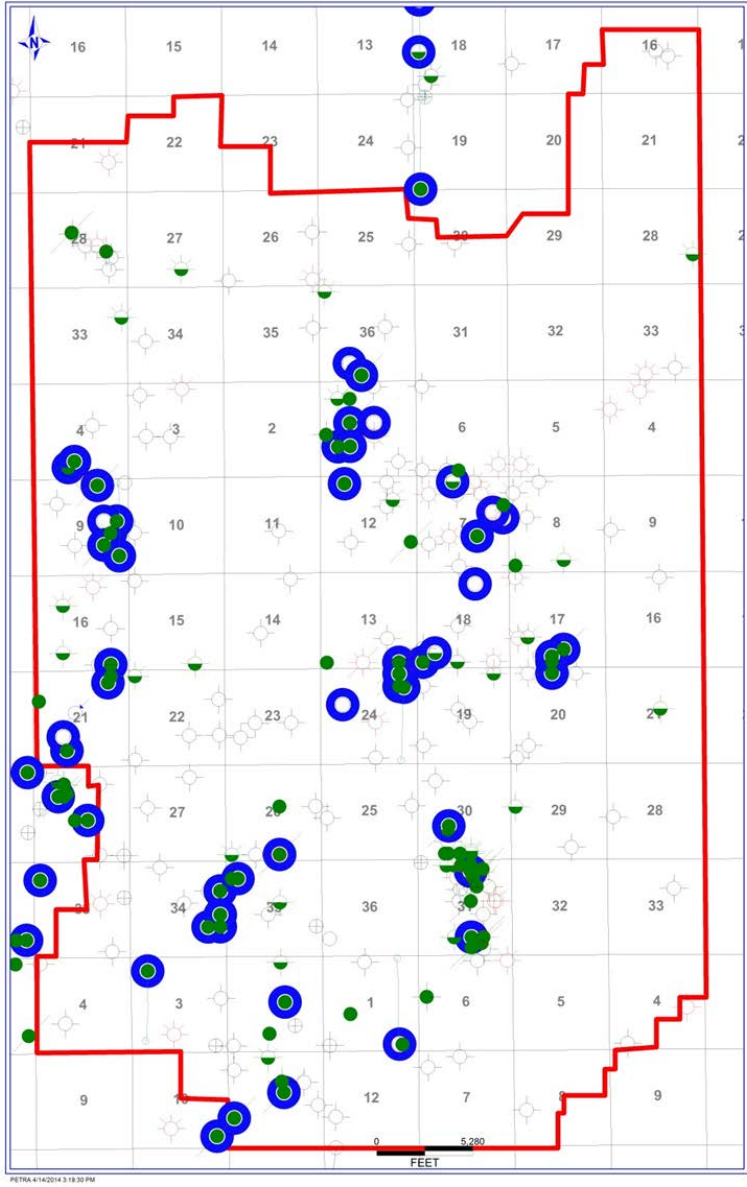
The Mississippi Lime in north-central Oklahoma and south-central Kansas is currently a 'hot' resource play for oil and gas. Though the Mississippi Lime has been a productive reservoir for at least 95 years, the application of horizontal drilling and modern completion techniques has breathed new life into an old play. As with other resource plays there is high variability in production with some wells being much, much better than others. This variability has been puzzling, if not economically disappointing to many of the people involved in the drilling of these horizontal Mississippi wells. The end members of the Mississippian Lime can be very complex and their seismic expression is not well understood. Furthermore, given the competitive acreage positions, little has been published on how to correlate lithologies seen in the wells to impedance and attributes computed from 3D seismic data.

In this mature oil and gas field, there are over one hundred existing vertical wells that penetrate the Mississippi Lime with available well log information. Only a few of these wells, however, have sonic logs that were run in the wellbore. The majority of the well logs are older, and provide little useful information about the Mississippi Lime in terms of the reservoir characteristics. The older wells will provide information pertinent to the structural setting within the survey limits, as well as well tops for time to depth conversion of the seismic survey. In total, there are eleven wells within the seismic survey that provide reliable sonic information. These logs will be most useful in running an inversion

on the seismic data set, but will also be helpful in tying the lithologic data to the seismic data in order to pick horizons effectively. All of the wells that fall within the limits of this seismic survey will also provide production data, when applicable. While not all of the wells in the 3D seismic survey targeted the Mississippian, there are a number that do provide production information from wells completed in the Mississippi Lime. This will allow me to be able to tie production back to seismic characteristics to determine if there is any correlation between the two.

The process of reservoir characterization of the Mississippi Lime using 3D seismic has been performed before, but little has been published on the Mississippi Lime in Northeastern Oklahoma and surrounding areas other than Dowdell (2013), in Osage County, Oklahoma, Rush et al. (2013), in Wellington, KS, and Snyder (2013) in Osage County, Oklahoma. More recent publications from a geologic point of view include Mazzullo (2009, 2010, 2011), Rogers (2001, 2012), and Rottman (2011). There have been a number of workshops recently held by professional societies with focus just on the Mississippi Lime in order to share recent findings and ideas by those willing to offer insight into a topic that has had relatively little openly published about it.

Unlike Dowdell's (2013) work based on only two horizontal wells and limited production, my survey encompasses 57 Mississippi Lime tested wells with up to 75 years of (perhaps disappointing) production data, making it an excellent calibration case study. Figure 1 shows the Mississippi tested wells that fall within the limits of the 3D seismic survey.



 **Mississippi Lime
Tested Wells**

Figure 1. 3D seismic survey outline in red showing wells symbols of wells within the survey area drilled to a depth of 3,750' or greater. Production tests in the Mississippi Lime are indicated by blue circles

In the following chapter, I will give a brief geologic history of the state of Oklahoma, along with a geologic focus on the Mississippi Lime in Kay County. In chapter 3, I will talk about how the geology of the Mississippi Lime in the 3D survey area correlates with the seismic measurements of the 3D survey. I follow with chapter 4, in which I discuss how the Mississippian production information that I have relates to the seismic measurements of the 3D survey. Finally I discuss my conclusions and potential limitations in chapter 5.

CHAPTER 2

GEOLOGIC BACKGROUND

GENERAL GEOLOGIC BACKGROUND

The geologic history of Oklahoma is one that is very lengthy and complex. Due to structural controls on deposition of sediments, Oklahoma has historically been a major contributor to the production of domestic oil and natural gas. Subsequently, there is a wealth of information available, in the form of well data, and 2D and 3D seismic surveys which provide the tools that create the opportunity to provide a clear interpretation for the geologic history of Oklahoma. This history of sediment deposition and structural deformation spans from pre-Cambrian time all the way through Permian time, with relatively minor depositional events occurring in Triassic, Jurassic, Cretaceous, and Tertiary time periods. Figure 2 shows a stratigraphic column of the rock units that can be found in Oklahoma. Basement rocks of Oklahoma consist of pre-Cambrian granites and rhyolites. These basement rocks were formed around 1.4 billion years ago. The first deposition of sediment in the state is that of the Reagan sandstone. This Cambrian aged rock lies unconformable on the granite and rhyolite surface. The deposition of the Reagan Sandstone was followed by a transgression of ocean water in middle Cambrian time around 500 million years ago. As you can see in Figure 3, this transgression covered most, if not all of the state in a shallow tropical sea. The subsequent deposition of the Arbuckle group carbonates and dolomites, with some interbedded shales, occurred from late Cambrian into the early Ordovician time, some 475 million years ago. In

middle to late Ordovician time, the Simpson group of rocks was deposited. This group consists mainly of sandstones with high silica content. Deposition of this sand was widespread throughout the state, and has been interpreted as a blanket sand beach environment. As stated by Johnson and Cardot (1992), early and middle Paleozoic sediments tend to be quite persistent laterally, and thus the same formations are recognized in most geologic provinces in Oklahoma outside of the Ouachita Uplift province. The Simpson sand group would be included in the early and middle Paleozoic sedimentation in the state.

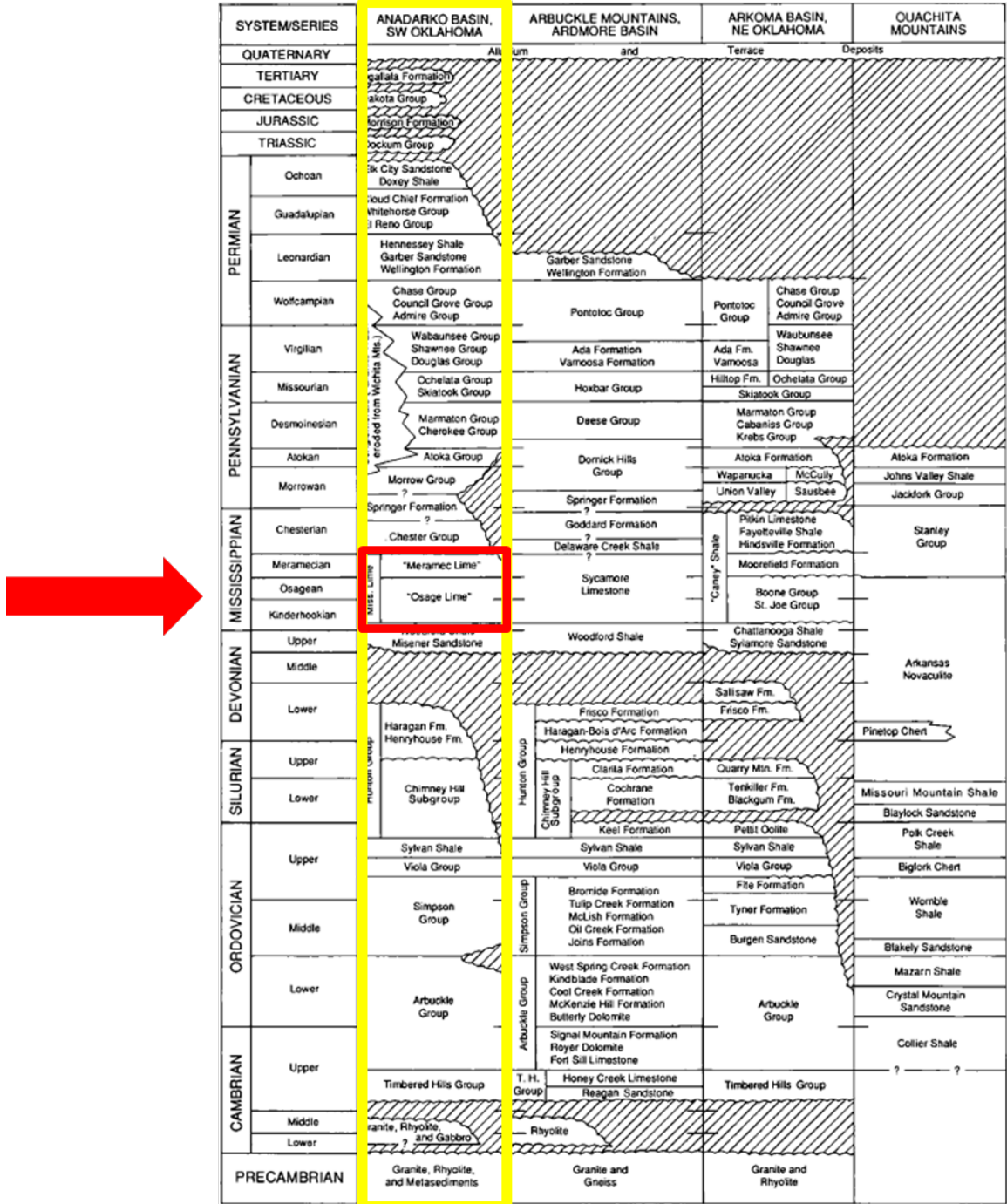


Figure 2. General Stratigraphic column of Oklahoma showing rock units with associated time periods. The red arrow indicates the Mississippian time period. (Johnson and Cardot, 1992)



Figure 3. Shallow seas covering Oklahoma at the beginning of the deposition of Arbuckle rocks. (Modified from Blakely, 2011)

At the end of the Ordovician time period, about 440 million years ago, the Viola Limestone and the Sylvan Shale were deposited on top of the Simpson Group of rocks. The Viola is a shelf carbonate and contains large amounts of invertebrate fossils. Deposition of sediment occurred from the Silurian and continued into the Devonian time period, between 440 million years ago and 415 million years ago. The Hunton, which is Silurian in age, has been characterized as limestone and dolomite, and was initially deposited over nearly the entire state. Northcutt et al (2001) state that Hunton strata are widely distributed in the Anadarko basin, Arkoma basin, and central and southern Oklahoma. During most of the Devonian time period, however, there was a time on non-deposition due to the regression of the seas. This regression in turn caused the erosion of the previously deposited Hunton formation over the entire state creating an unconformity surface.

Post deposition and erosion of the Hunton formation brought another transgression of the seas. At this time roughly 375 million years ago, in the late Devonian and early Mississippian, the Woodford Shale was deposited unconformably on top of the Hunton. Currently the Woodford is likely the most well-known shale in the state. It has been credited as being the major source rock for oil and natural for Oklahoma, and is now being exploited as a reservoir as well. Johnson and Cardot (1992) make the assertion that the Woodford shale is unquestionably the most prolific source rock for oil and gas in Oklahoma. The Woodford is an organic rich, carbonaceous shale that was deposited in a widespread event throughout Oklahoma in Devonian time. Beginning in

Mississippian time, 360 million years ago, the shallow, warm, tropical seas again arrived in Oklahoma. It was then that the Mississippian Limestone was deposited. This limestone has been documented as a shelf carbonate, deposited on or very near to the shelf that would have separated the shallow and the deep seas. The Mississippian is full of invertebrate fossils, and has abundant interbedded chert layers present throughout the entirety of the rock formation. Per Johnson and Cardot (1992), cherty limestone deposition was significant during the Osagean and Meramacian periods of the Mississippian, and the depositional environment for most of the Mississippian time period is classified as well-aerated, warm, shallow seas that supported an abundance of benthic life forms.

The end of Mississippian deposition and beginning of the Pennsylvanian time period, 318 million years ago, brought more deposition of sediment. During the Pennsylvanian time period, however, there is an influx of clastic sediment deposition as opposed to the more marine dominated depositional settings previously described. This increase in clastic sediments being deposited is due to a more terrigenous setting within the state that accommodated this influx of this type of sediment. Johnson and Cardot (1992) speak of the terrigenous sediment deposition during the Pennsylvanian, saying that thick wedges of terrigenous clastic sediments were shed from nearby uplifts while thinner carbonate deposition occurred in shallow water shelf areas distal to the uplifts that began around Pennsylvanian time.

More importantly, the beginning of the Pennsylvanian marks the start of the three major tectonic events in Oklahoma. These tectonic events contribute significantly to the complexity of the geology of Oklahoma. Johnson (2008) states that the principle mountain belts of Oklahoma, the Ouachita, Arbuckle, and Wichita Mountains were sites of folding, faulting, and uplift during the Pennsylvanian time period. The influx in clastic sediment deposition can be attributed to these orogenic events. These tectonic events began in the late Mississippian when the South American plate encroached upon the North American plate and the two collided. The first event can be termed the 'Wichita Orogeny', and is credited with the creation of the Arbuckle Mountains in present day southern Oklahoma, and the Nemaha ridge which is in present day central and north central Oklahoma. Johnson (2008) also states that folding and uplift of pre-Morrowan aged rocks characterized the Wichita orogeny which resulted in uplift of 10,000-15,000 feet in the Wichita Mountains and the Criner Hills of Oklahoma. Johnson goes on to say that during this orogenic event, a broad, north-trending arch rose above sea level in a narrow fashion and created fault block mountains extending from Oklahoma City into neighboring Kansas, known as the Nemaha Uplift. It was also during the Wichita orogeny that the Ozark region of Oklahoma in the northeastern part of the state experienced a broad uplift known as the Ozark uplift or Cherokee Platform according to Johnson (2008). The second major tectonic event is termed the 'Upper Wichita Orogeny'. This is simply a continuation of the first major tectonic compressional event, which included more mountain building. The orogenic events continued through

the Late Pennsylvanian with the 'Arbuckle Orogeny' event. This event is credited with the Arbuckle Anticline in southern Oklahoma, the Wichita Mountains in southwest Oklahoma, and the Ouchita deformation in southeast Oklahoma. Johnson (2008) calls the Arbuckle orogeny the last major Pennsylvanian orogeny and notes that strong compression and uplift occurred affecting many of the major mountain ranges in southern Oklahoma and caused prominent folding in the Ardmore, Marietta, and Anadarko basins. Not only did these orogenic events create mountains, but they are also responsible for the creation of the current day basins that we are familiar with, as well as other geologic 'provinces' of Oklahoma. Figure 4 shows the geologic provinces of Oklahoma. The largest basin, the Anadarko Basin, is recorded as accommodating 40,000 feet of sediment in its deepest regions. Northcutt et al (2001) claims that the largest basins in Oklahoma contain between 20,000-40,000 feet of sediment that rests on a basement complex of Precambrian and Cambrian igneous rocks. In addition to mountain building, basin creating, and influence on the deposition of the Pennsylvanian time period, these tectonic episodes are also the catalyst behind the creation of the main fault zones and structures that are present in current day Oklahoma. These fault zones and structures that are present in Oklahoma today are significant not only because they provide insight into the geologic history of Oklahoma, but they are important to the oil and gas industry as well. These structures and faults with related fault zones provide trapping mechanisms for oil and natural gas. This is important because without these trapping mechanisms, the oil and natural gas would migrate to other places. The

structures and faults are also important to the production of hydrocarbon as it turns out. These structures (in some cases) and especially the faults have fractures associated with them caused by the flexure of the rock from the compressional forces of the orogenic events of the Pennsylvanian. These fractures not only provide migration pathways for hydrocarbon, but they also provide permeability for production of hydrocarbon from wellbores. Figure 5 shows the geologic provinces of Oklahoma and how they relate to the major basins and tectonic uplifts that helped to shape these provinces.

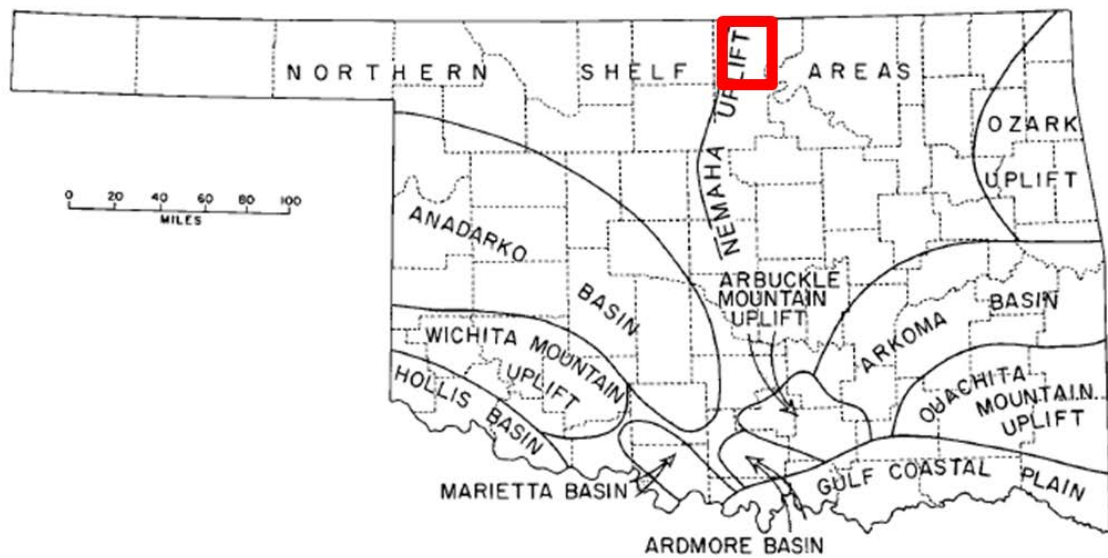


Figure 4. Image of basins and geologic provinces as created by the orogenic events that shaped Oklahoma. The study area is indicated by the red rectangle. (Johnson and Cardot, 1992)

GEOLOGIC PROVINCES OF OKLAHOMA
Robert A. Northcutt and Jock A. Campbell

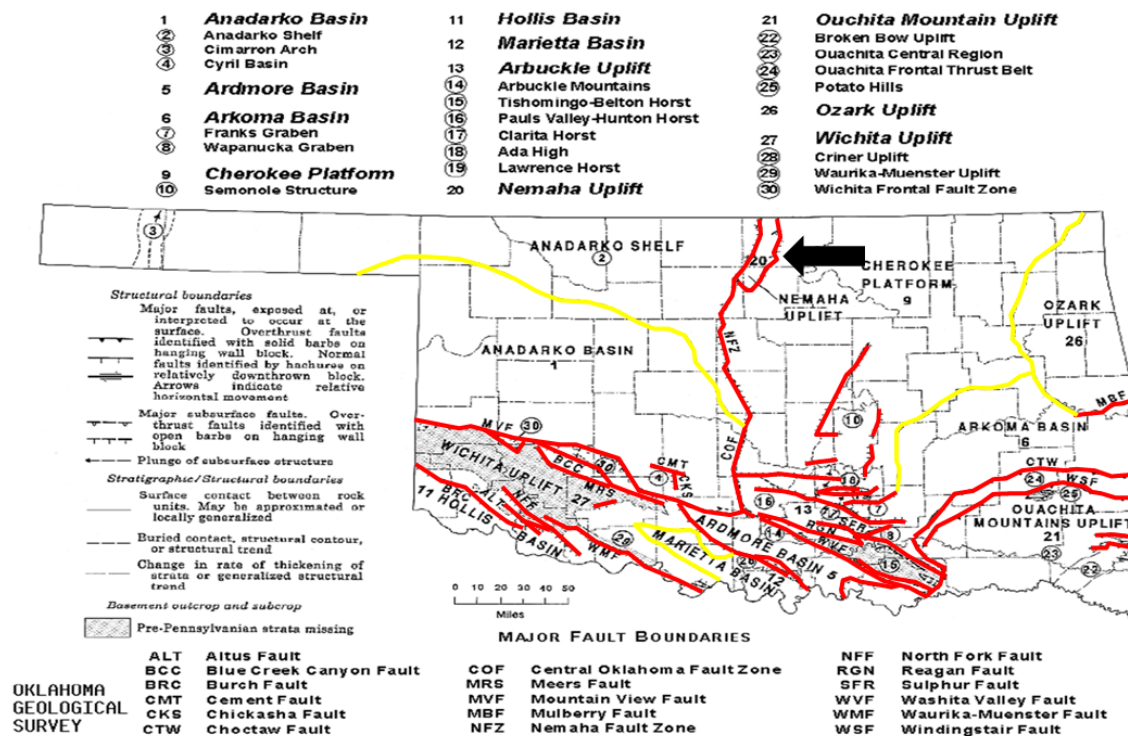


Figure 5. Major fault zones in Oklahoma as created by orogenic events with associated geologic provinces. The red lines indicate major faults in the state. The yellow lines indicate boundaries between geologic provinces. Black arrow points to study area. (Modified from Northcutt et al., 2001)

Out of the three major tectonic events, the Wichita Orogeny that created the Nemaha Ridge in central and north central Oklahoma is especially important when investigating the Mississippi Lime in Kay County, Oklahoma. The Nemaha Ridge is the main structural control that directly affects the Mississippi Lime in the study area. This large uplift is visible within the 3D seismic survey being studied, and the uplift is the main control on the deposition of the tripolitic chert in the seismic survey area. Figure 6 shows the Nemaha uplift as it relates to Kay County, Oklahoma and the subject 3D seismic survey.

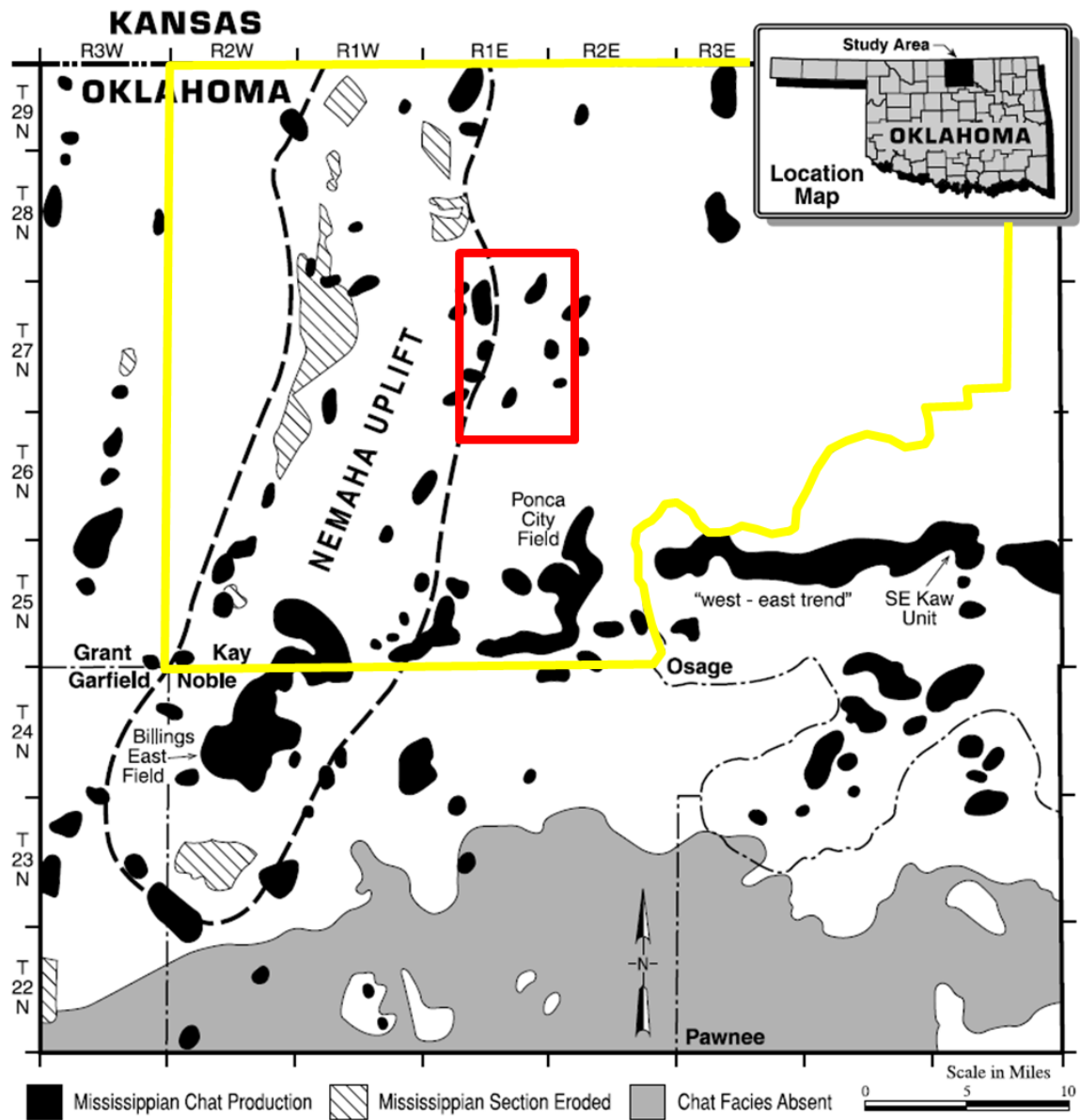


Figure 6. The Nemaha Uplift as observed within the study area with production from the Tripolitic Chert facies of the Mississippi Lime indicated by the black shapes. The red rectangle indicates the general area of the 3D seismic survey, and the yellow outlines Kay County. (Modified from Rogers, 2001)

After the Pennsylvanian Era, deposition of sediment continued in a wide fashion through the Permian age, beginning about 300 million years ago. This was the last major depositional event in Oklahoma that occurred across nearly

the entire state. According to Johnson (2008), the Wichita Mountains were still plenty tall during Permian time, providing much of the sediment for deposition during Permian time. There are two notable depositional events from the Permian that are present in the current day rock record. The early part of the Permian is noted by Johnson (2008) for the presence of widespread evaporite deposition in the central, southern, and western parts of Oklahoma. Johnson then goes on to describe the deposition in Late Permian time period as red shales and sandstones, with the presence of gypsum. These red shales and sandstones are the most recognizable rocks in the state because of their red color which is caused by the presence of iron oxide, namely hematite, in the mineral matrix of these rocks. The Permian sandstones and shales have turned this color over time because of the reaction of water with the iron oxides present. It is also worth noting that the state rock of Oklahoma, the barite rose rock, is Permian in age.

GEOLOGIC BACKGROUND OF THE AREA OF STUDY

The area of study in Kay County, Oklahoma lies in the Cherokee (Central Oklahoma) Platform geologic province as defined by the Oklahoma Geological Survey. This platform is bounded to the east by the Ozark Uplift and to the west by the Nemaha Uplift. The more specific area of study lies just to the east, and directly adjacent to the Nemaha Uplift. The Ozark and Nemaha Uplifts were formed from the late Mississippian through the early Pennsylvanian time. Figure 7 shows the location of the area of study in relation to the geologic provinces.

Major geologic provinces of Oklahoma.

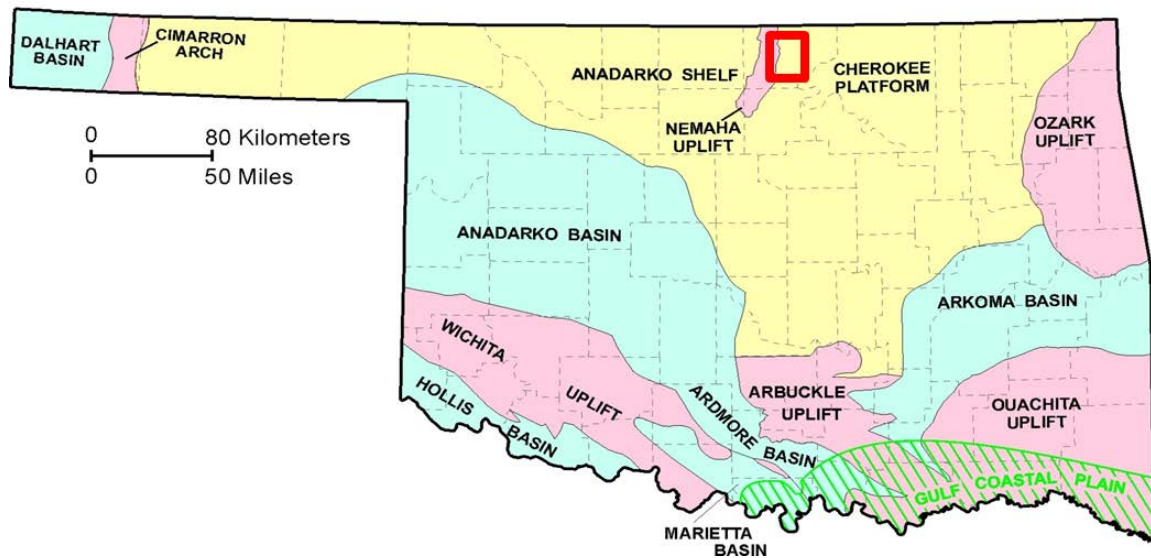


Figure 7. The area of study in the red box in relation to the geologic provinces of Oklahoma. Courtesy of the Oklahoma Geologic Survey.

The Mississippian Limestone was deposited in this area of study over the time between the Devonian and early Pennsylvanian. Deposition occurred in a setting which most consider today to be a shallow marine sea. Figures 8 and 9 are a representation of what the sea level looked like in reference to Oklahoma during early Mississippian and late Mississippian time, respectively. The warm marine sea was conducive to carbonate formation and deposition Craig and Varnes, (1979). See Figure 10 for stratigraphic positioning of the Mississippian Lime in Kay County, Oklahoma.

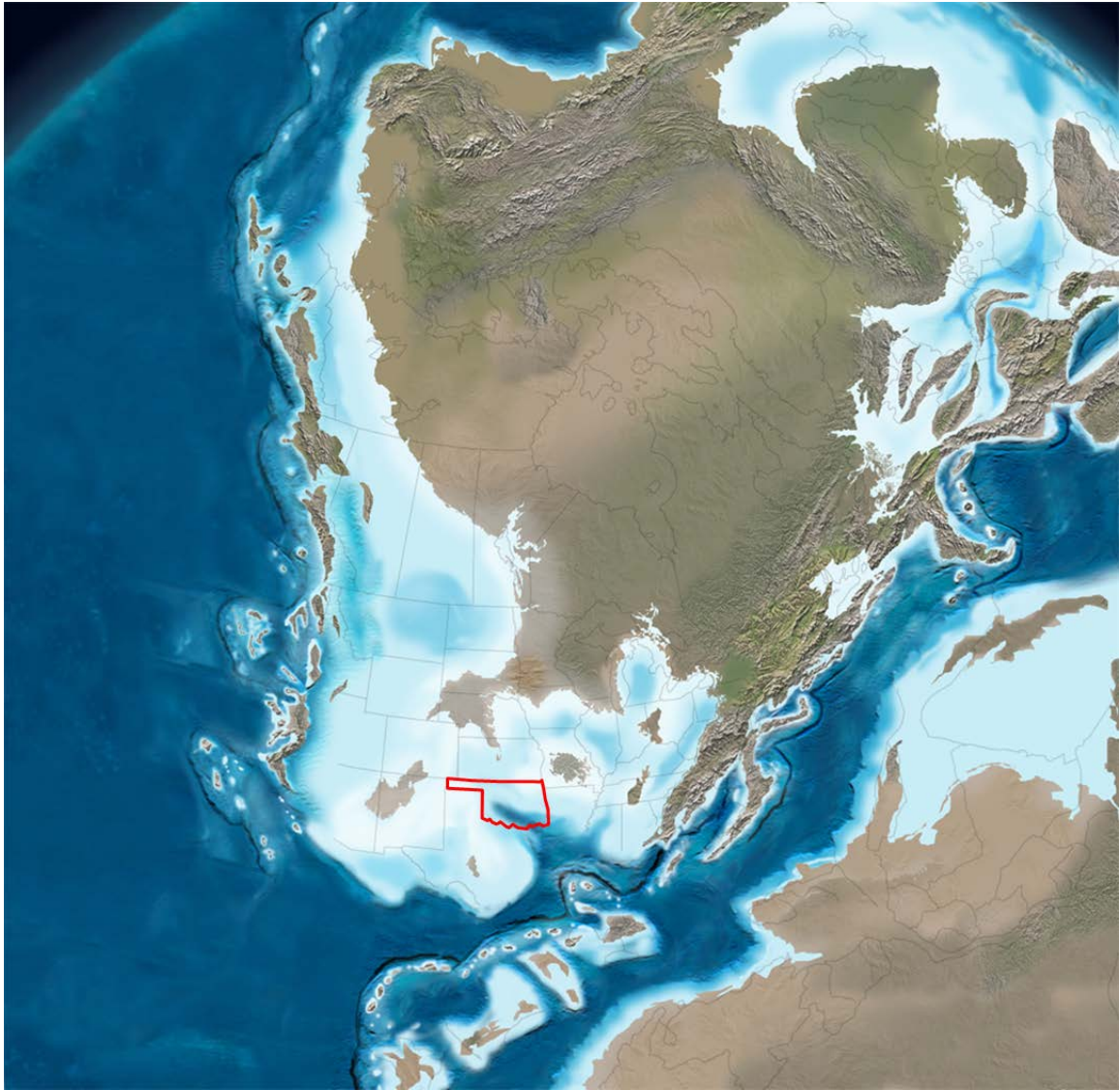


Figure 8. Shallow seas covering northern Oklahoma during early Mississippian time. (Modified from Blakely, 2011)

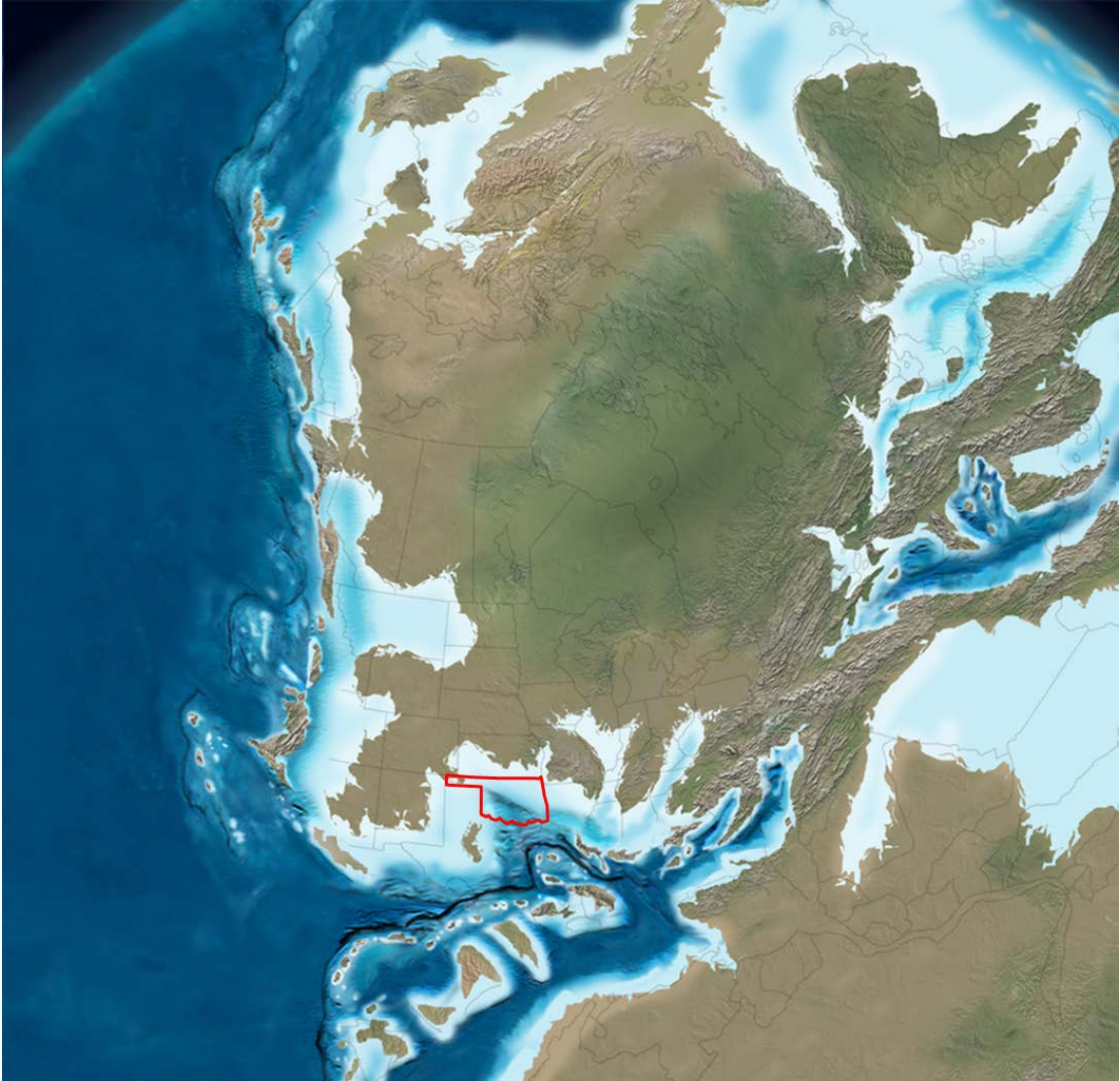


Figure 9. Shallow seas covering northern Oklahoma during late Mississippian time. (Modified from Blakely, 2011)

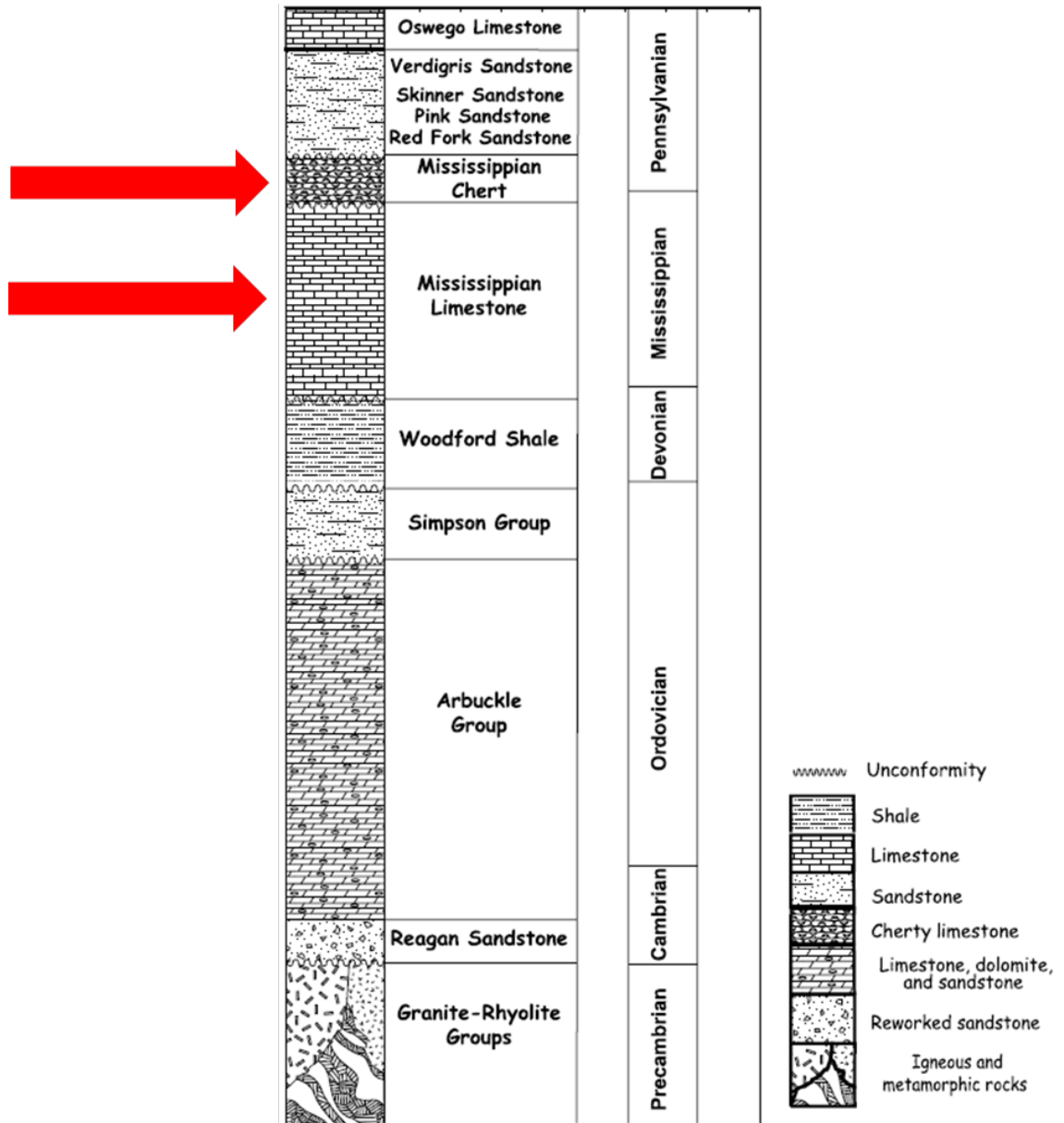


Figure 10. Stratigraphic relationship of the Mississippi Lime in Kay County, Oklahoma. The red arrows point to the stratigraphic location of the Tripolitic Chert member of the Mississippian and the Mississippian Solid member of the Mississippian. (Elibiju et al. 2011)

An issue with the Mississippi Lime is that there are several different end members or stratigraphic intervals exist throughout the rock unit. Rottman, (2011) cites five different “reservoir systems” within the Mississippi Lime. These include talus deposits, secondary dolomites, spiculitic deposits, tripolitic cherts informally known as “chat”, and fractured cherts. Watney et al (2001) describe the Mississippian Limestone that is present in south-central Kansas, just to north of my study area, as containing as many as seven different lithofacies within the rock unit. The documented heterogeneity of the Mississippi Limestone creates a rock unit that is extremely variable both laterally and vertically. This variability makes the Mississippian Limestone very enigmatic, especially when one is attempting to interpret or economically evaluate the Mississippi Lime in the subsurface. Most of the variations of the Mississippian that Rottman and Watney describe are facies changes that are readily identifiable when observing outcrops or thin sections of the Mississippian. Identification of these characteristics of the Mississippian can be very difficult to impossible when using well logs and other lithologic measurements used in creating an interpretation of the subsurface. Many of the different characteristics that Rottman and Watney describe are beyond the scope of observation for these tools, and therefore are difficult to consider when only subsurface data is available for interpretation.

The two main reservoir systems of the Mississippi Lime to consider here, based on production information from within the seismic survey area, are the tripolitic cherts or more informally ‘chat’, and fractured limestone with interbedded chert layers. Rogers, (2001) describes two means of tripolitic chert formation. In

the first model, uplift of the Mississippi Lime gives cause for the silica rich limestone or diagenetic chert to be eroded into topographic lows. This limestone is silica rich because it contains sponge spicules that were part of a coral reef system as a result of the Mississippian deposition in a shallow warm sea environment. This shallow warm sea was favorable for the formation and growth of many types of organisms. Diagenetic alteration of the limestone would occur as a result of exposure to environmental elements, namely meteoric waters. Carbonates are very basic in chemical composition. If carbonates are exposed to meteoric water that is even slightly more acidic than the depositional waters, the acidic nature of these waters will in essence dissolve the limestone. In the second model, the tripolitic chert forms as a result of a sub aerially exposed and diagenetically altered portion of the Mississippi limestone. This second model that Rogers describes is mostly a function of sea level. A carbonate mound or reef is built up over time in the shallow tropical sea environment. As the sea level regresses, the carbonate buildup becomes exposed to the weather elements of the surface. The environmental elements cause a sort of alteration in place of the limestone through diagenesis. The first model describes a portion of the Mississippian that typically occurs at the top of the stratigraphic interval, and is identified as a pre-Pennsylvanian unconformity. This portion of the Mississippi exhibits high porosity and permeability, as well as low density, and can be a desirable target for drilling. Figure 11 shows the two models of tripolitic chert formation that Rogers (2001) describes. Rodgers (2001) goes further and defines the tripolitic chert as a rock unit that is weathered and/or detrital, highly

porous or dense chert that is up to two hundred feet thick and serves as a significant hydrocarbon reservoir rock in north-central Oklahoma. The fractured limestone portion of the Mississippi occurs toward the lower portion of the deposition. This exhibits fracture porosity, which likely occurs due to the presence of a brittle chert facies interbedded with the limestone, and provides the desirable reservoir characteristic. The fractures would form as a result of flexure of the rock unit due to tectonic events. These fractures enhance permeability, or the ability of fluid to flow through the rock, which creates better production from the rocks.

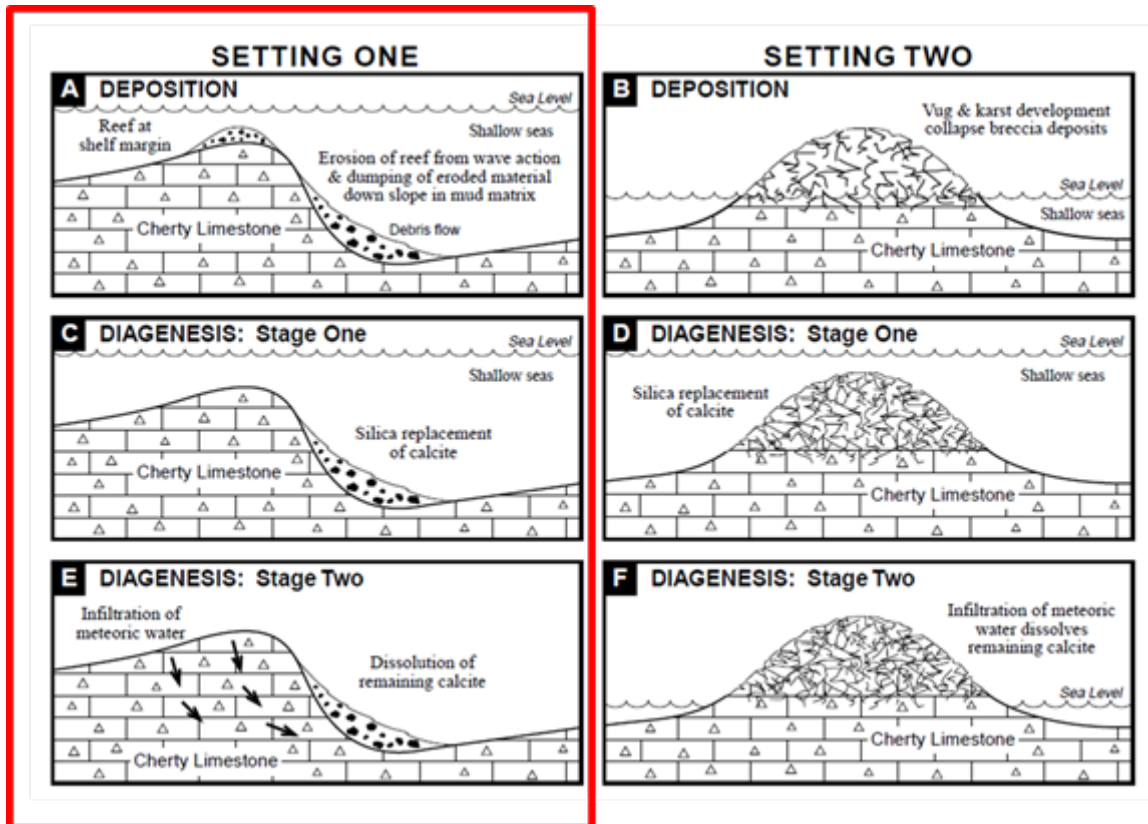


Figure 11. The two types of tripolitic chert formation described by Rogers (2001). The red box surrounding Setting One indicates that this is the type of tripolitic chert deposition seen within the study area, with Mississippi Limestone rocks being uplifted by the Nemaha Ridge after deposition and then eroded into adjacent areas. The tripolite is deposited unconformably on top of the Mississippi Solid in areas of closer proximity to the Nemaha fault with a propensity to accumulate in paleotopographic lows within the study area. (Modified from Rogers, 2001)

The deposition of the Mississippi Lime is 100 ft to 600 ft thick in the region of discussion. Because of the lateral variability, especially of the tripolitic chert, one cannot simply extrapolate log measurements to map with confidence commercially productive portions of the Mississippi Lime versus commercially non-productive portions. The tripolitic chert can be traced using 3D seismic Snyder, (2013) where it is sufficiently thick. Studies have shown that 3D seismic

is capable of identifying areas within the Mississippi Lime that have higher fracture density than other areas. White et al. (2012) discuss the correlation of surface seismic attributes to the occurrence of natural fractures in the Mississippian Lime in Osage County, Oklahoma, an area just to the east of my area of study. However, it is difficult to identify the other three reservoir systems that Rottman, (2011) describes using 3D seismic data due to the fact that they are all characteristics that occur on a sub-seismic scale.

CHAPTER 3

CORRELATION OF GEOLOGY TO SEISMIC MEASUREMENTS

There are many methods to developing a subsurface geologic interpretation. There are also many different sources and types of data available to aid in developing these subsurface geologic interpretations. No matter the method used to develop these interpretations, it is important to consider and use all available pertinent data when developing such interpretations. This is important because in many instances, one piece of data or portion of information does not provide all of the necessary input needed to form a complete interpretation. Much of the data is complimentary to one another and when considered all together will create the most thorough interpretation.

GEOLOGIC WELL LOG INTERPRETATION

One of the more common mediums for studying the subsurface, in an exploration sense, is the well log. Well logs provide geoscientists measurements of rock characteristics that are observed directly from the well bore. Traditionally, characteristics such as fluid content, density, acoustic properties, permeability, and lithology are the measurements made by these tools. More recently, however, advances in technology have made it possible for these logs to actually take images from the well bore, and measure production rates in real time. These advancements are very helpful, but can be expensive and are not common place due to differences in reservoir regimes (drilling with water or oil based muds), bottom hole temperature, and cost.

Kay County Oklahoma has a long history of exploration and drilling. Because of this, there is a lot of well data to consider when performing a subsurface study in this area. One of the problems encountered in this type of study is the advancement in technology of the oil and gas industry. Newer techniques and technologies in the well logging realm have made the older information more difficult to use and rely upon for all of the pertinent data necessary for a quality interpretation. Older well logs, namely logs that are older than 1970, provide a minimal amount of data compared to the logs that were collected after that time. These older logs mainly provide resistivity, SP, and sometimes microlog information. In comparison, the more modern suite of logs provide many other types of information including gamma ray (lithology), rock density, sonic characteristics (mainly compressional waves), and sometimes photo-electric information. Figure 12 shows a modern electric log suite from the Mississippi Lime within the seismic survey. All of this petrophysical information provided by the more modern suite of logs provides for a much more thorough and comprehensive subsurface study. Taking this and the purpose of this study into consideration, only wells that have information provided by the more modern suites of logs will be used in this analysis.

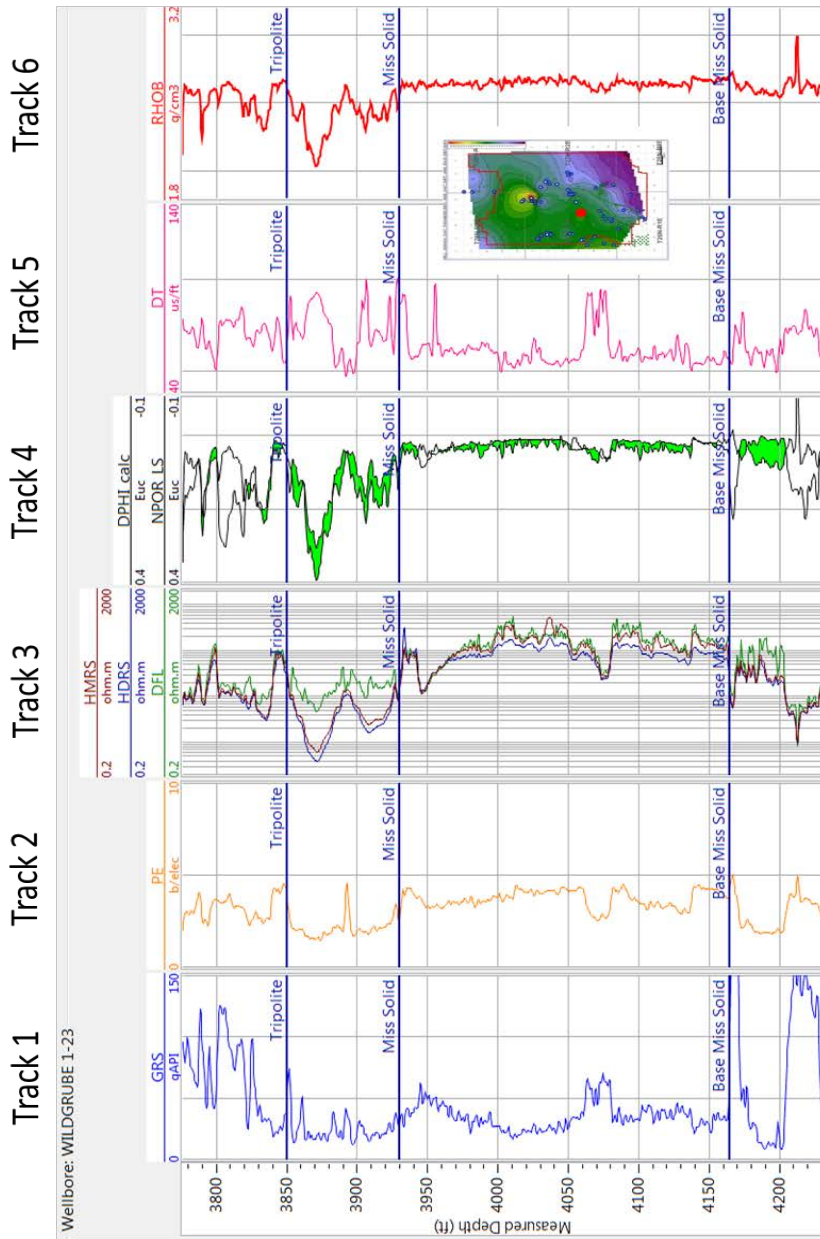


Figure 12. Modern electric log suite over the Mississippi Lime from a well within the 3D seismic survey. Tops of the tripolitic chert and Mississippi Solid facies are noted. Logs in the different tracks are described below.
 Track 1 – Gamma Ray Log (Scale = 0-150 gAPI); Track 2 – PE Log (Scale = 0-10 b/elec); Track 3 – Resistivity Log (Scale = 0.2-2000 ohm/m; green curve is shallow DOI resistivity, yellow curve is medium DOI resistivity, blue curve is deep DOI resistivity); Track 4 – Density/Neutron Porosity Log (Scale = -0.1-0.4 Euc); green shaded area indicates gas effect; Track 5 – Delta T Sonic Log (Scale = 40-140 us/ft); Track 6 – Bulk Density Log (Scale = 1.8-3.2 g/cm³)

In the study area shown in Figure 1, log characteristics exhibit a good deal of variation from top to bottom in the entire Mississippi Lime formation. Dowdell (2012) makes the assertion that the Mississippian Lime in Osage County, Oklahoma can be broken out into 3 different end members, Tripolitic chert, the St. Joe 'A', and the St. Joe 'B'. I believe, however, that in this particular area of study, that it is very difficult to discern the differences that would make up the St. Joe 'A' and the St. Joe 'B' end members of the Mississippi Limestone identified by Dowdell. It is my assertion that there are only two significant facies of the Mississippi Lime present on a consistent basis throughout the study area. The Tripolitic chert facies, and what I refer to as the Mississippi Solid facies. It is very easy to distinguish between these two facies when observing their petrophysical characteristics on open hole logs. Figure 12 shows a modern electric log suite from within the seismic survey with differentiation between the Mississippian Tripolitic Chert facies and the Mississippi solid facies.

Figure 12 shows a modern suite of logs from one well in the study area with the various logs identified by track number. The logs in this well and others are used to characterize the Mississippi Lime in Kay County. In general, the Mississippi Lime formation ranges in thickness from 300-400 feet. The dominant facies, Mississippi Solid, makes up roughly seventy five percent of this thickness in most areas. The dominant characteristic of this end member of the Mississippi Lime is tight porosity. Track four in Figure 12 shows porosity values range from 2 to 4 percent from the density porosity curve through this interval, with the occasional reading of up to six percent porosity. These porosity values are

considered to be very low by conventional porosity standards. In general, there is 'gas effect' cross over throughout this entire interval, where the neutron porosity curve reads lower than the density porosity curve shown in green fill. When this effect occurs, it indicates that the neutron curve is reading hydrogen molecules in place, which is an indicator of the presence of natural gas. The characteristics of the sonic log over the Mississippi Solid interval shown in track five of Figure 12 can be characterized as fast velocity. Average readings from the compressional wave velocity are 55-60 microseconds/foot. In track one of Figure 12, the gamma ray log detects the presence of clay particles by sensing the radioactive nature of the clays. This is a lithology indicator that mostly distinguishes between shale and non-shale bearing intervals of rock strata. In the Mississippi Solid, the gamma ray is mostly homogenous, with readings ranging between 15-45 API units. There is the presence of the occasional 'shaley' bed with a higher gamma reading. These instances are very localized instances, and should not be taken into account if trying to classify the Mississippi Lime into end members. Resistivity values shown in track three of Figure 12 read well over 100 ohms and in some cases up to 500 ohms over the majority of the Mississippi Solid interval. This is not necessarily due to fluid content of the rock, but can also be contributed to the nature of the tight porosity found within this facies as described earlier. There are portions of this facies in which the resistivity does read much lower than 100 ohms, and sometimes as low as 10 ohms. This is not just attributed to the fluid content of the formation at that point, but can be affected by the mineralogy as well. Like with the gamma

ray, these variations within the resistivity readings are localized in nature, and should be treated as such. One of the most telling indicators or characteristics of the Mississippi Solid facies comes from the photoelectric log in track two of Figure 12. The photoelectric log assigns values to rock formations based on their mineralogy. The logging tool records the absorption of low energy gamma rays by the formation and records these values as barns per electron. This value is a direct function of the aggregate atomic number of the elements from within the formation (Kansas Geologic Society, 2003). This log then assigns specific values to minerals such as quartz (1.81), dolomite (3.14), and calcite (5.08). Table one shows the values assigned to mineral constituents that make up common rock formations. The Photoelectric values throughout the interval of the Mississippi Solid read between 3 and 5, with only the occasional values reading truly 5, which would indicate pure limestone. I attribute these erroneous values, less than 5, to thin bedding of other minerals within the Mississippi Solid. The interbedded chert likely affects the reading the most. Photoelectric logs are not sensitive to thin bedding characteristics, so the values being read are more of a running average. With chert being silica rich (quartz has a Pe value of 1.81) and true limestone having a value of 5.08 on the Pe log, the expectation should be a Pe reading of 3.5-4 on the Pe log if there is interbedded chert in the limestone formation. The Pe log is a valuable tool in this case when it comes to distinguishing the Mississippi Solid facies, from the Tripolitic chert facies.

Material	PEF (barns/electron)	<i>U</i> (barns/cm ³)
Quartz	1.80	4.80
Calcite	5.10	13.80
Dolomite	3.10	9.00
Kaolinite	1.80	4.40
Illite	3.50	8.70
Chlorite	6.30	17.00
Fresh water	0.36	0.40
Brine (120 kppm NaCl)	0.81	0.96
Oil	0.12	0.12

Table 1. PE values of different rock types as indicated by the photoelectric logging tool. The red box shows the PE values representative of different rock and mineral types. (Modified from SPE PetroWiki 2014.)

The second major facies, Tripolitic chert facies, of the Mississippi Limestone in Kay County is very unique, and is also easily identifiable when observing open hole logs. This rock unit lies on top of the Mississippi Solid facies, and is at the basal Pennsylvania unconformity. Thickness of this unit in the study area ranges from 0-150 feet in thickness. The tripolitic chert is present over the vast majority of the study area, and is not present only in the far southeastern portions of the area. Figure 13 shows a cross-section of density logs from within the seismic survey demonstrating the variation in thickness of the tripolitic chert facies of the Mississippi Lime. In comparison to the Mississippi

Solid facies, the Tripolitic chert is remarkably different. The most defining well log characteristic of the tripolitic chert is the high porosity shown in track four of Figure 12. The density porosity curve readings from the tripolite in the study area range from twenty to forty percent, with readings as high as forty five percent. There is also 'gas effect' cross over with the neutron porosity curve observed in some of the logs, but it is not present in every well, and should not be used as a defining characteristic when identifying this facies. Track five of Figure 12 shows the values observed from the compressional sonic log to range between ninety to one hundred five microseconds per foot in the most porous parts of the tripolite. The gamma ray log over the tripolite is less homogenous than those characteristics observed in the Mississippi Solid, but are still generally low. Track one in Figure 12 shows these values range from fifteen to thirty-five API units, with the occasional reading of as high as seventy-five API units. These higher API readings can be attributed to higher clay content, likely as a result of the depositional setting of the tripolite. There is also likely an element of diagenetic alteration within the tripolite that contributes to the higher clay content observed in some places by the gamma ray. The resistivity of the tripolite is also drastically different from the Mississippi Solid. The tripolite is characterized in many areas by having especially low resistivity values. According to Rogers (2001), good quality productive tripolitic chert should have a reading of one to two ohms on the deep resistivity log. In the study area, the tripolite can have resistivity values ranging from below one ohm to roughly ten ohms as shown in track three of Figure 12. In the most porous parts of the tripolite, the resistivity

values can be expected to very low, and are rarely higher than five ohms. These low resistivity values are caused by two things. First is the high porosity exhibited in the tripolite. The second reason for the low resistivity values can be attributed to the amount of water present in the tripolite. The tripolite contains a significant amount of water from the production records of the wells within the study area. Finally, the photoelectric log provides a nice confirmation mechanism when identifying the tripolite facies. In the case of the tripolite, the main constituent of this facies is quartz since the main component is chert. When observing the Pe values of the tripolite in track two of Figure 12, the curve reads below a value of two for nearly the entirety of the tripolite. This confirms that the tripolite facies is in fact chert, since quartz is assigned a value of 1.81 on the photoelectric scale. The photoelectric log may be the most useful tool in discriminating between the facies changes within the Mississippi Lime.

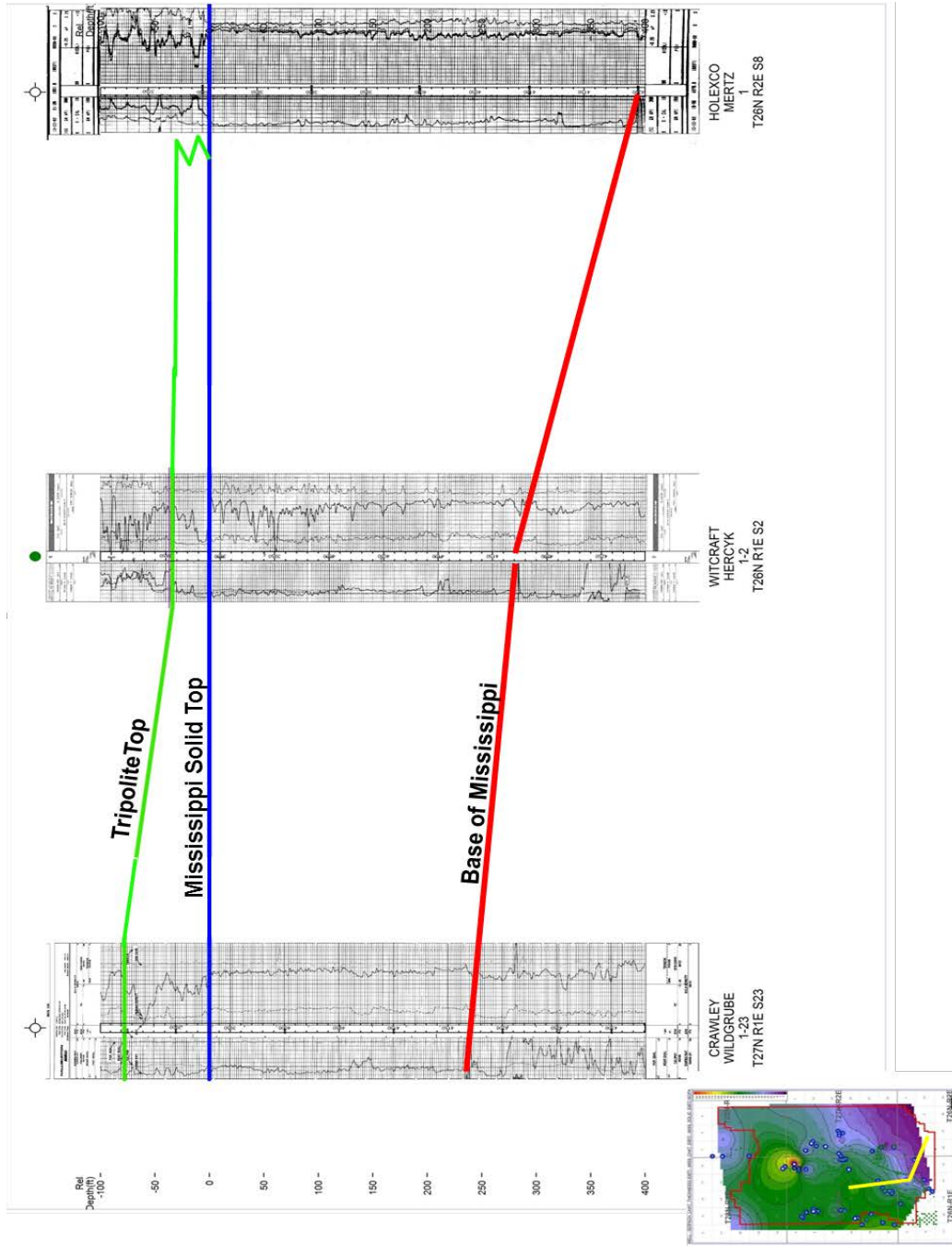


Figure 13. Stratigraphic cross section through Mississippi Lime within the area of study as seen by bulk density logs. Mississippi solid top used as datum. Note the lateral variation from north to south within the study area. The tripolite thins where solid thickens. Inset tripolitic chert isopach thickness map shows location of wells used in cross section. The green line indicates the top of the tripolite. The blue line indicates the top of the Mississippi solid. The red line indicates the base of the Mississippi Solid.

GEOLOGIC MAPPING

Another valuable tool geologists utilize in their interpretation of the subsurface is their skill in geologic mapping. There are a number of different types of maps geologists create and utilize in order to paint a picture of what the subsurface looks like in a particular location. These maps can include structure maps, isopach thickness maps, interval thickness maps, and production maps to name a few. Typically, a geologist will harvest information provided from well logs, and use that information to create a contour type of map that is representative of how the subsurface is behaving based on the data provided from the wells in a given area. Geologic maps can be both generated by hand or by computer. Generating these maps by hand can be time consuming and cumbersome at times, but can be a better representation of the subsurface since they are created by someone that has more understanding of the geologic behavior of the geologic feature being mapped. Using a computer to generate geologic maps is useful because it eliminates the time consumption of creating the maps by hand, and can identify many different geologic characteristics very easily. However, creating geologic maps with a computer can also have setbacks because the computer software is trained only to honor the data input into said software without any existing understanding of rock behavior. While a computer is capable of manipulating the data very easily, it is not capable of necessarily understanding the data the way a geologist would understand it. These maps are commonly used to identify new drilling opportunities by identifying potential reservoirs as well as subsurface hazard detection (faults)

and structural settings of various rock units in the subsurface. The information provided by these geologic maps is unique in respect to each type of map, but is very important to consider as whole by combining the information that each particular map provides to the interpreter.

For the purposes of this study I generated several different geological maps, using geologic software, over the same area that the subject 3D seismic data covers. I generated structure maps on several different formations tops including the Mississippi 'Chat' tripolitic chert interval at the top of the Mississippian interval, and the Mississippi Solid top. These structure maps provide, from a geologic perspective, what the structural orientation of the rock formations are, and a look into different geologic structures that are present and capable of being observed through traditional subsurface evaluation methods using well logs. Selley (1998) refers to structure contour maps as the simplest, but probably most important geological maps used in petroleum exploration. Another map I generated is an isopach thickness map of the tripolitic chert interval at top of the Mississippi Formation. This map shows how the thickness of the tripolitic chert varies laterally across the study area. Lastly, I generated an isopach thickness map of the Mississippi Solid facies of the Mississippi Lime deposited in the study area. This map, like the isopach map of the tripolitic chert, shows how the thickness of the Mississippi Solid changes across the study area. Selley (1998) calls the isopach thickness maps the next maps in importance to the structural contour maps. The combination of these maps provide evidence for how the Mississippi Lime was deposited, what type of geologic changes the

Mississippi Lime has undergone through time, and ultimately what the current geologic setting of the Mississippi Lime and its associated facies looks like today.

The previously mention structure maps were generated through observations made on well logs from existing wells that were drilled to a depth deep enough to penetrate the Mississippi Lime. Wells that were drilled and subsequently logged with density logging tool were used in identifying the formation tops for these maps. Using this technique does exclude some of the potential data points from consideration in the generation of these maps because the logging tools that were used in the wellbore did not include a density tool. I employed this technique of not including all of the potential data for the sake of consistency. In using only well logs that contained a density tool measurement, I was able to pick the tops of the tripolite and the Mississippi solid with a greater deal of confidence than if I was attempting to correlate different types of well logs in order to pick the tops. The density logging tool expresses the difference in density of the tripolite and the Mississippi solid much more clearly than the other logging tools, therefore making it easier to pick the tops more accurately on a consistent basis. In order to get the values needed to generate these structure maps, I picked the top of the rock formations based on the density characteristics provided by the well logs. These tops are all considered to be a true vertical depth drilled with no deviation. These tops are then assigned a negative value (subsea) because they are distances from the surface of the Earth down to the top of the formations. The tops are then adjusted relative to sea level to get the true subsea value of the formation. This adjustment is done by taking the ground

level elevation at the specific well site and adding the elevation datum to this elevation. The elevation datum is the point above the ground level where the logging tools enter the wellbore, and is typically the kelly bushing (KB) height on the drilling rig floor above the ground level at the well site. After combining the ground level elevation with the elevation datum, this value is then added to the NEGATIVE value of the formation top picked from the well log. The remaining value from this seemingly simple arithmetic is the true subsea depth of the rock formation top with respect to sea level, which is zero. This true subsea value is then plotted on a map with the corresponding wellbore from which the formation top was picked. After posting all of these values, a contour map is then generated taking into consideration the measured formation tops from the wellbores in which they were picked. The contours represent what the surface of the formation top looks like relative to sea level in the study area.

Figures 14 and 15 are structure maps that I generated using the process described above of the top of the Mississippi tripolitic chert facies and the Mississippi Solid facies, respectively. Generally speaking, these structure maps are very similar in appearance. This is due to the fact that the tops identified for these facies of the Mississippi Lime in this area are separated by one hundred feet or less in virtually all of the study area. Both maps reflect roughly the same structural features present in the study area. Independent of the structural features present on these maps, the overall trend of the surface of both the tripolite and the solid are an east-west strike with a general southerly dip of the rock formations. There are some structural features that are worthy of note that

are present on the structure maps. On the far west side of the study area, especially the northwest and southwest, the contour lines shift to a more north-south attitude as opposed to the general east-west trend observed over the majority of the maps. This abrupt change in direction of contour lines with respect to the overall structural trend of a given area is typically indicative of the presence of a fault. Another feature that is prominent in the structure maps occurs nearly right in the middle of the study area. Here there is a feature that reflects a structural low and a structural high directly adjacent to one another. A structural feature like this could be caused by a couple of different circumstances. One such possibility is the existence of basement highs left over as a relic of the formation of the basement rocks. Another possibility is that the feature is caused by a pop up fault block along a strike slip fault plane giving the appearance of a basement high. Elebiju et al. (2011) describe the behavior of the basement rocks saying that the basement is an irregular erosional surface that contains a series of domes which control the distribution and thickness of the overlying Paleozoic sediment. There are a few other localized structural highs and lows present within the study area. These little structural features could be paleotopographic features present at the time of Mississippian deposition, but most likely are due to structural deformation influenced by the presence of a compressional strike slip fault regime as part of the Nemaha Ridge fault complex.

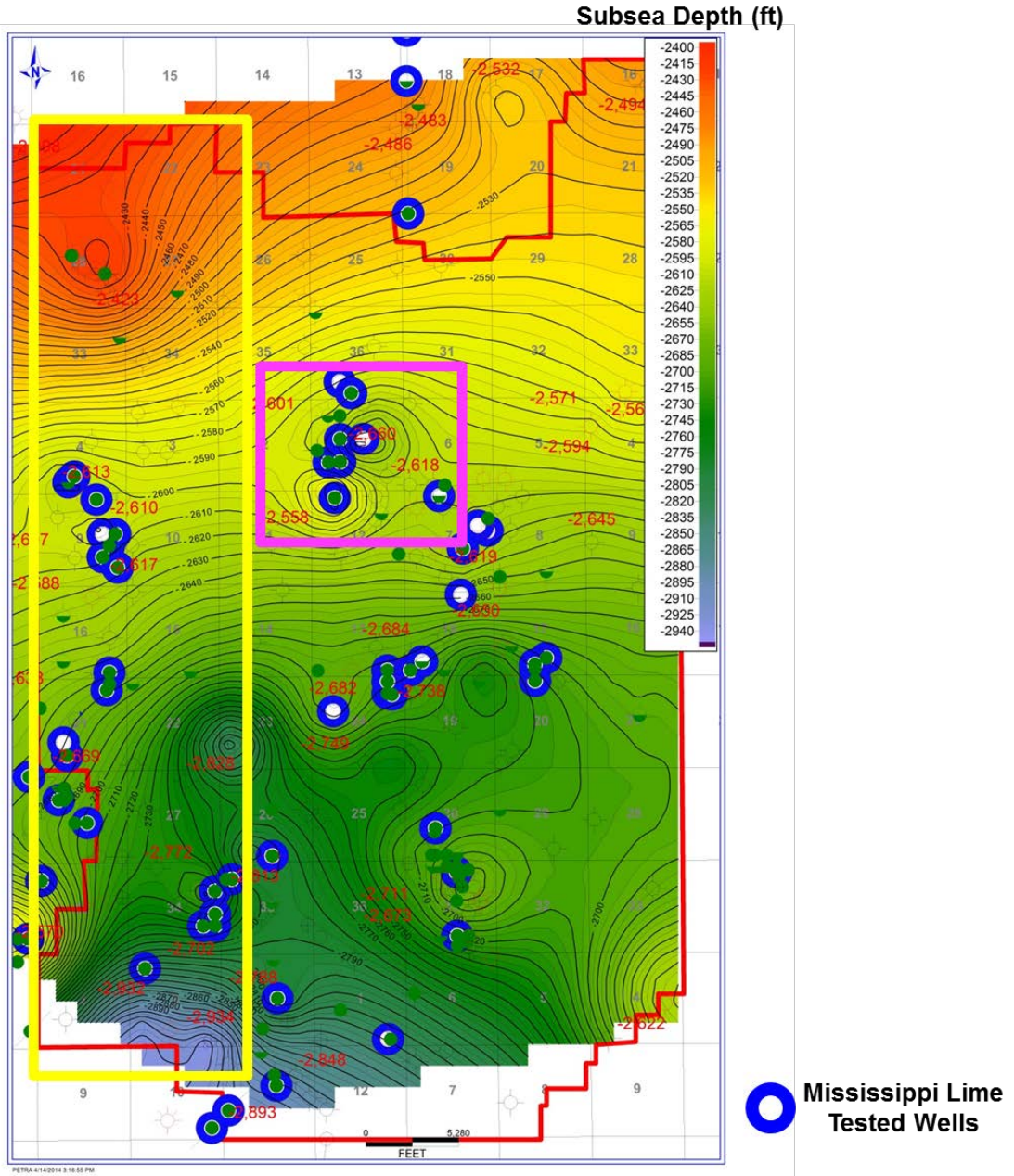


Figure 14. Structure map of top Mississippi Tripolitic Chert generated from geologic picks from well logs. The yellow box highlights where contours shift to a more north south direction, indicating the presence of a fault. The magenta box highlights a structural low and structural high directly adjacent to one another which is indicative of a paleotopographic high feature. 3D seismic survey boundaries are delineated by red.

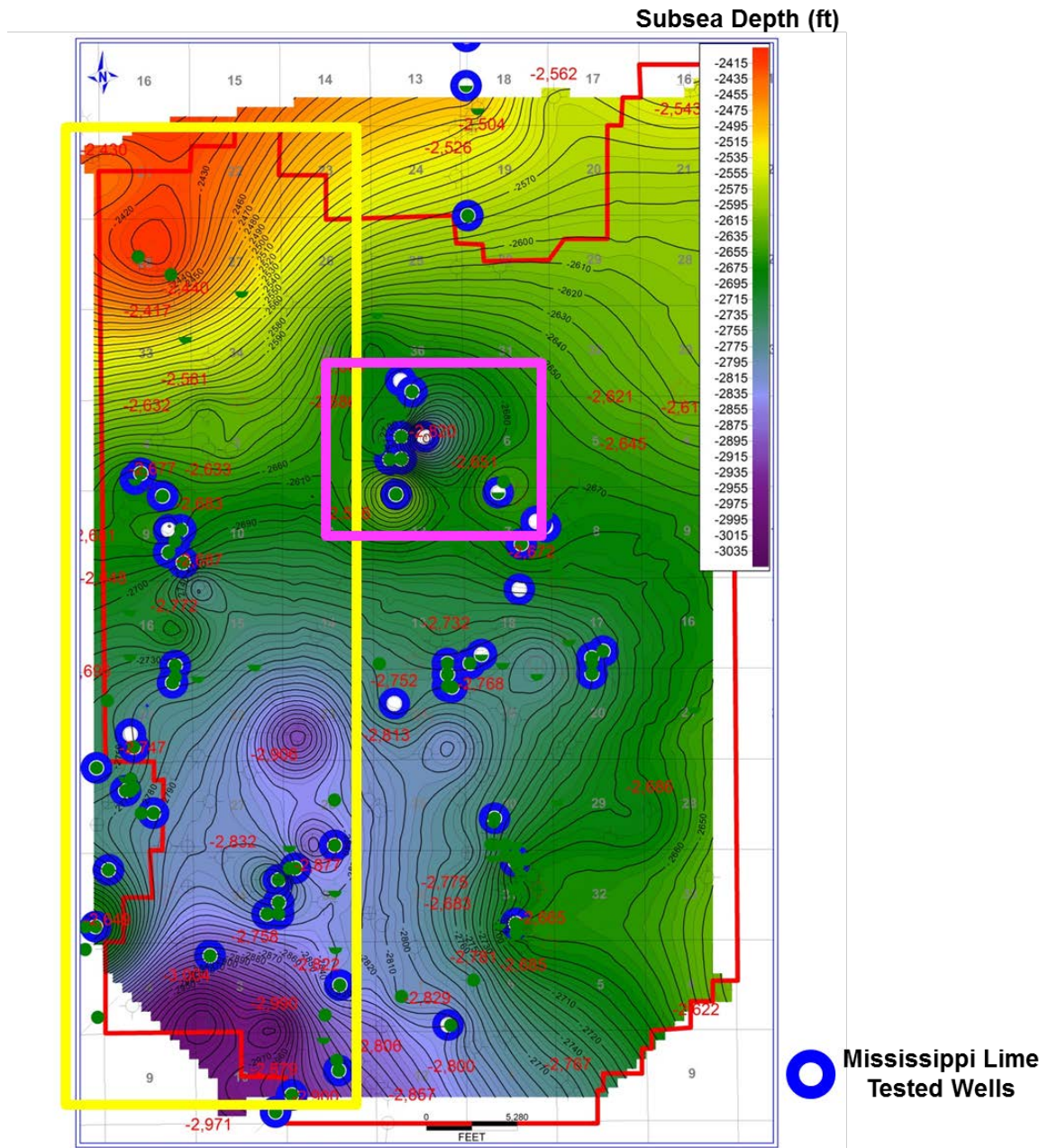


Figure 15. Structure map of top Mississippi Solid generated from geologic picks from well logs. The yellow box highlights where contours shift to a more north south direction, indicating the presence of a fault. The magenta box highlights a structural low and structural high directly adjacent to one another which is indicative of a paleotopographic high feature. 3D seismic survey boundaries are delineated by red.

Figure 16 is an isopach thickness map of the tripolitic chert facies member of the Mississippi Lime found in the study area. This map was generated quite simply by calculating the difference in feet from the top of the tripolitic chert and the top of the Mississippi solid. These tops are the same tops that were used in generating the aforementioned structure maps, using the information provided by wells that were logged using density well logging tools. Because the tripolitic chert member of the Mississippi lies directly on top of the Mississippi Solid, this measurement gives a true and accurate representation of the thickness of the tripolite. It is important to consider the thickness of the tripolitic chert member of the Mississippi because it possesses the more desirable reservoir characteristics of the two facies discussed, and the tripolitic chert is the most production tested of the two facies in the study area.

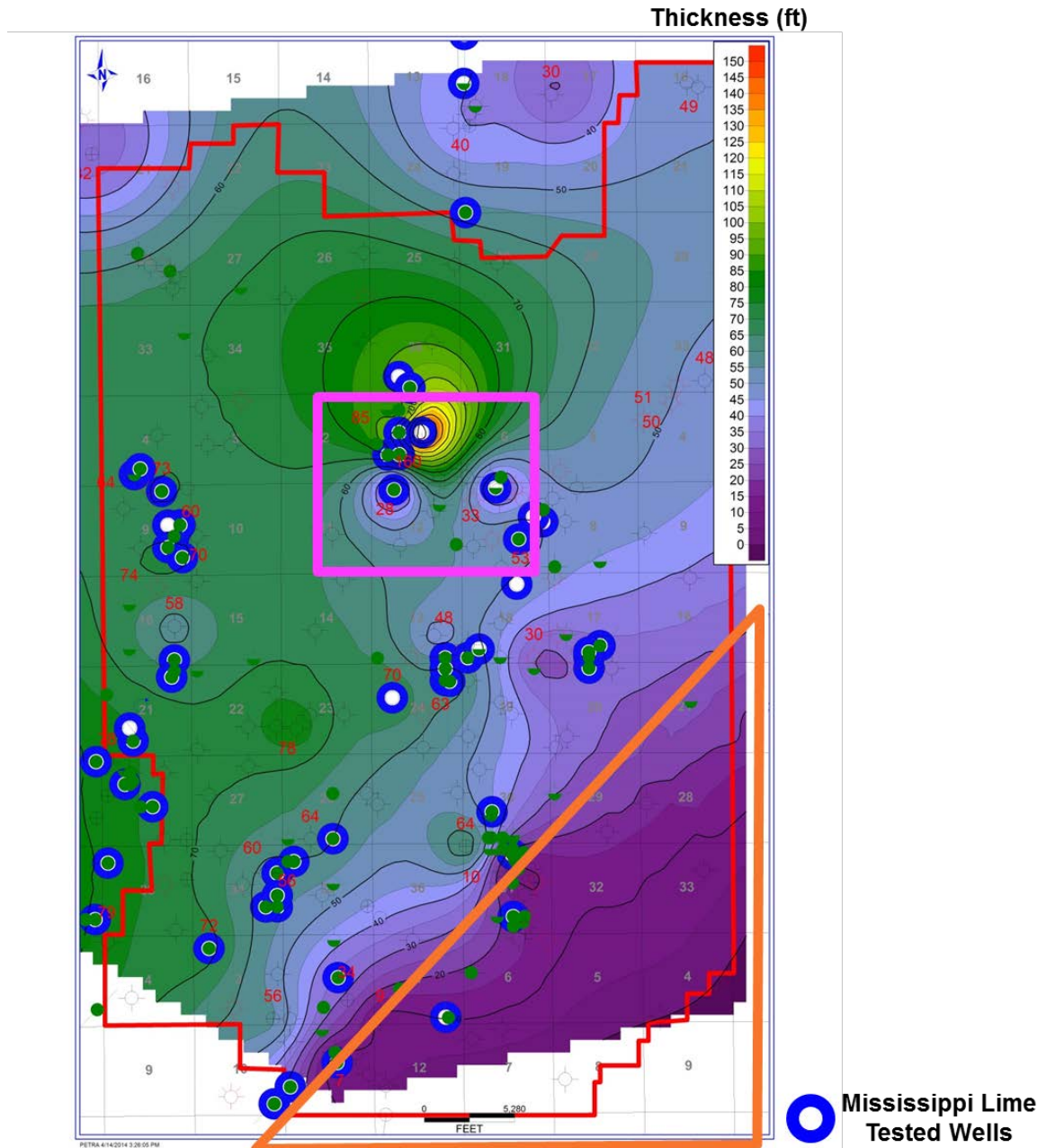


Figure 16. Mississippi Tripolitic Chert Isopach Thickness map generated from geologic picks from well logs. The magenta box highlights the thickening and preservation of tripolitic chert in the topographic lows and thinning of tripolitic chert on topographic highs. The orange triangle highlights where the tripolitic chert thins to the southeastern portion of the study area. Thinning occurs due to distal proximity to the Nemaha fault. Thinning of tripolite deposition may also be controlled by paleotopographic high features. 3D seismic survey boundaries are delineated by red.

There are several different characteristics of the tripolite that are of geologic significance shown in Figure 16. The first is that over the majority of the study area, the tripolite is of a fairly consistent thickness. This is demonstrated by the widespread presence of the green shades of color which indicate a thickness range of between fifty five and eighty five feet. Secondly, there is a small area in the north central portion of the map that shows the thickest presence of the tripolite indicated by the warmer colors. This thickness of the tripolite in this well is over 160 feet thick. Just to the south, and nearly directly adjacent to this thick, are two small areas that demonstrate a much thinner section of the tripolite. These are represented by the much cooler purple colors. This is significant because it indicates that the deposition of the tripolite in this area was likely a function of accommodation space available influenced by the paleotopography at the time of the deposition of the tripolite during Mississippian time. If you refer back to Figure 15, the structure map of the Mississippi Solid, you will observe that in the exact same spot that these thickness anomalies occur there is a structural low where the thickest occurrence of the tripolite exists, and two structural highs where the thin tripolite values exist. This provides the evidence to be confident in saying that at the time of the tripolite deposition, paleotopographic lows are where more tripolite was deposited, while the tripolite deposition on paleotopographic highs are much thinner due to the space available for deposition. Lastly, the lateral continuity of the tripolite can be observed when looking at this map. In the far southeastern portion of the study area, there is a data point that indicates that there is no tripolite present in that

wellbore. This shows that the deposition of the tripolite does not occur over the entire area of study, and therefore is not laterally continuous over a large area. I believe that there is a lack of deposition of tripolite in the southeastern portion of the seismic survey is because this particular area is too distal from the source of the sediment that makes up the tripolite, the source being the up thrown Mississippi rocks associated with the Nemaha Ridge. Local structural highs at the time of deposition of the tripolite could have served as a control on the aerial extent of the deposition of the tripolite as well. Rogers 2001 states that while the deposition of the tripolitic chert is widespread in north-central Oklahoma, it is not continuous.

Figure 17 shows an isopach thickness map of the Mississippi Solid member of the Mississippi Lime. This map was generated by measuring the thickness of the Mississippi Solid from the top of the solid to the top of the Ordovician aged Wilcox sandstone, which the Mississippian lies on top of unconformably in the study area. There are fewer data points used in the generation of this map when compared to the other geologic maps presented in this study. This is because not all of the wells used in generating the other maps penetrated the subsurface deep enough to observe the top of the Wilcox sand. The map shows an overall thickening of the Mississippi Solid from west to east, with the thinner portions of the Mississippi Solid being represented by the warmer colors, while the thicker values of the Mississippi solid are represented by the cooler colors. There is a large discrepancy from the thinnest mapped value and the thickest mapped value shown on this map, over three hundred feet in

difference. This discrepancy is caused by one of two things. The map is either showing a representation of what would be considered a slope margin and slope break that is near a shoreline where the Mississippi Solid was being deposited, or it is showing a representation of the uplift and subsequent erosion of the Mississippi Solid post deposition. I believe that this map is representative of the uplift and subsequent erosion of the Mississippi Solid after it was deposited. This belief is based on the indication of the presence of a fault exhibited by the two contour maps discussed previously. This change in thickness of the Mississippi Solid is evidence that further supports the existence of a fault.

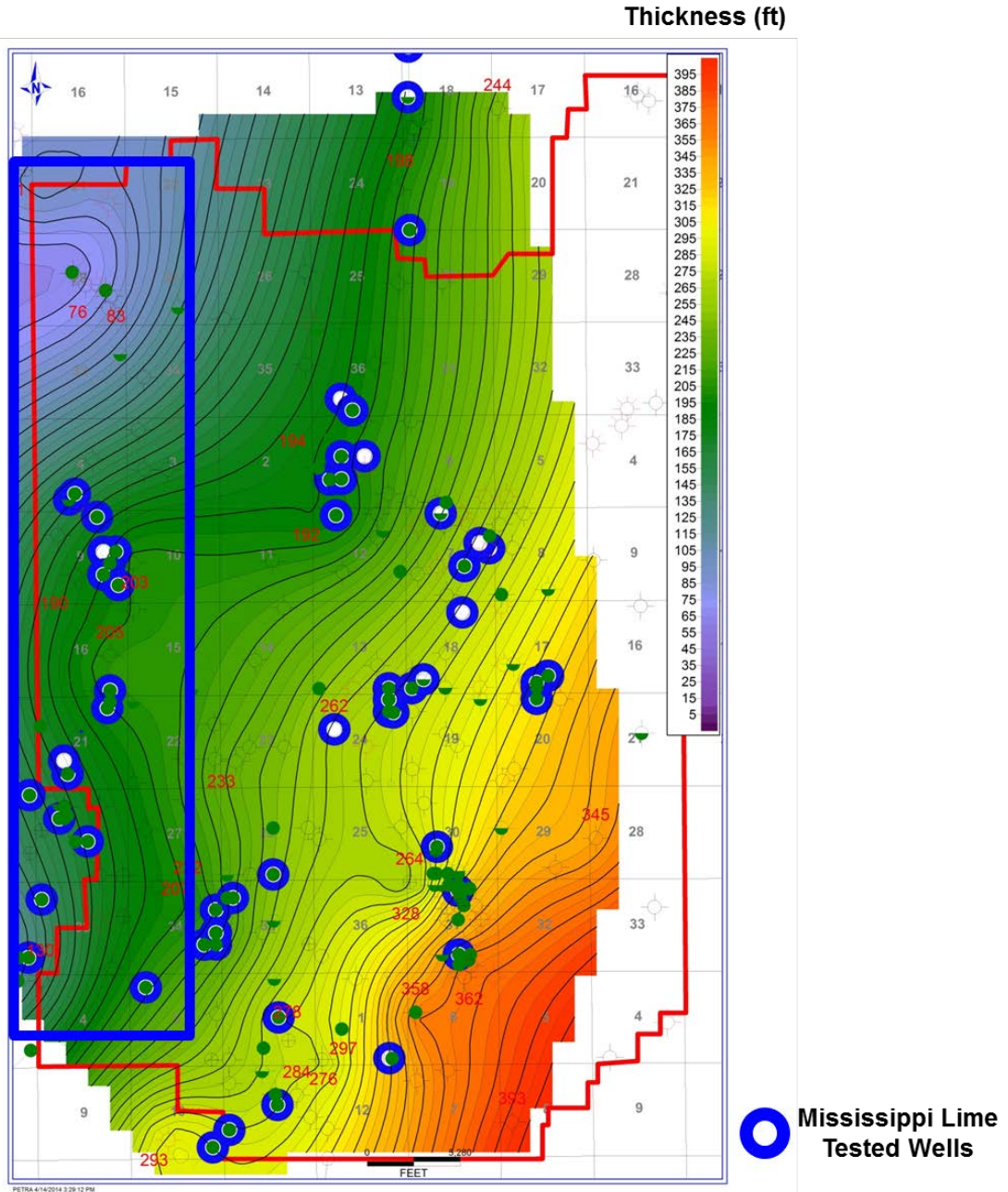


Figure 17. Mississippi Solid Isopach Thickness map generated from geologic picks from well logs. The blue box highlights the thinnest values of the Mississippi solid. This indicates the presence of a fault up throwing the Mississippian, and subsequent erosion caused the thinning of the Mississippi Solid on this up thrown fault block. 3D seismic survey boundaries are delineated by red.

When the information provided by the isopach thickness maps of the tripolite and the Mississippi Solid is considered, my contention is that the tripolite that is present in the study is the result of the uplifting of the Mississippi Solid via the Nemaha uplift, and the subsequent erosion and deposition of the Mississippi Solid to the east off of the uplift. In other words, the Mississippi Solid is the source of the sediment of which the tripolite consists. This geologic process of formation of tripolitic chert is also one of the two situations that Rogers, (2001) describes in her hypothesis of the formation of tripolitic chert. The isopach thickness map of the tripolitic chert shown in Figure 16 lends even more evidence to this belief. It makes sense that the source of the tripolite in this study area would be from the west based on the absence of the tripolite shown in the southeastern parts of the map. This would indicate that this area was more distal to the source and therefore did not experience the deposition that the rest of the study area experienced. Further evidence for this belief provided by the isopach thickness map of the tripolitic chert is shown in the preference of the tripolite to be deposited in paleotopographic lows shown by the structure map of the Mississippi Solid. In principle, because the Mississippi Solid was uplifted by the Nemaha uplift on the western parts of the study area, the preference of the eroded material would be to move from the higher points to lower points because of the effects of gravity.

SEISMIC EXPRESSION OF GEOLOGIC FEATURES

Creating geologic maps of the Mississippian Lime by utilizing the information provided by well logs presents a fairly complete set of information

that can be used in interpretation. These maps were compiled and generated using enough data points from the well logs to have a high degree of confidence in the interpretation expressed by the maps. While these maps are full and complete in their presentation of the Mississippi Lime data, there are more helpful data to be considered in the geologic interpretation of the Mississippi Lime of Kay County. By utilizing 3D seismic data to support and enhance what has already been shown through conventional log-based geologic mapping techniques, a more accurate portrayal of the characteristics of the Mississippi Lime become evident. Even though there may be an abundance of subsurface well data available, these mapped geologic interpretations are based on projections of characteristics observed from well data at a particular point. 3D seismic data supplements the subsurface well data, providing a more complete picture of what is happening in the subsurface. 3D seismic data can aid in identifying structural anomalies as well as reservoir characteristics, or provide further support in confirming the existence of geologic features that have already been documented. The subject seismic survey was re-processed prior to my interpretation. While the survey is of excellent quality, there are some limitations that come along with the interpretation. With respect to the Mississippi Lime, it was very difficult to choose a horizon top to pick throughout the survey. This is due to a couple of things. First, the Mississippi top is an unconformity surface. Because of this, it is difficult to be consistent with horizon picks because the phase of the data may shift in a lateral sense due to a highly variable depositional surface. Secondly, the tripolitic chert that is deposited at the top of

the Mississippi Lime within the seismic survey does not provide a reliable reflector to pick a horizon on. The tripolitic chert is highly heterogeneous as a rock unit, both laterally and vertically. These characteristics of the tripolite cause the seismic data to have the appearance of brightening and dimming throughout the tripolitic chert member, also making it difficult to consistently pick a horizon right at the top of the Mississippi.

For the purposes of this study, the 3D seismic data was run through the Attribute Assisted Seismic Processing and Interpretation (AASPI) software suite of attributes, in which new volumes of seismic data were created with each new volume having the ability to highlight different seismic characteristics found within the original seismic data volume. Of the volumes created by the AASPI software, the volumes that provided the most insight and support to the geologic interpretation of the Mississippi Lime are curvature, coherency, and spectral decomposition. Each of these volumes provide some unique information that helps to enhance the previously discussed geologic picture of the study area.

The first step in creating a seismic interpretation is to tie the digital well data that are available to the seismic data. Such tying is done to ensure that horizons are picked in the correct locations within the seismic data, and to confirm the phase of the data is correct so that the interpretation of the seismic data will represent the geologic interpretation as closely as possible. The process of tying well data to seismic data starts by converting sonic log data to velocity data, and then using this velocity data to create impedance logs by multiplying the velocity data by density data. The impedance logs created in this

process indicate what kind of acoustic response one should expect at different formation boundaries within the wellbore. Increases in impedance give rise to positive reflections and decreases to negative reflections. Next, a wavelet is extracted from the seismic data over a window of time to produce the synthetic. In this case, I extracted a wavelet over a 300 ms window. The result of this process is shown in Figure 18, with the synthetic data with a correlation of 53.5%, which is an acceptable degree of correlation, but perfect. This process was repeated for 10 other wells within the seismic survey. In all, 11 wells had digital information available to tie to the seismic data. After this process was complete, I used this information to aid in picking seismic horizons. Figure 19 shows the locations of the wells within the seismic survey that had digital well log data available to tie to the seismic data.

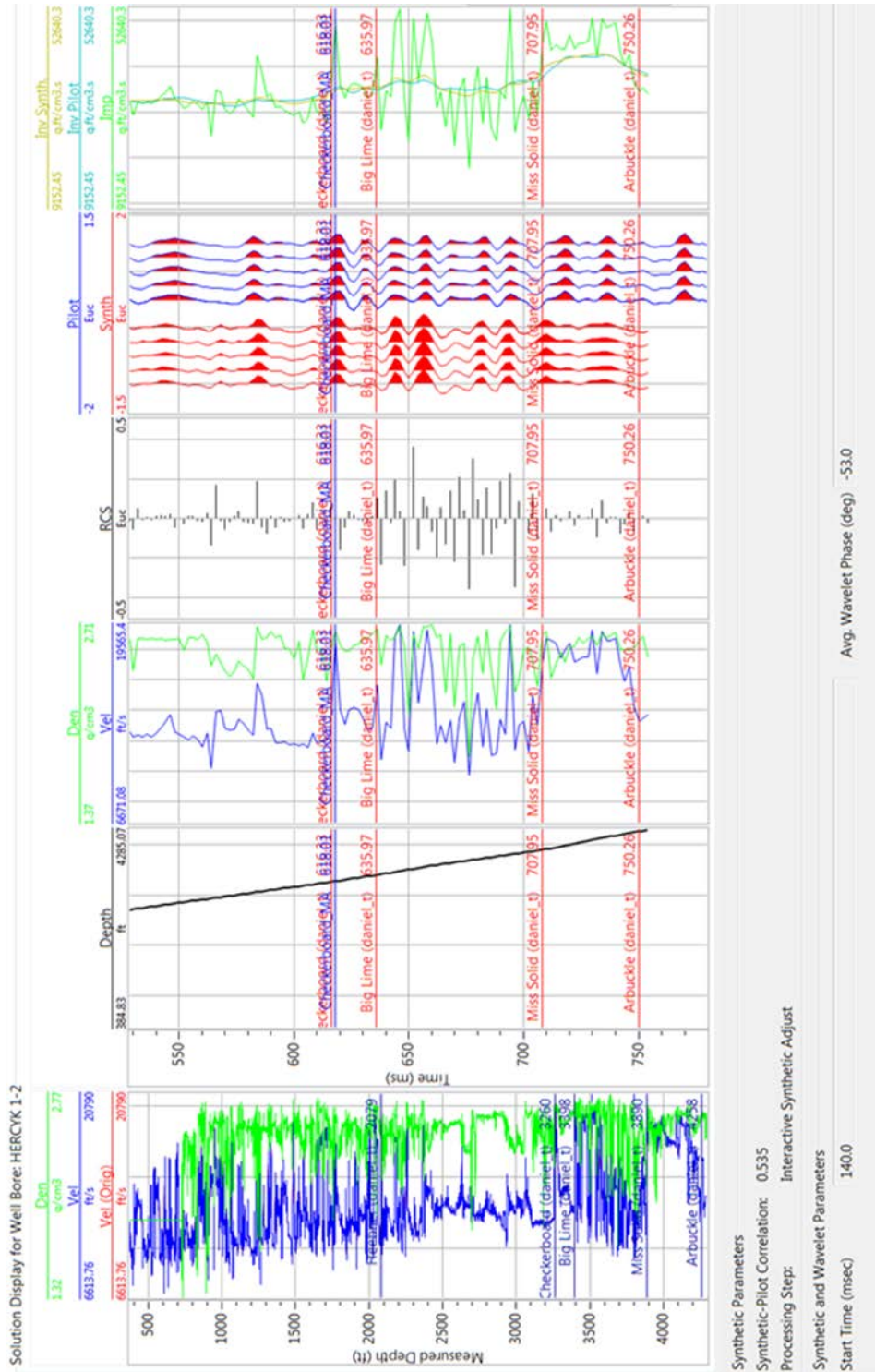


Figure 18. Seismic synthetic (in orange) with measured seismic (in blue) between 500-800 ms. Synthetic correlation is 0.535.

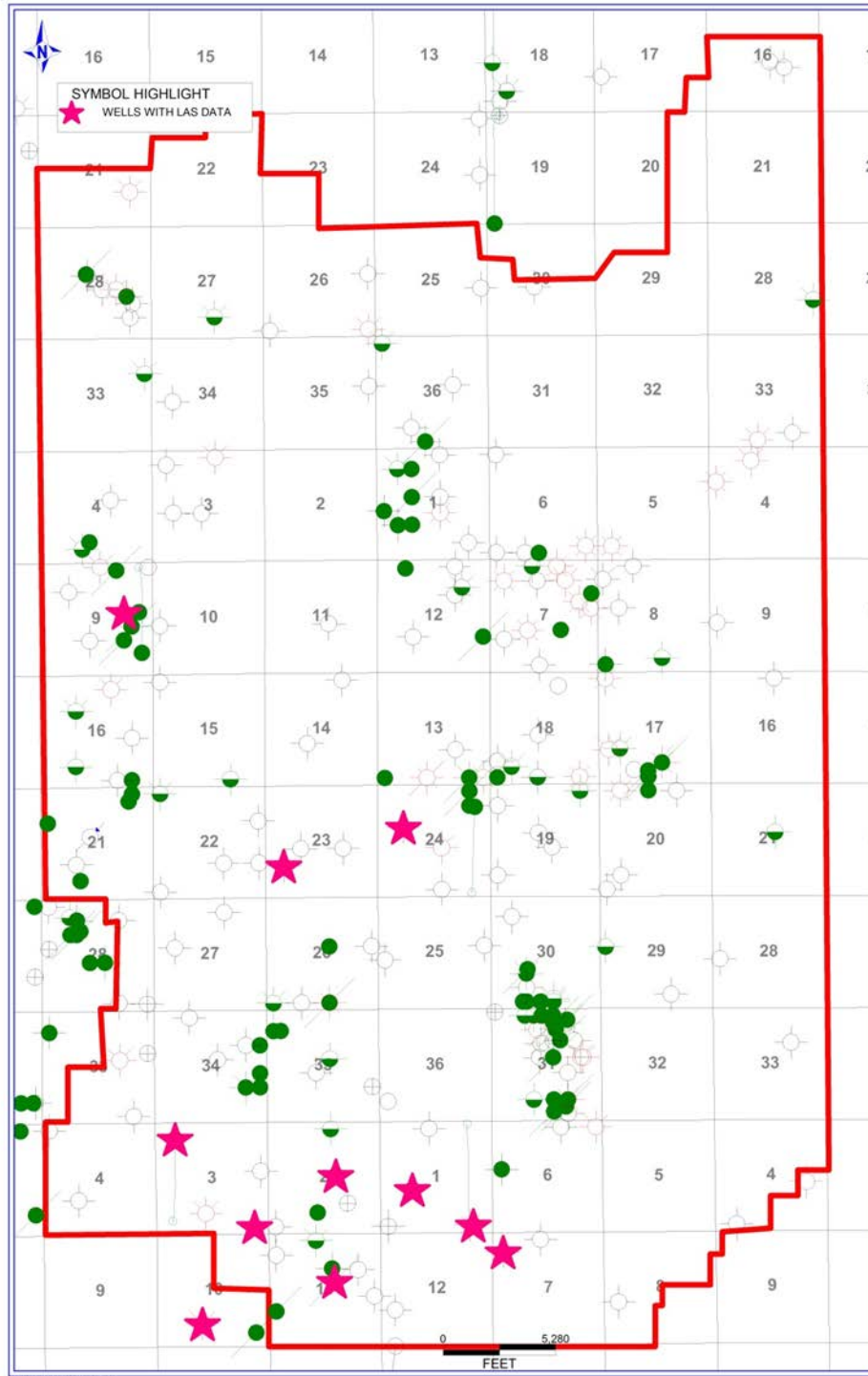


Figure 19. Map of the 11 wells with digital well log data (indicated by magenta stars) available for use in creating synthetics. Wells shown penetrated entirely through the Mississippian. 3D seismic survey boundaries are delineated by red.

Figure 20 is a time structure map along the top Mississippian horizon in the seismic data. This figure represents a seismic (time) expression of the structure maps of the tripolite and Mississippi Solid shown in Figures 14 and 15. Instead of contour lines delineating the gradient and changes present on the Mississippian surface like expressed on the subsurface maps, color is indicative of the change in elevation along the Mississippian surface in this map. The warmer colors indicate a higher portion of the surface, while the cooler colors indicate spots along the surface that are lower. In comparison to the depth structure map in Figure 15, this time structure map gives greater lateral detail highlighting structural features such as the north-south trending Nemaha fault on the far western portion of the time structure map. Aisenberg (2013) describes this fault that cuts the Mississippi as a large, nearly vertical fault with almost 40 ms of displacement at the south and north parts of the survey with lessening relief toward the crest of the fault in the center of the 3D survey. This is most prominently observed by the sharp contrast in color from green to dark blue and pink which would indicate an abrupt change in elevation along the Mississippian surface. In the southern portion of this map, you can observe the aforementioned localized topographic highs and lows. These features are shown by the intermingling of the green and yellow colors with the blue shaded areas. Finally, in the north central portion of this map, you can easily spot the oblong red shape set in the middle of the green shaded area, a localized high that was mentioned previously. The time structure map along the Mississippi horizon as expressed by the seismic data is a good example of supporting evidence for the

existing subsurface geologic data. The time structure map largely mimics the same features shown on the subsurface geologic maps, and even enhances some of the structural features observed in the study area.

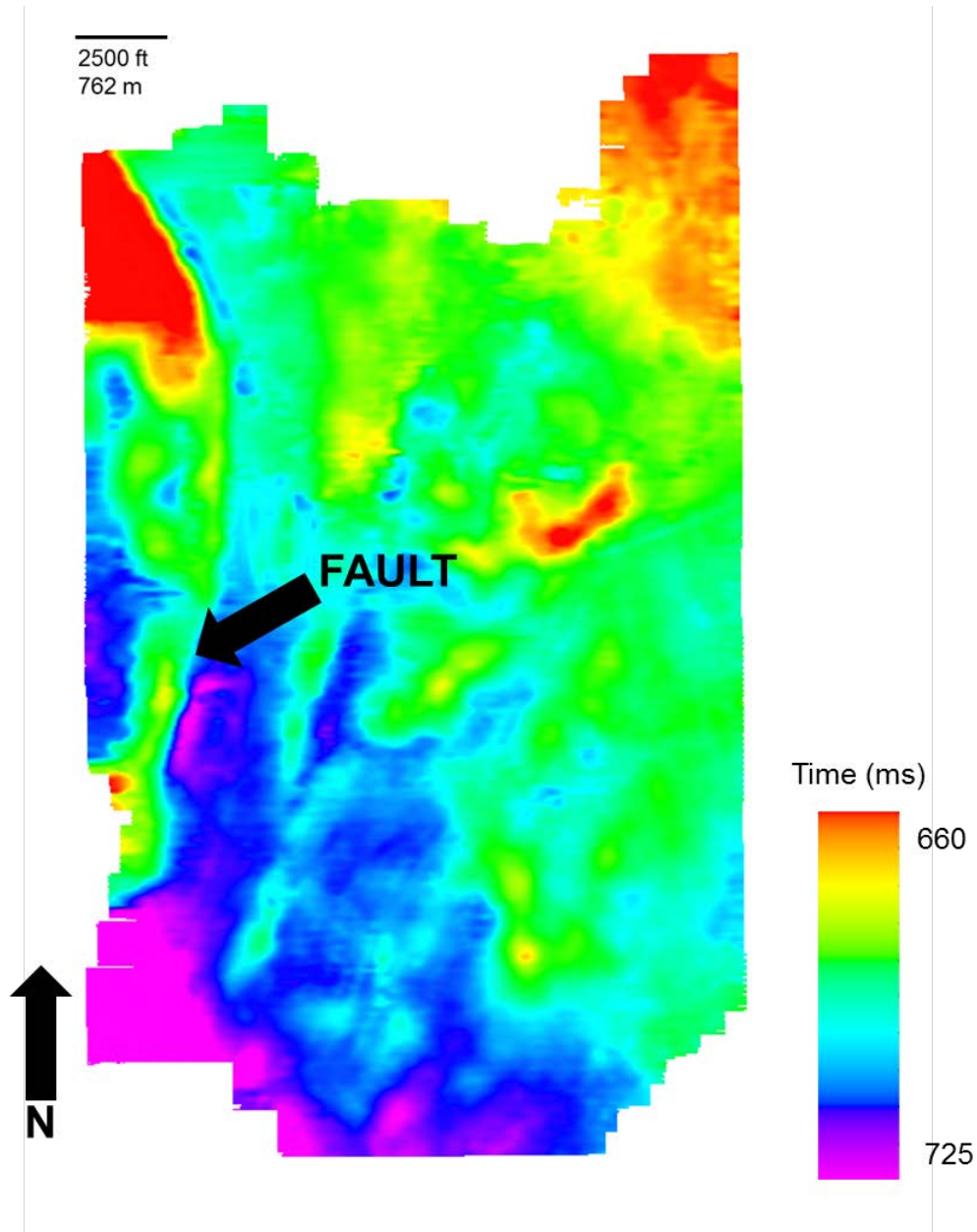


Figure 20. Top Mississippi time structure from 3D seismic data. The black arrow points to a major fault that is part of the Nemaha Ridge fault complex.

Figure 21 shows a phantom horizon slice 40 ms below the Mississippi horizon through the outer product similarity volume. Outer product similarity is used in this instance to identify structural features such as faults and karsts that exhibit discontinuous amplitude data. Figure 21 shows the most prominent structural features to be on the far west side of the survey. There are two large faults here with a north to south orientation. The fault that lies furthest to the west is the same fault seen in Figure 15. The second fault is located just west of the center of the survey. This fault is not readily observed in Figure 15. Figure 17, the Mississippi Solid thickness map, is key in identifying the large fault that lies furthest to the west in the survey, but did not show any indication that this second fault was present. This is likely due to the fact that this fault occurred after the initial large fault, and likely does not give rise to a very large amount of displacement. It is important to note that the well control only supported the existence of only one of these faults. These faults are part of the Nemaha Ridge that runs through Oklahoma in a north to south orientation and was created as a part of the 'Wichita Orogeny' that occurred in the early Pennsylvanian time period. These faults are part of a much larger complex that runs from central Oklahoma northward all the way into Kansas. Gay (1999) describes the Nemaha fault complex as being a compressional orogenic regime. He uses the analogy of the Rocky Mountains to describe the conditions in which the Nemaha ridge was created. Gay cites several instances along the Nemaha Ridge in which the fault zone exhibits the characteristics of the thrust fold model of compressional mountain building. Figure 22 shows this model. Gay also cites the existence of

strike slip faults that occur in association with the Nemaha Ridge fault complex. Gay states that these faults likely occurred after the primary compressional event that formed the Nemaha ridge. In review of the seismic data, I concur with Gay's assertion of a compressional regime being responsible for the creation of the Nemaha ridge. Figure 23 shows a vertical section of grayscale amplitude co-rendered with most positive (k_1) curvature coupled with most positive (k_1) curvature co-rendered with outer product similarity extracted on the Mississippi horizon. The yellow arrows indicate the two faults associated with the Nemaha Ridge present in the seismic survey. The yellow circle highlights the primary fault found in the survey and shows quite a bit of vertical displacement. The seismic reflectors seen on the up thrown side of this primary fault exhibit the same characteristics shown in the thrust fold model found in Figure 22. The characteristics of most positive (k_1) curvature exhibited on the up thrown side of this fault would also indicate that there is an anticlinal shape associated with this structure. The green circle in Figure 23 highlights the secondary fault associated with the Nemaha Ridge found in the seismic survey. This fault exhibits little vertical displacement, and at times seems to even show pull apart characteristics. This secondary fault is likely a strike slip fault, which according to Gay, would have occurred after the primary compressional event that formed the Nemaha Ridge. In addition to the faults associated with the Nemaha Ridge, Figure 21 also illuminates other structural features to be considered in the survey. There are several small circular features that occur throughout the survey. These can be interpreted as either karst collapse features, or structural

highs. These features account for some of the small structural variability that is observed in the structural maps. The interpretation of these features will be addressed further later on in this chapter.

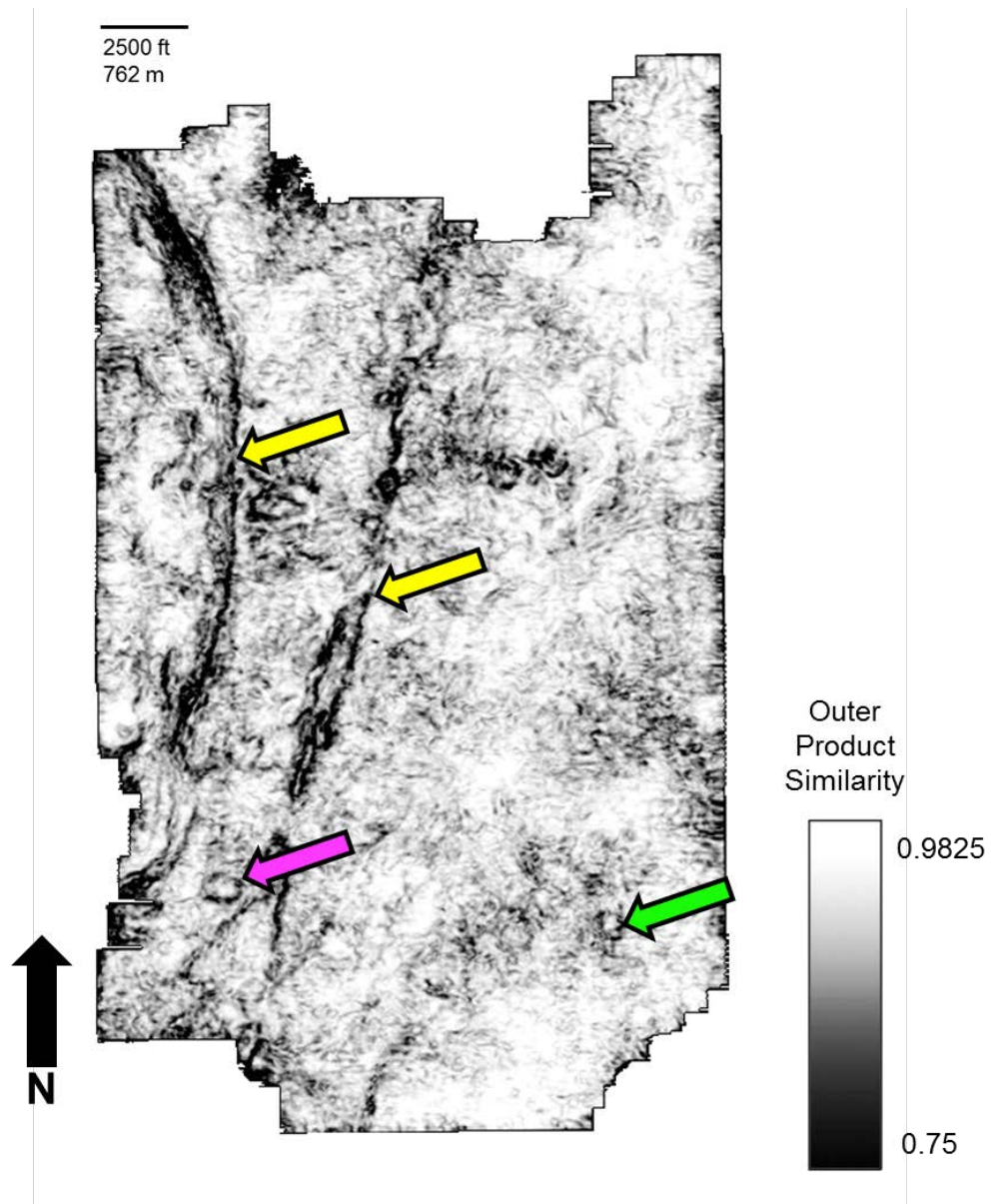


Figure 21. Outer Product Similarity extracted 40 ms below the top Mississippi horizon. Yellow arrows indicate faults. Green arrow indicate karst/collapse features. Magenta arrow indicates potential paleotopographic high feature.

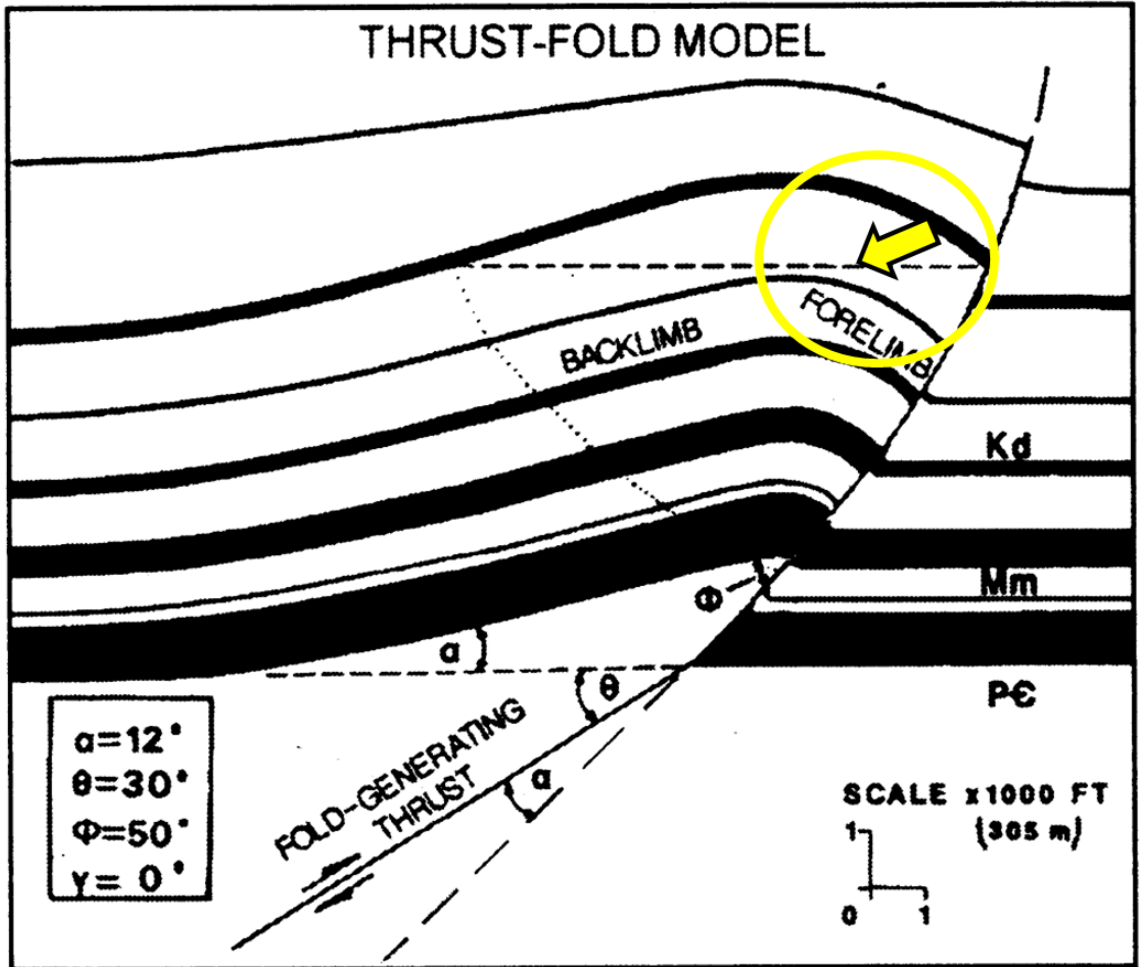


Figure 22. Thrust fold model as described as an analogue to the Nemaha Ridge compressional event by Gay (1999). Yellow circle and arrow indicate how the rock layers behave on the forelimb of the fold, which is caused by thrust faulting.

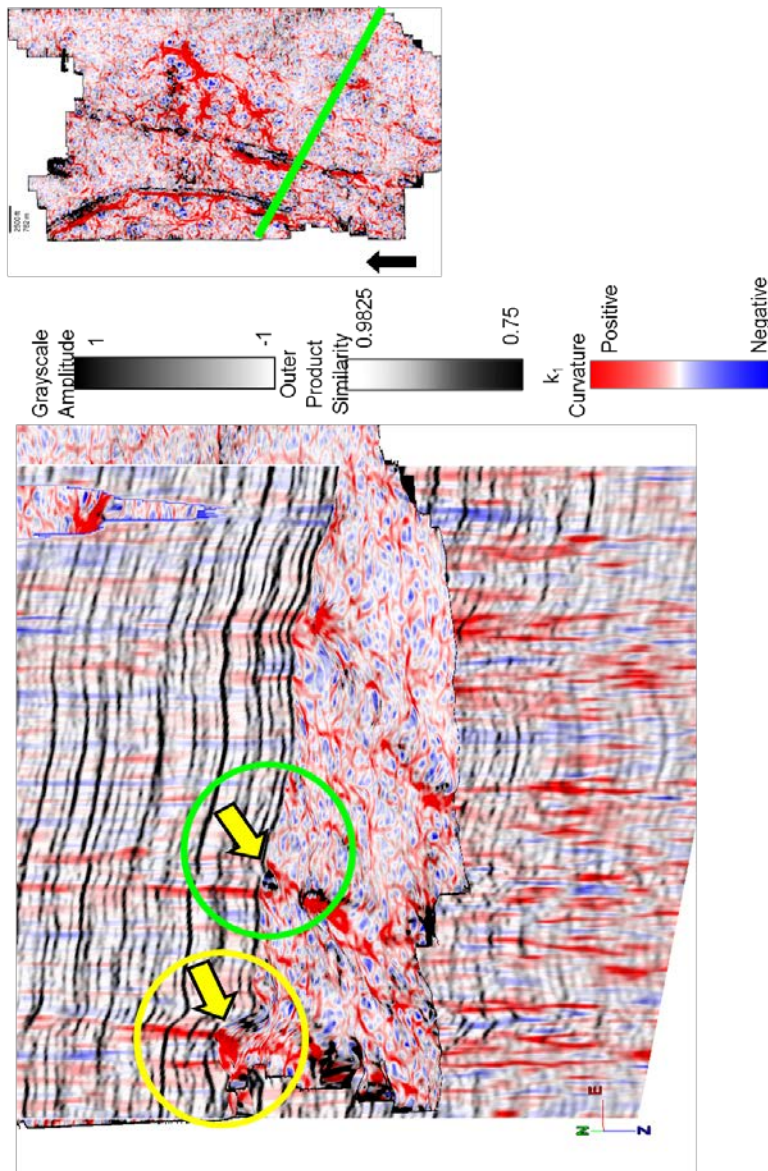


Figure 23. Most positive (k_1) curvature vertical slice co-rendered with amplitude (grayscale) along cross section A-A'. Most positive (k_1) curvature shown co-rendered with outer product similarity extracted on the Mississippi horizon. Yellow arrows indicate the faults associated with the Nemaha Ridge observed within the survey. Yellow circle highlights the larger of the two faults with significant displacement. Within the yellow circle, the behavior of the seismic reflectors is similar to the thrust fold model that Gay (1999) refers to. The green circle highlights the second of the 2 faults found in the survey. This fault exhibits the characteristics of a strike-slip fault, which are also found in association with the Nemaha Ridge, according to Gay (1999). The fault highlighted by the green circle shows little vertical displacement. Inset map shows location of cross section.

Figures 24 and 25 show phantom horizons 40 ms below the top Mississippian of most positive (k_1) and most negative (k_2) curvature volumes. In a simplistic sense, Chopra and Marfurt (2007) define anticlines having a positive curvature and synclines having a negative curvature. Chopra and Marfurt (2007) further state that curvature provides excellent images of subtle flexures, folds, and collapse features that are not commonly seen on coherence volumes. Furthermore, White et al. (2012) states that an indirect association between curvature and fracture density can be made when trying to predict fractures by employing surface seismic attributes. With this in mind, the goal of introducing curvature images into this study is to further define the type of structural features that have been discussed to this point. This is done by correlating the curvature characteristics back to structural features in an attempt to understand the shape(s) of the features.

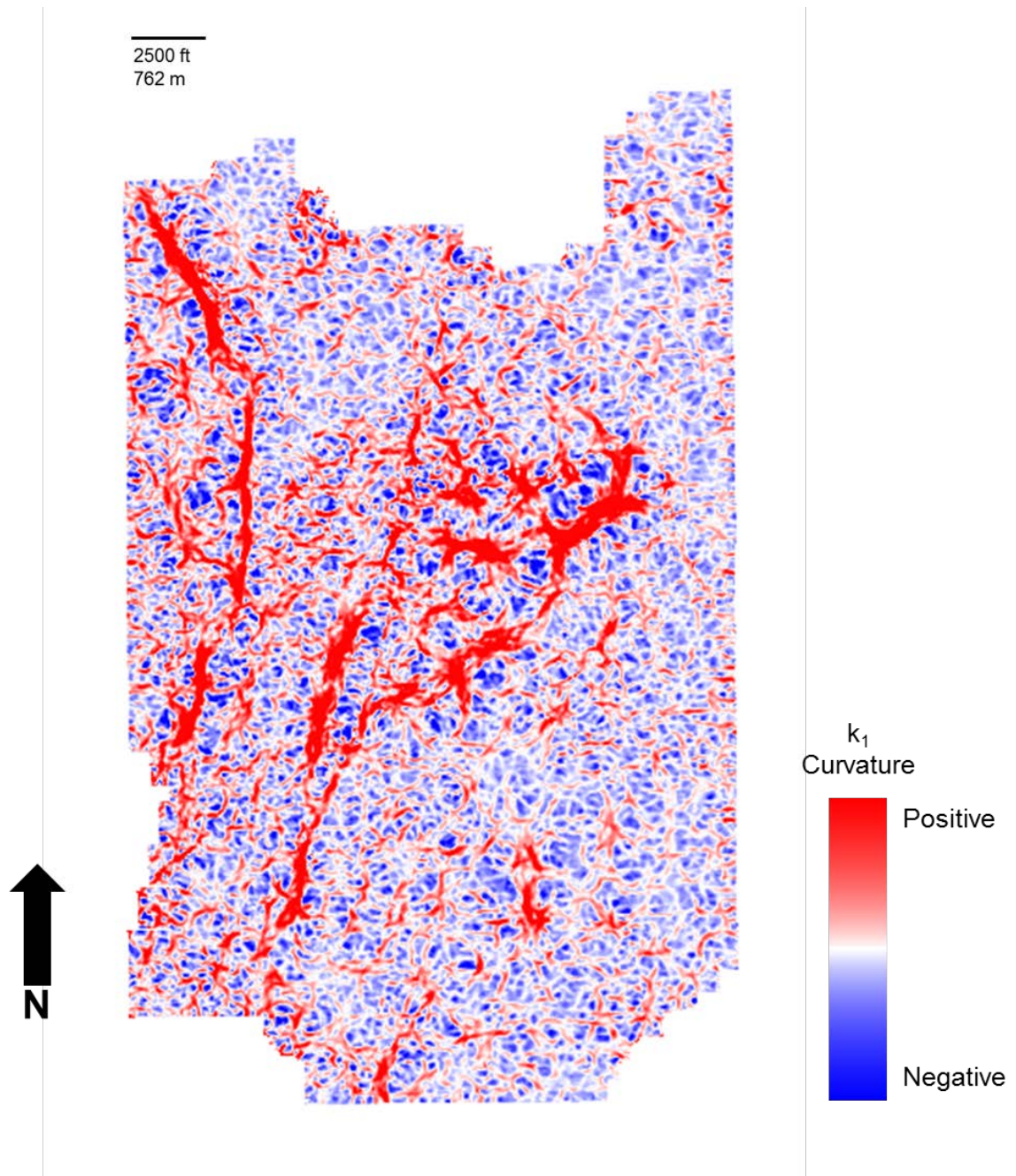


Figure 24. Most positive (k_1) curvature extracted 40 ms below the Mississippi horizon.

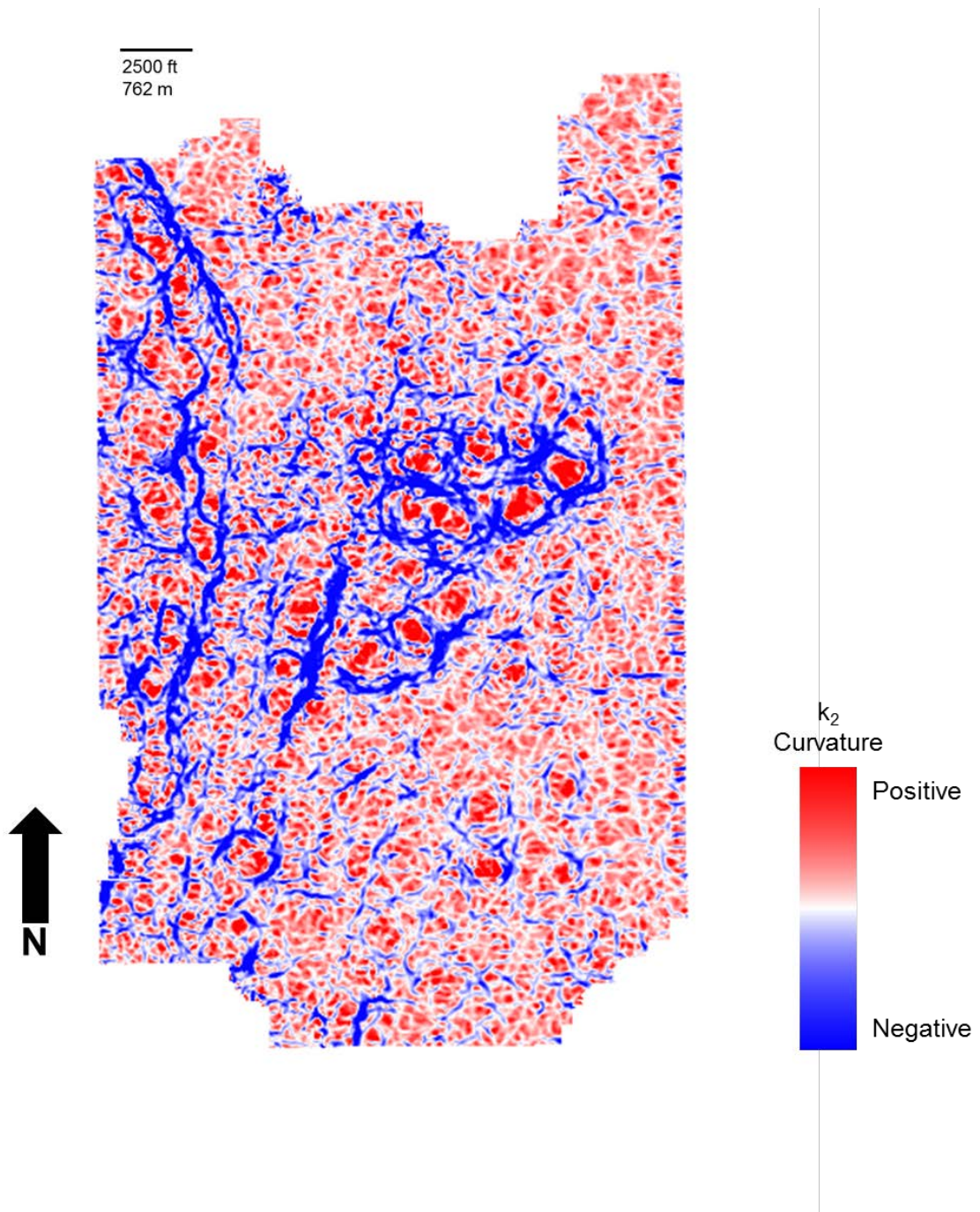


Figure 25. Most negative (k_2) curvature extracted 40 ms below the Mississippi horizon.

Figure 26 shows a phantom horizon slice through most positive (k_1), but now co-rendered with the outer product similarity. With the addition of the outer product similarity to the curvature images, it becomes easier to visualize the structural features associated with the shapes indicated by the curvature. Figure 26 highlights karst/collapse and paleotopographic high features in the southeast portion of the survey, as well as in the north central portion of the survey. These collapse features account for some of the structural low areas that are observed on the geologic structure map, while the paleotopographic high features account for some of the structural high points in the survey. Figure 26 also shows how the faulting in the area takes on a negative characteristic of most positive curvature, shown by the broad blue colors located close to the fault plane. Figure 27 shows vertical grayscale seismic amplitude co-rendered with most positive curvature along the cross section A-A'. The yellow line indicates the Mississippi horizon, yellow arrows point to faults, magenta arrow points to paleotopographic high features, and green arrow points to karst/collapse features. This confirms the data displayed in the phantom slice shown in Figure 26. Figure 28 represents the same vertical data present in Figure 27, but now coupled with most positive curvature co-rendered with outer product similarity extracted on the Mississippi horizon. This figure adds the third dimension to most positive curvature, and supports the characteristics of most positive curvature observed in the phantom slice in Figure 24. Figure 29 shows a phantom horizon slice through most negative (k_2), but now co-rendered with the outer product similarity. Figure 29 shows the presence of the karst/collapse and

paleotopographic high features across the survey. The faults in this image are highlighted by positive values of most negative curvature as indicated by the red coloring present along the fault plane. Figure 30 shows grayscale amplitude co-rendered with most negative curvature along the cross section B-B'. This supports the characteristics exhibited by the phantom horizon slice seen in Figure 29 with yellow arrows indicating faults and magenta arrows indicating paleotopographic high features. Figure 31 shows the same vertical slice data shown in Figure 30 coupled with most negative curvature co-rendered with outer product similarity extracted along the Mississippi horizon. This figure adds the third dimension to Figure 30 and again identifies faults with yellow arrows and paleotopographic highs with magenta arrows.

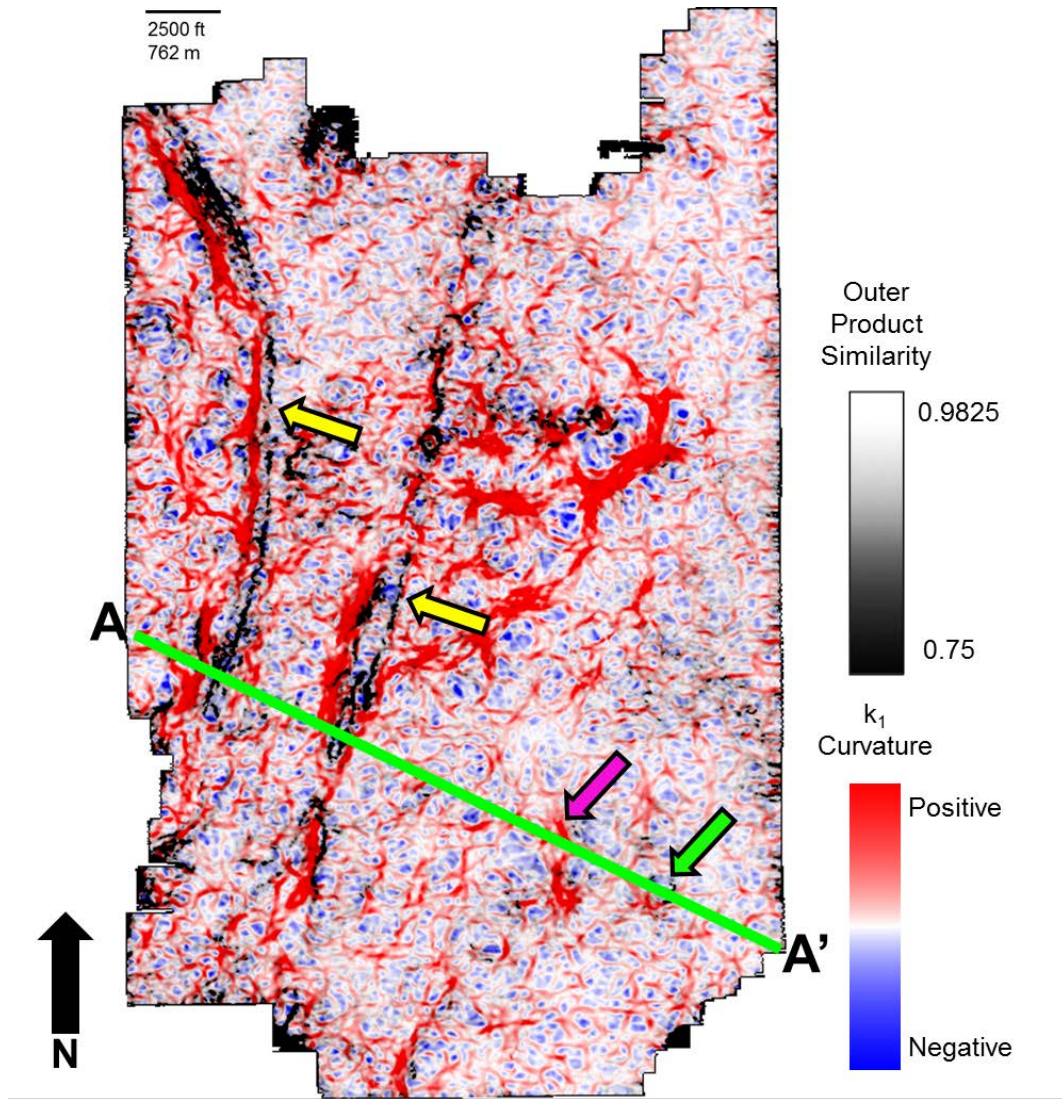


Figure 26. Most positive (k_1) curvature co-rendered with outer product similarity, both extracted 40 ms below the Mississippi horizon. Yellow arrows indicate faults. Green arrows indicate potential karst/collapse features. Magenta arrow indicates curvature demonstrated high features. Green line indicates vertical slice A-A' through the seismic data.

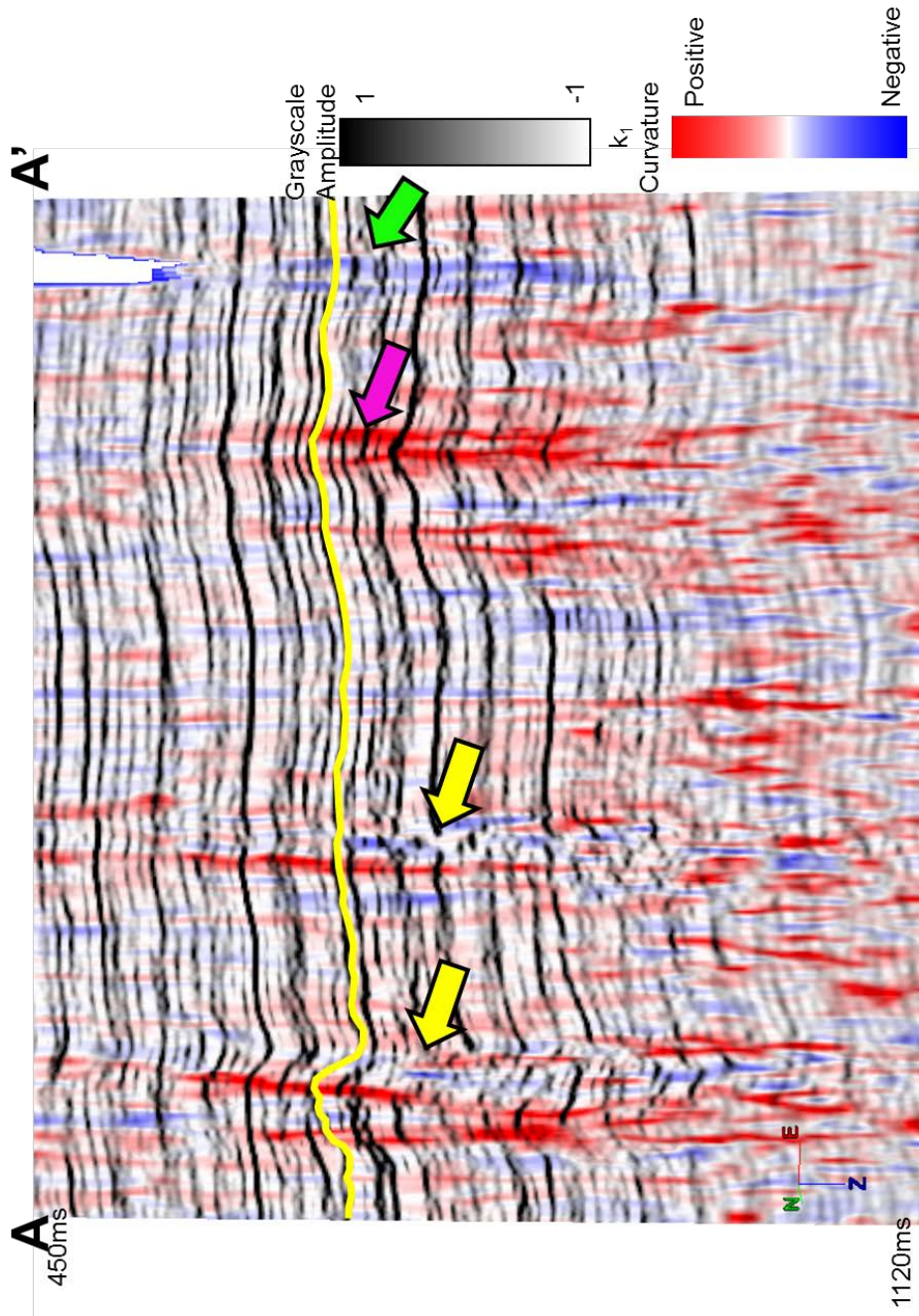


Figure 27. Most positive (k_1) curvature vertical slice co-rendered with amplitude (grayscale) along cross section A-A'. Mississippi horizon shown by yellow line. Faults are indicated by yellow arrows. Potential karst/collapse feature indicated by green arrow. Potential karst/collapse feature is likely influenced by lack of data access and may be an artifact of acquisition. Magenta arrow indicates either a paleotopographic high, or more likely, a structural deformation influenced by the presence of a compressional strike slip fault regime as part of the Nemaha Ridge fault complex.

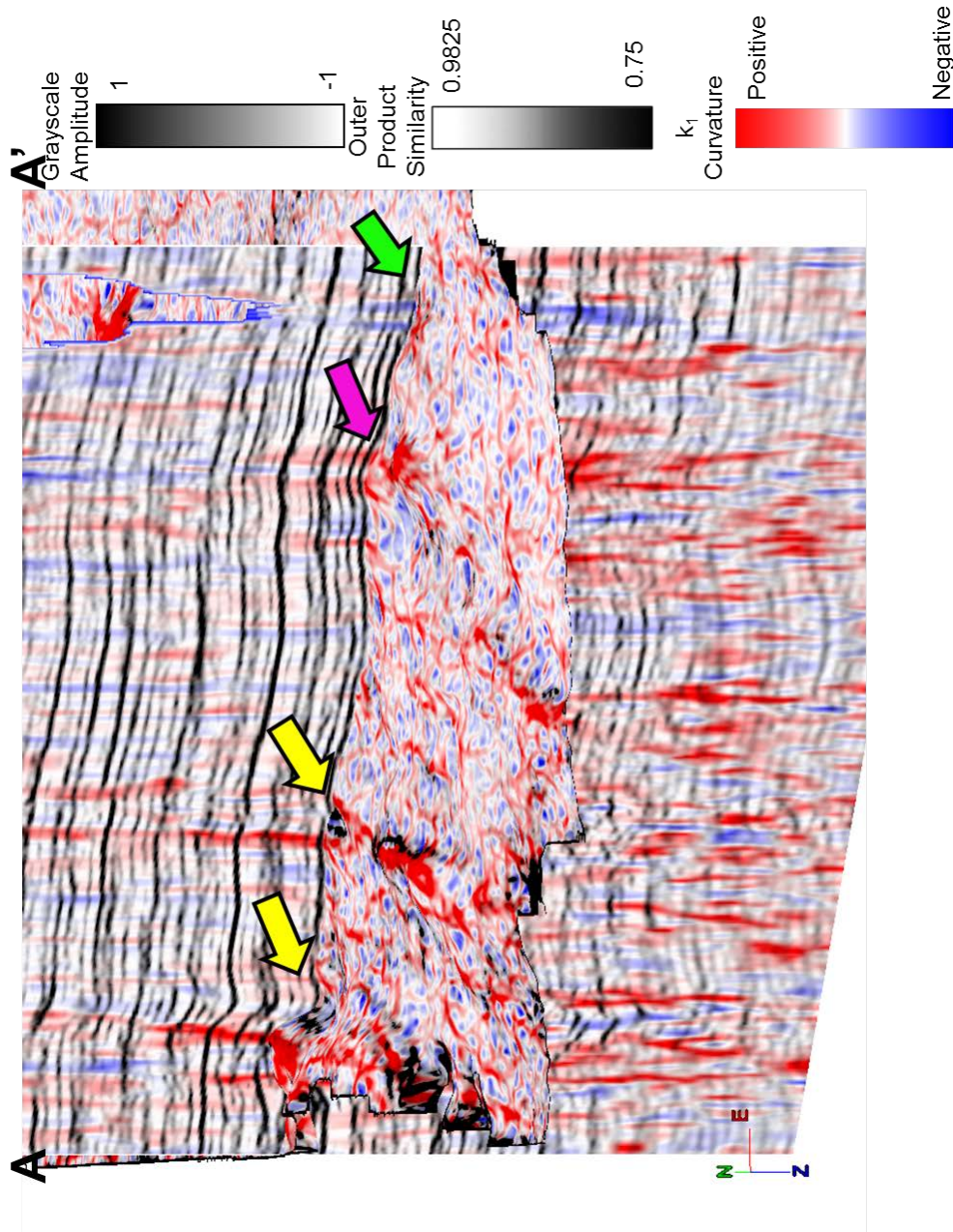


Figure 28. Most positive (k_1) curvature vertical slice co-rendered with amplitude (grayscale) along cross section A-A'. Most positive (k_1) curvature shown co-rendered with outer product similarity extracted on the Mississippi horizon. Faults are indicated by yellow arrows. Potential karst/collapse feature indicated by green arrow. Potential karst/collapse feature is likely influenced by lack of data access and may be an artifact of acquisition. Magenta arrow indicates either a paleotopographic high, or more likely, structural deformation influenced by the presence of a compressional strike slip fault regime as part of the Nemaha Ridge fault complex.

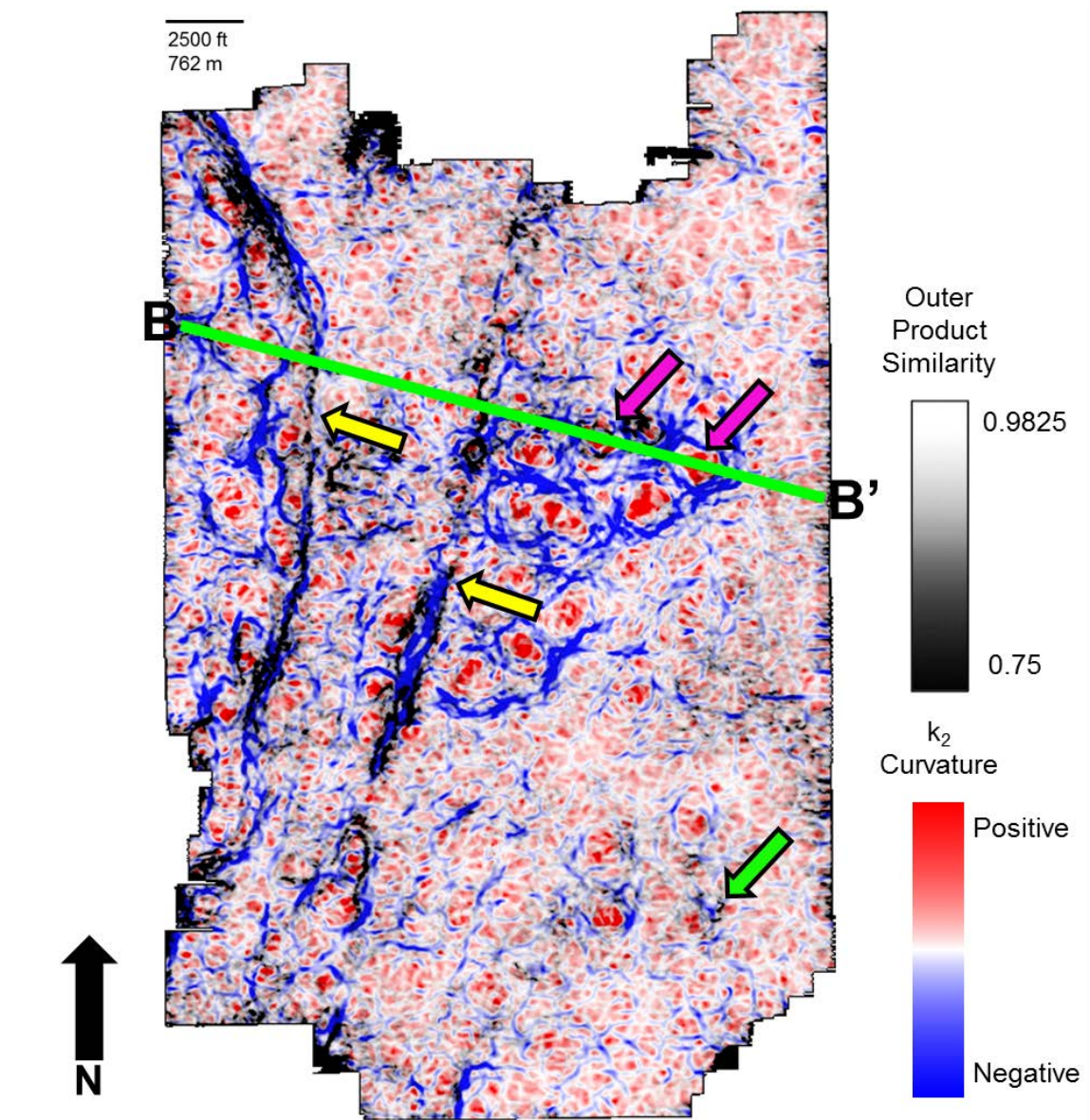


Figure 29. Most negative (k_2) curvature co-rendered with outer product similarity, both extracted 40 ms below the Mississippi horizon. Yellow arrows indicate faults. Green arrows indicate potential karst/collapse features. Magenta arrows indicate curvature indicated high features. Green line indicates vertical slice B-B' through the seismic data.

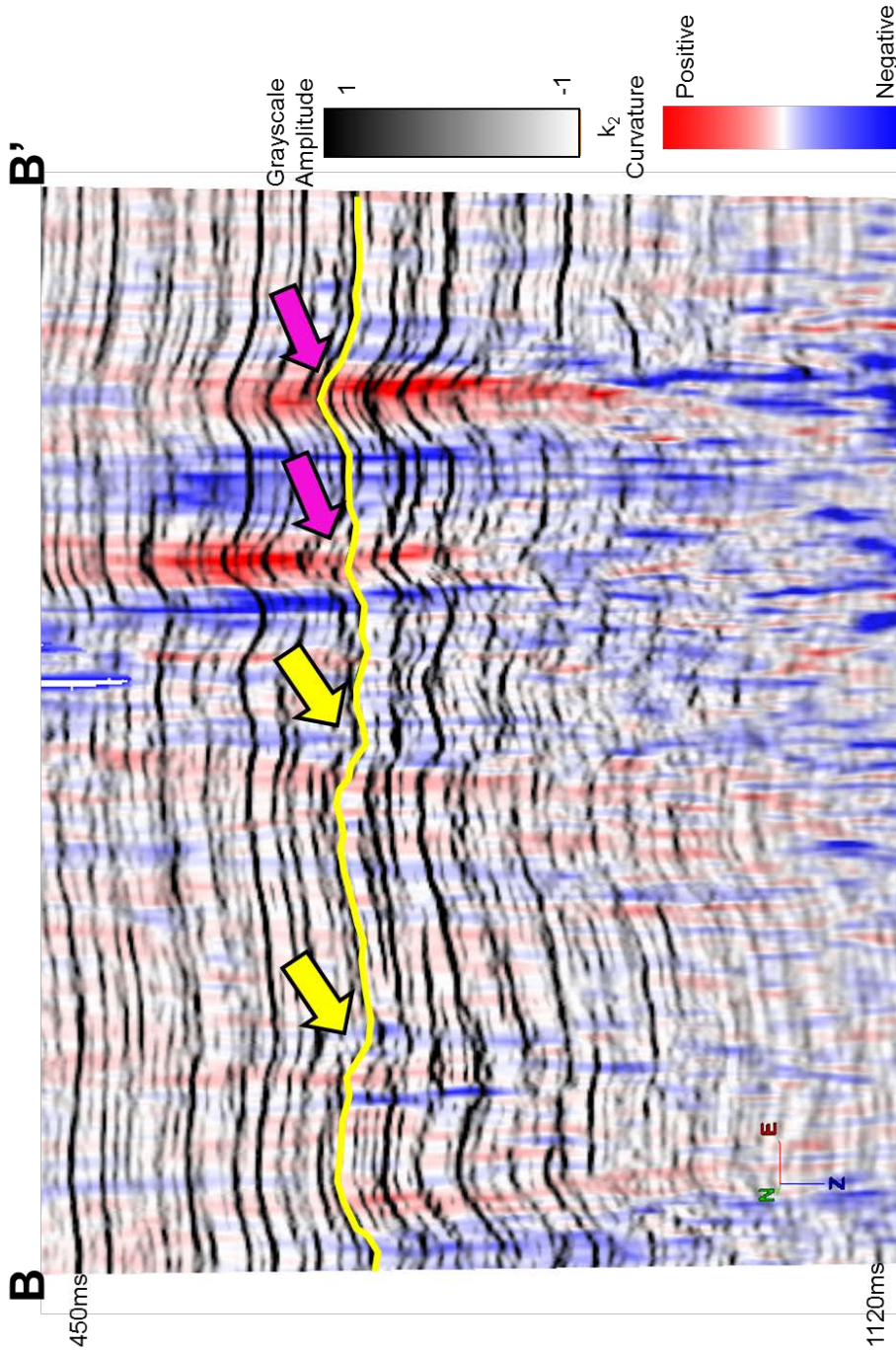


Figure 30. Most negative (k_2) curvature vertical slice co-rendered with amplitude (grayscale) along cross section B-B'. Mississippi horizon shown by yellow line. Faults are indicated by yellow arrows. Magenta arrows indicate either a paleotopographic high, or more likely, structural deformation influenced by the presence of a compressional strike slip fault regime as part of the Nemaha Ridge fault complex.

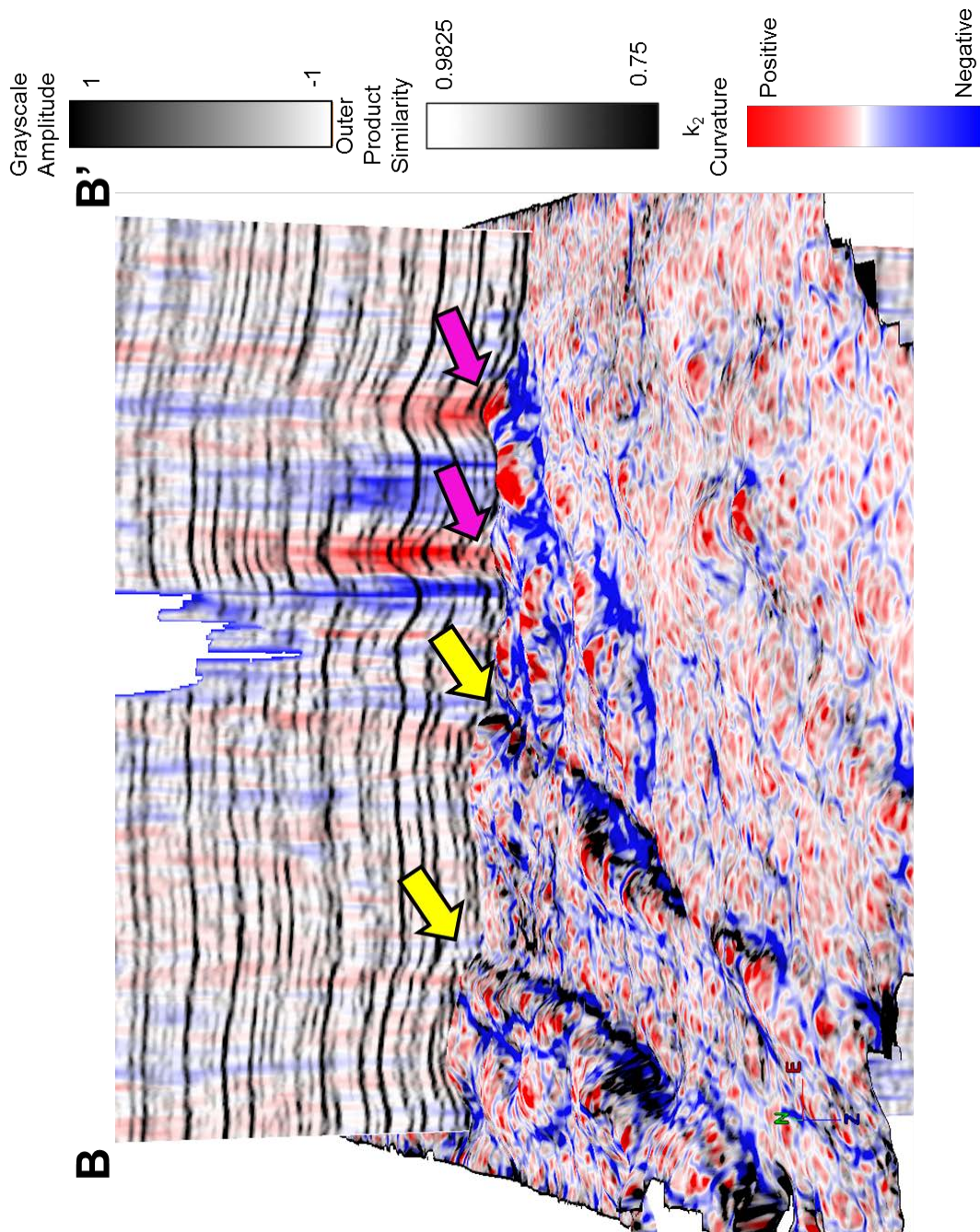


Figure 31. Most negative (k_2) curvature vertical slice co-rendered with amplitude (grayscale) along cross section B-B'. Most negative (k_2) curvature shown co-rendered with outer product similarity extracted on the Mississippi horizon. Faults are indicated by yellow arrows. Magenta arrows indicate either a paleotopographic high, or more likely, structural deformation influenced by the presence of a compressional strike slip fault regime as part of the Nemaha Ridge fault complex.

In an attempt to identify the presence of the tripolitic chert using the seismic data, I employed the use of spectral decomposition. As demonstrated by the geologic mapping of the tripolitic chert, there are variations in the thickness and continuity of the tripolite. Partyka et al. (1999) found spectral decomposition to be very useful in identifying changes in thickness and lateral continuity. Figures 32 and 33 both show examples of the expression of the presence of the tripolitic chert using spectral decomposition. Figure 32 is a horizon extraction at the top Mississippi horizon showing spectral magnitude at 22 Hz. The low magnitude expressed in the far southeast portion of the seismic survey correlates with the thinning tripolite deposition expressed by the isopach thickness geologic map in Figure 15. Figure 33 is a horizon extraction at the top Mississippi horizon showing spectral magnitude at 49 Hz. Again, this shows that the low amplitude expressed in the far southeast portion of the seismic survey correlates back to the isopach thickness geologic map in Figure 15. These figures provide seismic support of the deposition of tripolitic chert to the geologic interpretation generated through the information provided by well logs.

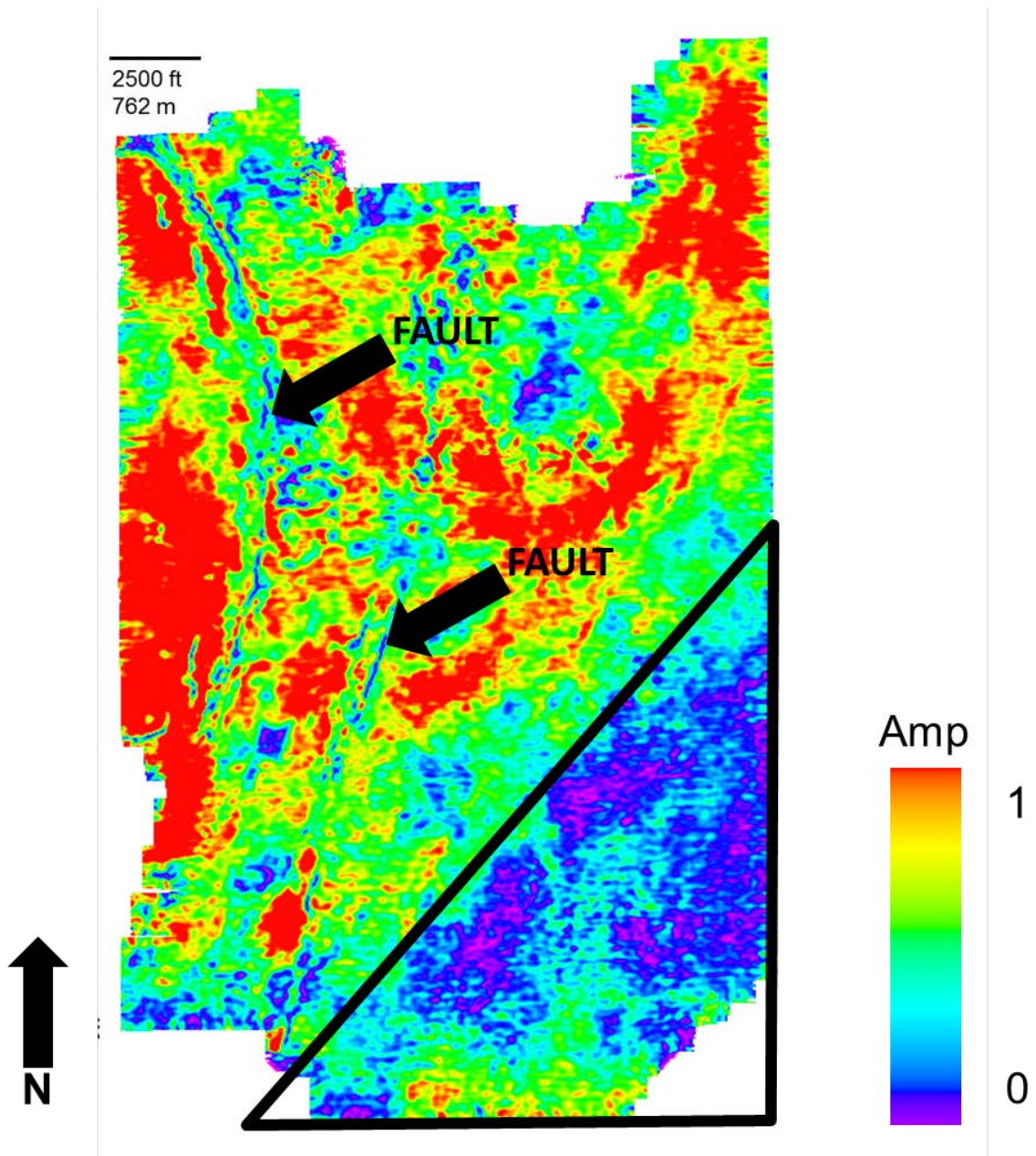


Figure 32. 22 Hz Spectral magnitude component extracted 40 ms below the Mississippi horizon. Low magnitude in the far southeast portion of the seismic survey (shown by black triangle) correlates with thinning tripolite deposition measured by logs in figure 18. Low magnitude also illuminates faulting locations at this frequency, indicated by black arrows.

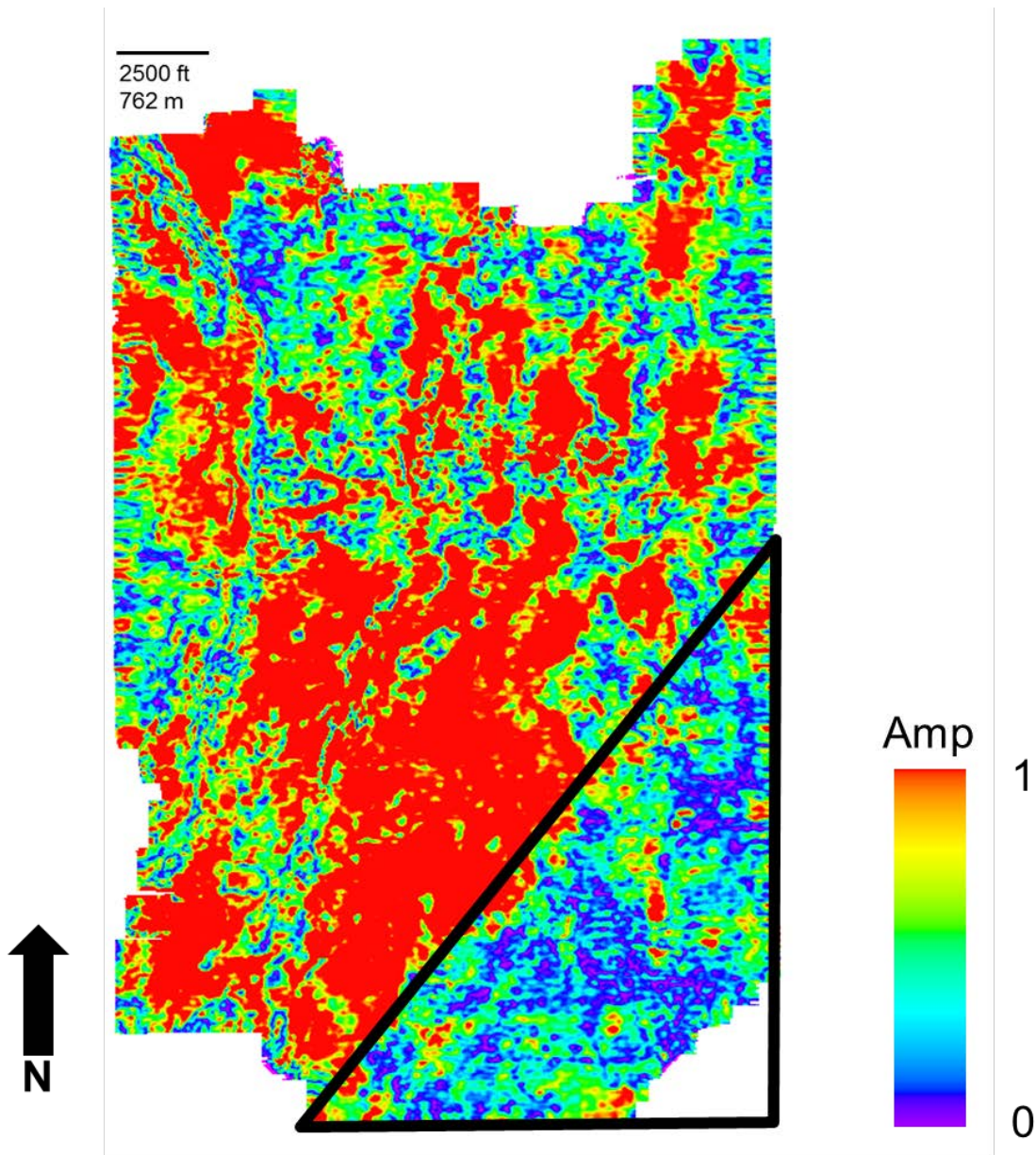


Figure 33. 49 Hz Spectral magnitude component extracted 40 ms below the Mississippi horizon. Low magnitude in the far southeast portion of the seismic survey (shown by black triangle) correlates with thinning tripolite deposition measured by logs in figure 18.

CHAPTER 4

CORRELATION OF PRODUCTION TO SEISMIC MEASUREMENTS

3D seismic data are routinely used as an exploration tool to identify new oil and natural gas fields. 3D seismic data can also aid in the development of a geologic framework. Much has been published about how seismic attributes are used to identify geologic features and correlate these features back to production. It is difficult to tie production of oil and gas back to just a single attribute. There are many factors that can effect production ranging from well completion techniques to reservoir quality to geologic structure. At present, seismic correlation to well completion techniques are limited to estimates of brittleness, geohazards, stress direction, and presence of natural fractures. Seismic data are more commonly correlated to geologic structure and reservoir volume and quality.

I hypothesize that production from the Mississippi Lime in this portion of Kay County, Oklahoma is influenced by and can be correlated to three factors. The first of these factors is the presence of the tripolitic chert facies of the Mississippi Lime. The tripolite is deposited in this area as a result of silica rich limestone being eroded from the up thrown block of the Nemaha Ridge. The deposition and preservation of tripolite in paleotopographic lows is important to existence of reservoir quality rock. Tripolite should appear as a strong negative amplitude reflector and exhibit low impedance values. Secondly, production from the Mississippi Lime in this area should be enhanced by the presence of natural fractures. Natural fractures will appear as discontinuities, folds, faults, and

flexures. Natural fractures enhance the permeability of the rock. These fractures are best identified by features that possess most positive (k_1) curvature characteristics, but can sometimes be identified by low values of most negative (k_2) curvature. Lastly, production from the Mississippi Lime is influenced by structural highs. Structural highs provide a trapping mechanism for oil and natural gas. Because oil and natural gas is more buoyant than water, they will accumulate in these structural highs, making them desirable targets for producing from the Mississippi Lime.

CORRELATION OF GEOLOGIC STRUCTURE TO PRODUCTION

Geologic structure serves as one of the primary trapping mechanisms for oil and natural gas in rocks, and is correlated to production of oil and natural gas from the Mississippi Lime within the limits of this 3D seismic survey. Evidence for this is provided by plotting production bubbles on corresponding structural attributes including dip magnitude, most positive (k_1) curvature, most negative (k_2) curvature, and time structure. Figure 34 shows oil production plotted on dip magnitude extracted 40 ms below the top Mississippian horizon. Note, production from the Mississippi Lime occurs in conjunction with localized structural highs, as well as along or in very near proximity to the 2 large faults that have been previously discussed. Production along or in near proximity to these faults is likely enhanced by increased fracturing of the rock along these faults. The localized structural highs create a small structural trap for oil and natural gas, making these features more productive. Figure 35 is a time structure map of the Mississippi Lime with oil production bubble plotted on it.

Again, oil production is observed on localized structural highs and along or in very near proximity to the 2 large faults.

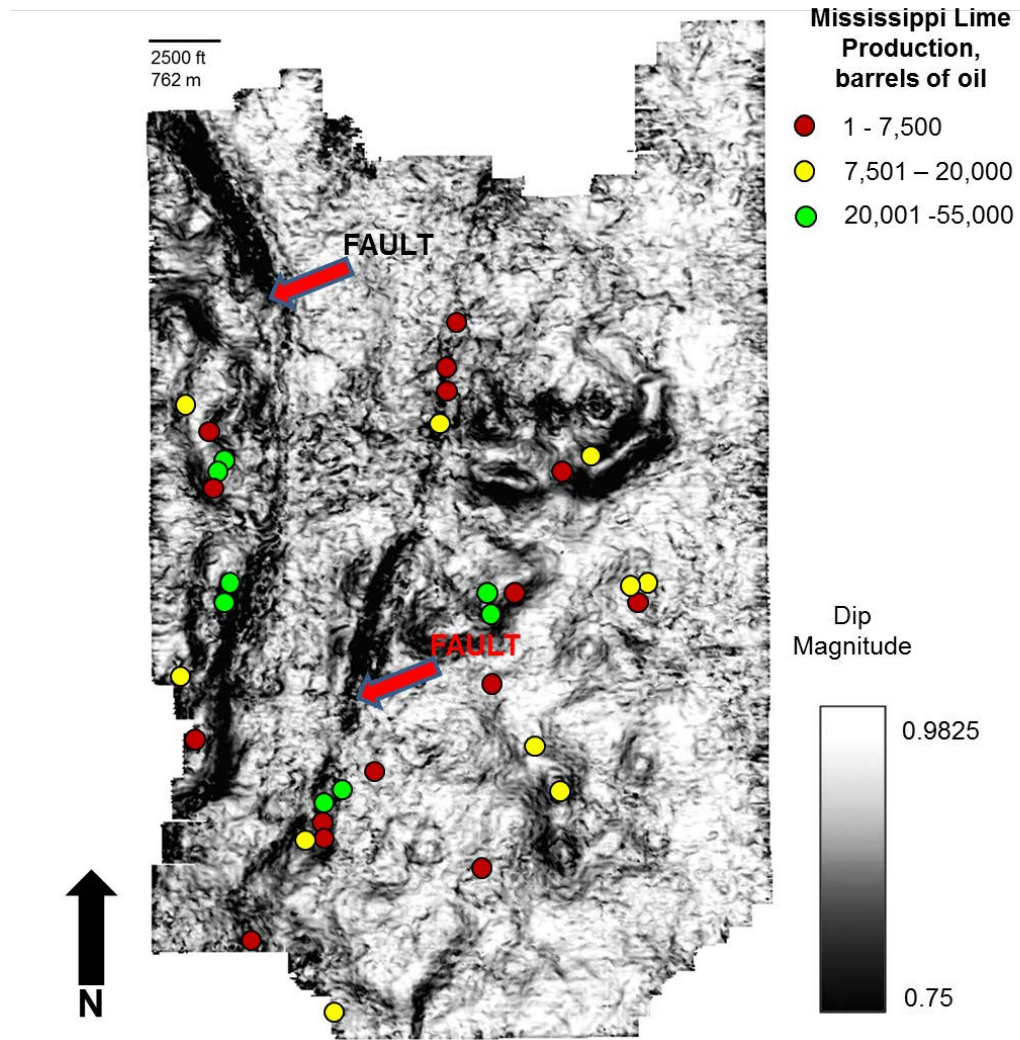


Figure 34. Dip Magnitude covering the seismic data survey. Cumulative oil production from Mississippi Lime indicated by red, yellow, and green circles. Magnitude of production indicated in legend.

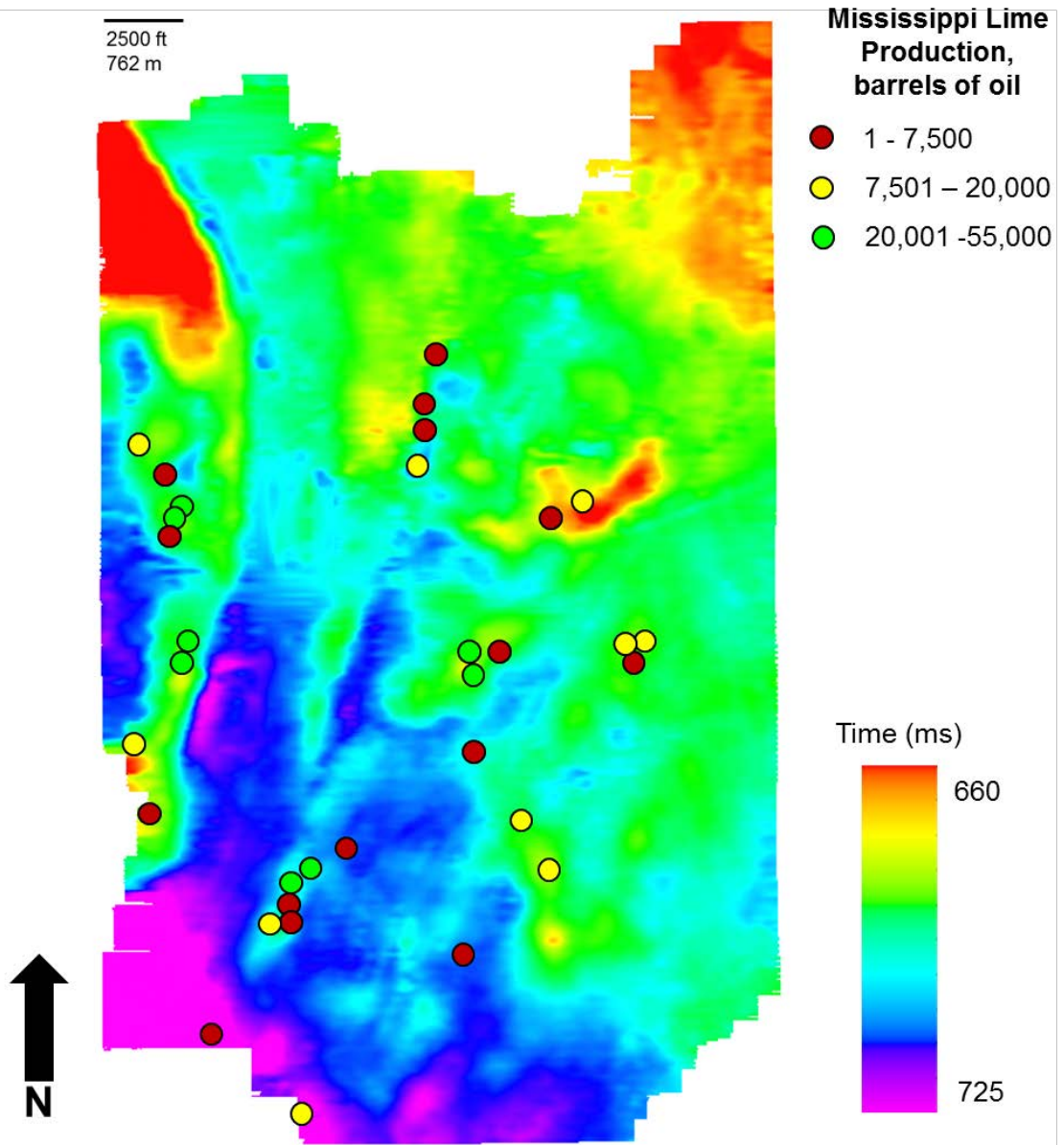


Figure 35. Mississippi time structure map with cumulative oil production from the Mississippi Lime. Cumulative oil production from Mississippi Lime indicated by red, yellow, and green circles. Magnitude of production indicated in legend.

Figures 36 and 37 show most positive (k_1) and most negative (k_2) curvature, respectively, extracted 40 ms below the top Mississippi horizon with oil production bubbles plotted at the wellbore locations. In Figure 36, there is a strong relationship between production and structural ridges. These areas have undergone greater flexure which would cause more natural fracturing within the rock formation. This natural fracturing creates better permeability, which would in theory provide better production of water and oil. Figure 37 does not show any correlation of production with most negative curvature. This is further evidence to support that production from the Mississippi Lime in this area is highly influenced by structure, especially structural highs and structural lineaments such as the large faults found within the survey.

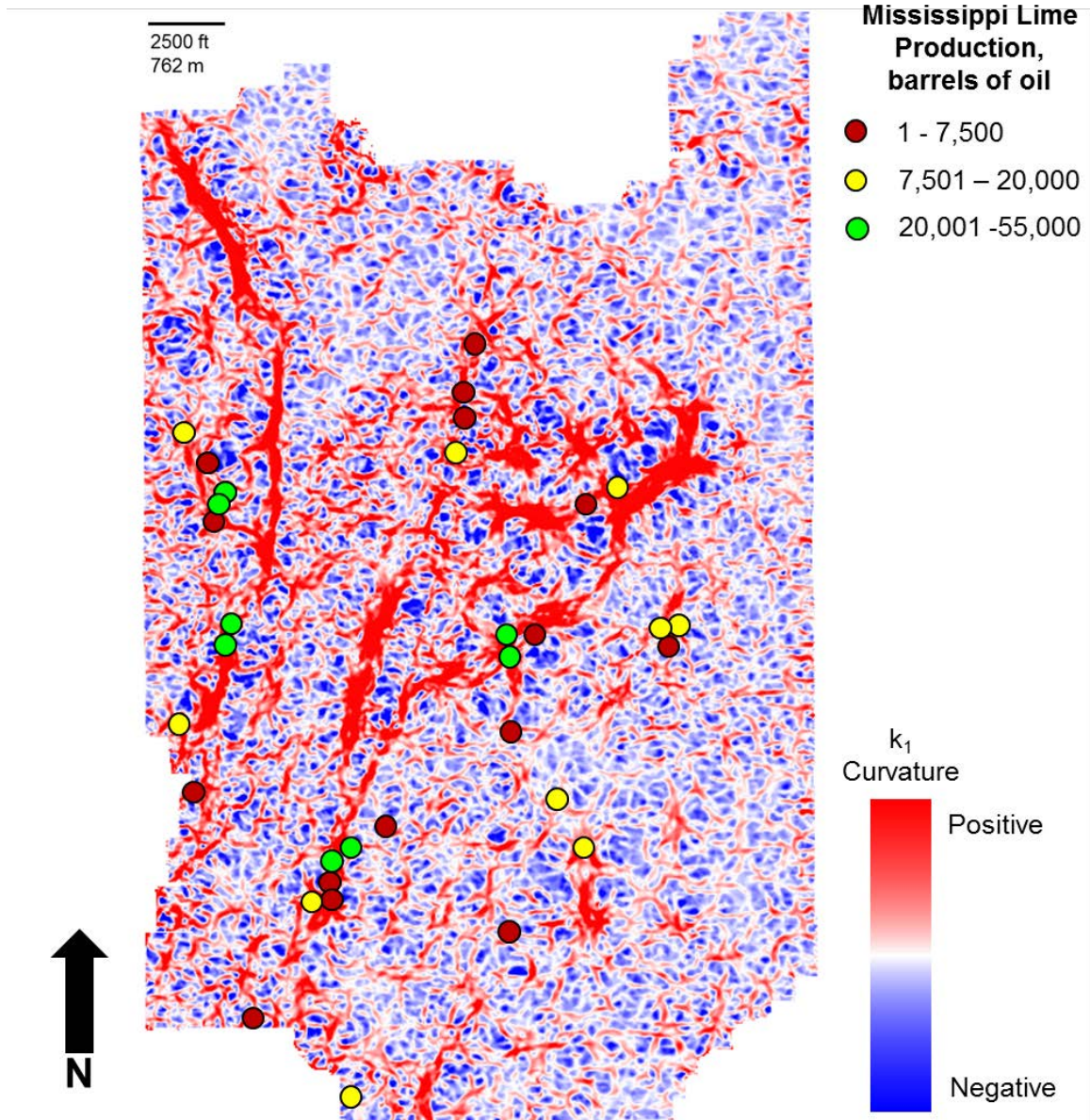


Figure 36. Most positive (k_1) curvature with cumulative oil production from the Mississippi Lime. Cumulative oil production from Mississippi Lime indicated by red, yellow, and green circles. Magnitude of production indicated in legend.

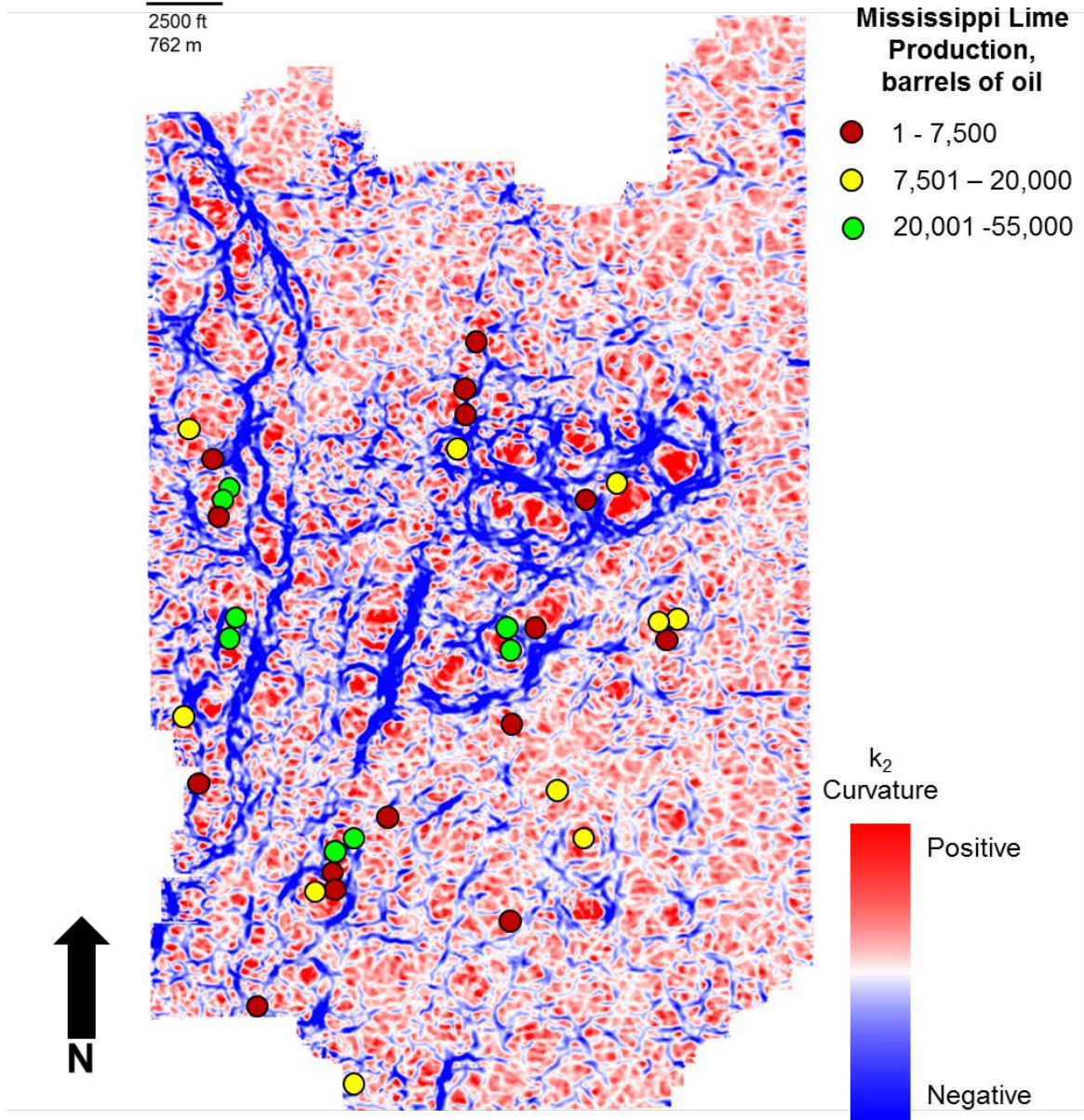


Figure 37. Most negative (k_2) curvature with cumulative oil production from the Mississippi Lime. Cumulative oil production from Mississippi Lime indicated by red, yellow, and green circles. Magnitude of production indicated in legend.

CORRELATION OF POST-STACK ACOUSTIC IMPEDANCE INVERSION ATTRIBUTES TO PRODUCTION

Seismic inversion removes the effect of the seismic wavelet and better approximates the impedance of the reservoir. Post-stack seismic amplitude inversion, and post-stack seismic attribute analysis and modeling, are frequently employed to perform quantitative prediction of reservoir properties from surface seismic data (Wagner et al. 2012). When observing a seismic volume in terms of amplitude, one observes the contrast in impedance between two adjacent layers of rocks. Post-stack impedance inverse “unravels” these changes. With the elimination of the wavelet post stack impedance better represents the rock matrix, porosity, and fluid fill.

It is important to verify that the same acoustic impedance values observed at well bores tie with the values from the seismic survey. Acoustic impedance logs are created by converting sonic P-wave values to velocity values and multiplying the velocity values and bulk density logs together to gain acoustic impedance values within the well bore. Once the acoustic impedance values are determined, a comparison of the acoustic impedance values is made to reservoir characteristics observed by other logging tools such as PE and gamma ray. This comparison of acoustic impedance to well logs provides the template between lithology and surface seismic measurements. Figure 38 shows a cross plot of density porosity with acoustic impedance from a well located within the 3D seismic survey. This cross plot indicates zones of high porosity exhibit lower acoustic impedance. Figure 39 shows the same cross plot with one population of

the values within the cross plot isolated. The accompanying well log shows that this population of low acoustic impedance and high density porosity corresponds to the tripolitic chert member of the Mississippi lime found in this study area. Figure 40 Shows a cross plot of PE values with acoustic impedance and density porosity from another well located within the 3D seismic survey. This cross plot shows that low values of the PE log correlate with high density porosity values and low values of acoustic impedance. Figure 41 shows this same cross plot with a population within the cross plot isolated. The corresponding well log shows that this isolated population makes up the values found within the tripolitic chert member of the Mississippi Lime. Figures 38-41 exemplify the methods used to tie acoustic impedance to known geologic characteristics from within well bores found in the limits of this seismic survey. This is also important because these figures demonstrate that reservoir characteristics of the Mississippi Lime are capable of being correlated to the post-stack acoustic impedance data.

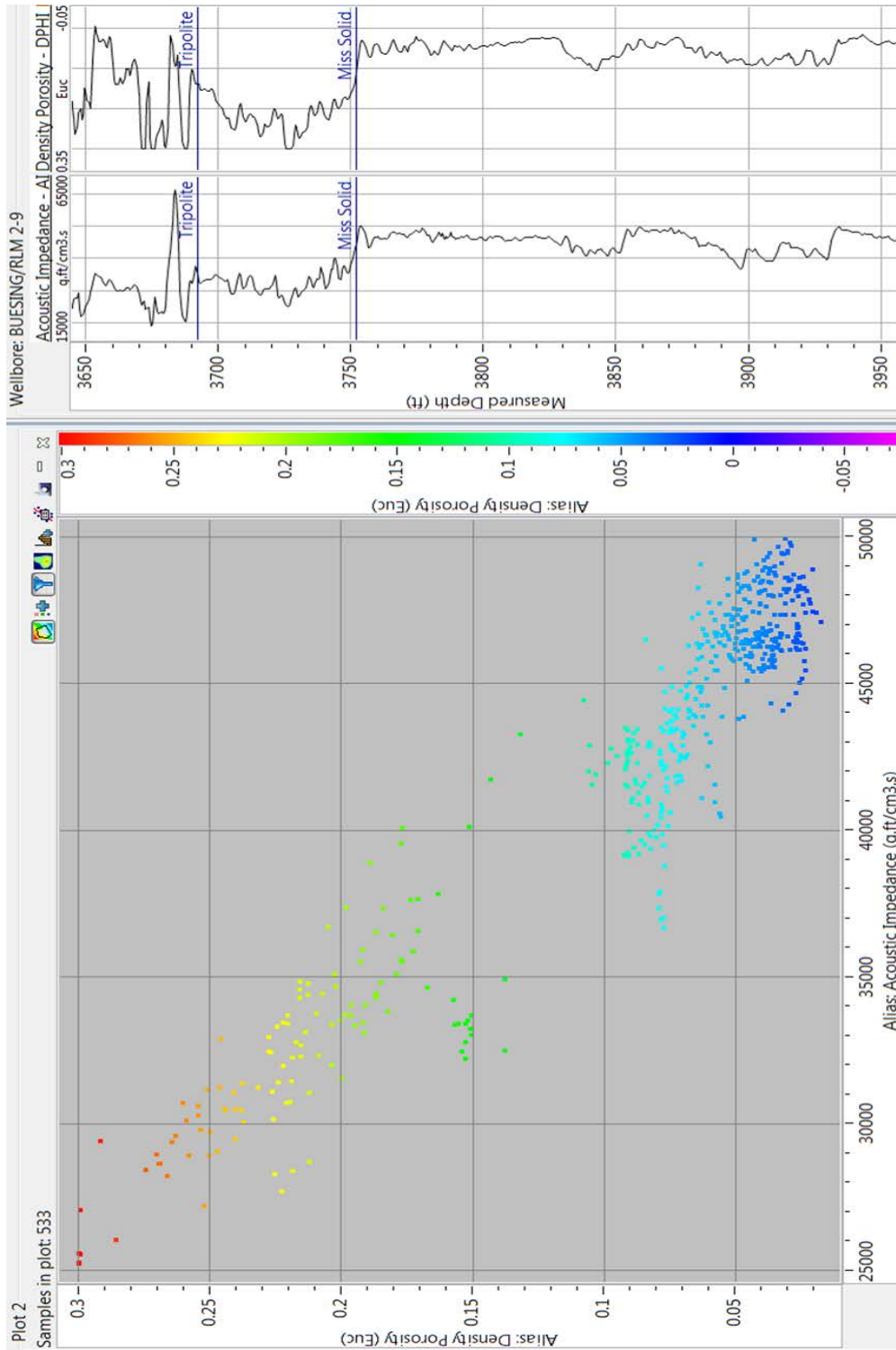


Figure 38. Post-stack acoustic impedance plotted against density porosity colored by density porosity for the zone 3650-3950 ft shown on the logs at right. Higher density porosity correlates to lower acoustic impedance.

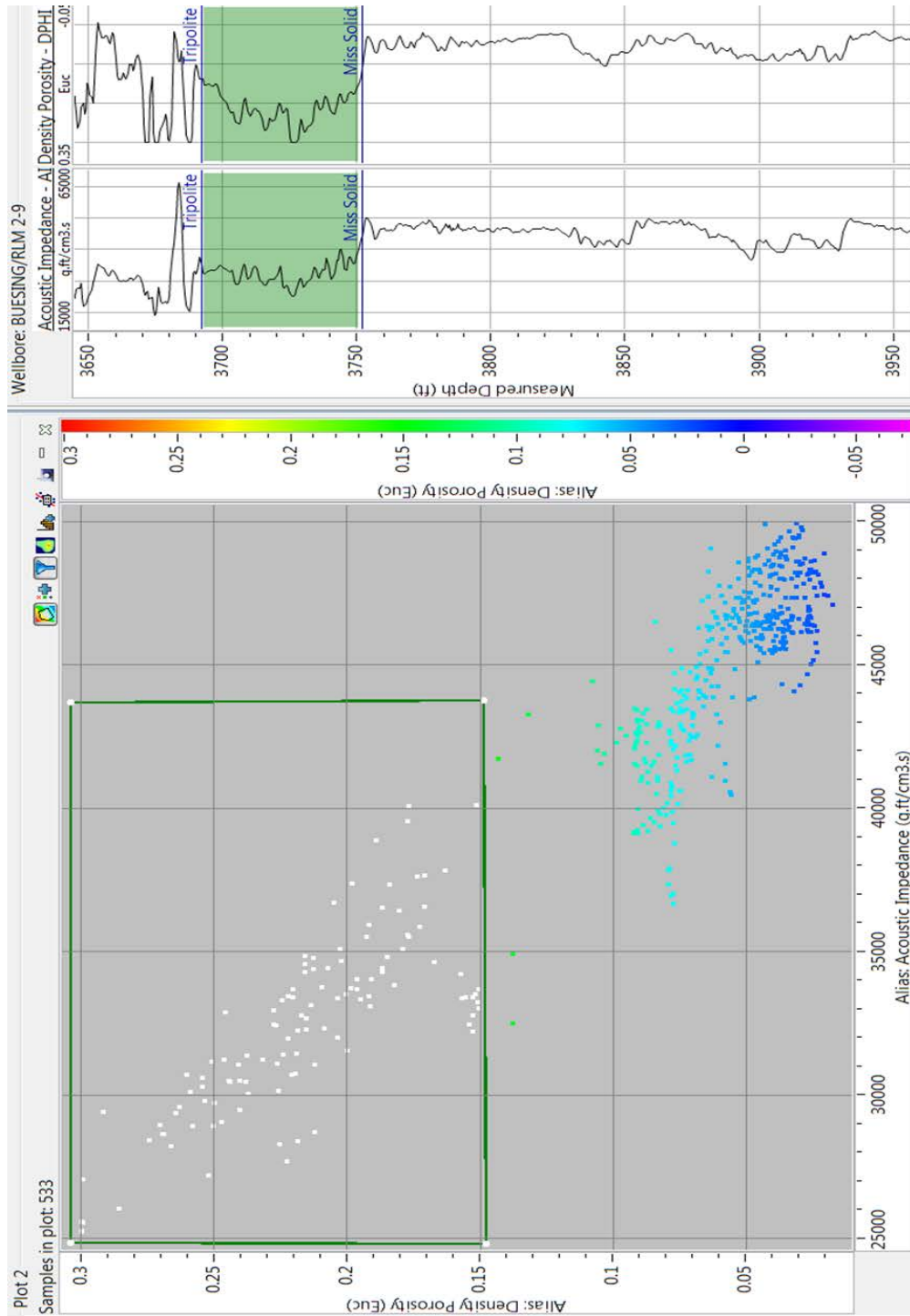


Figure 39. Post-stack acoustic impedance plotted against density porosity colored by density porosity for the zone 3650-3950 ft shown on the logs at right. Higher density porosity correlates to lower acoustic impedance. Isolated data population corresponding to highlighted tripolite as shown in the well logs appears as white in crossplot.

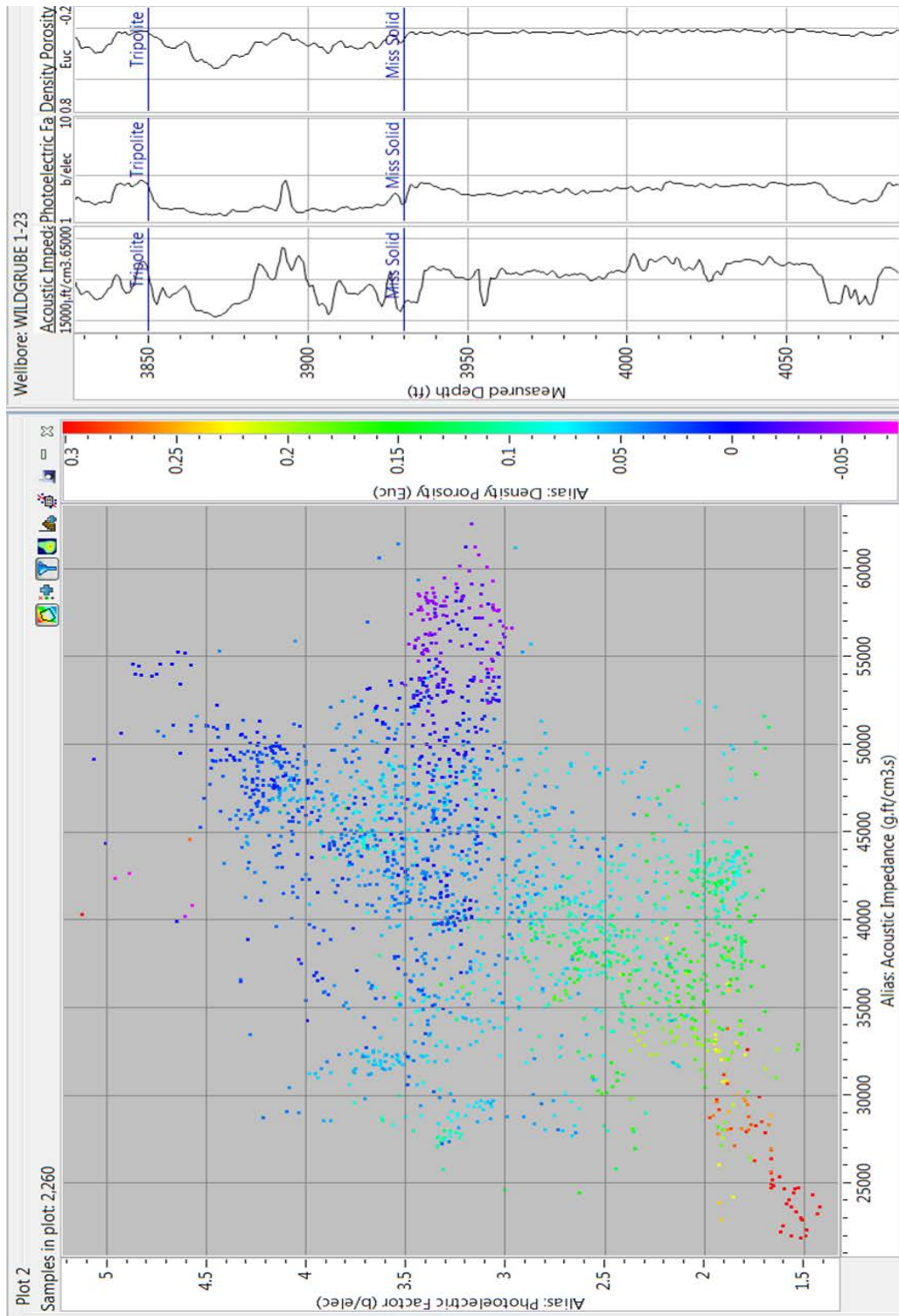


Figure 40. Post-stack acoustic impedance plotted against photoelectric factor colored by density porosity for the zone 3850-4050 ft shown on the well logs at the right.

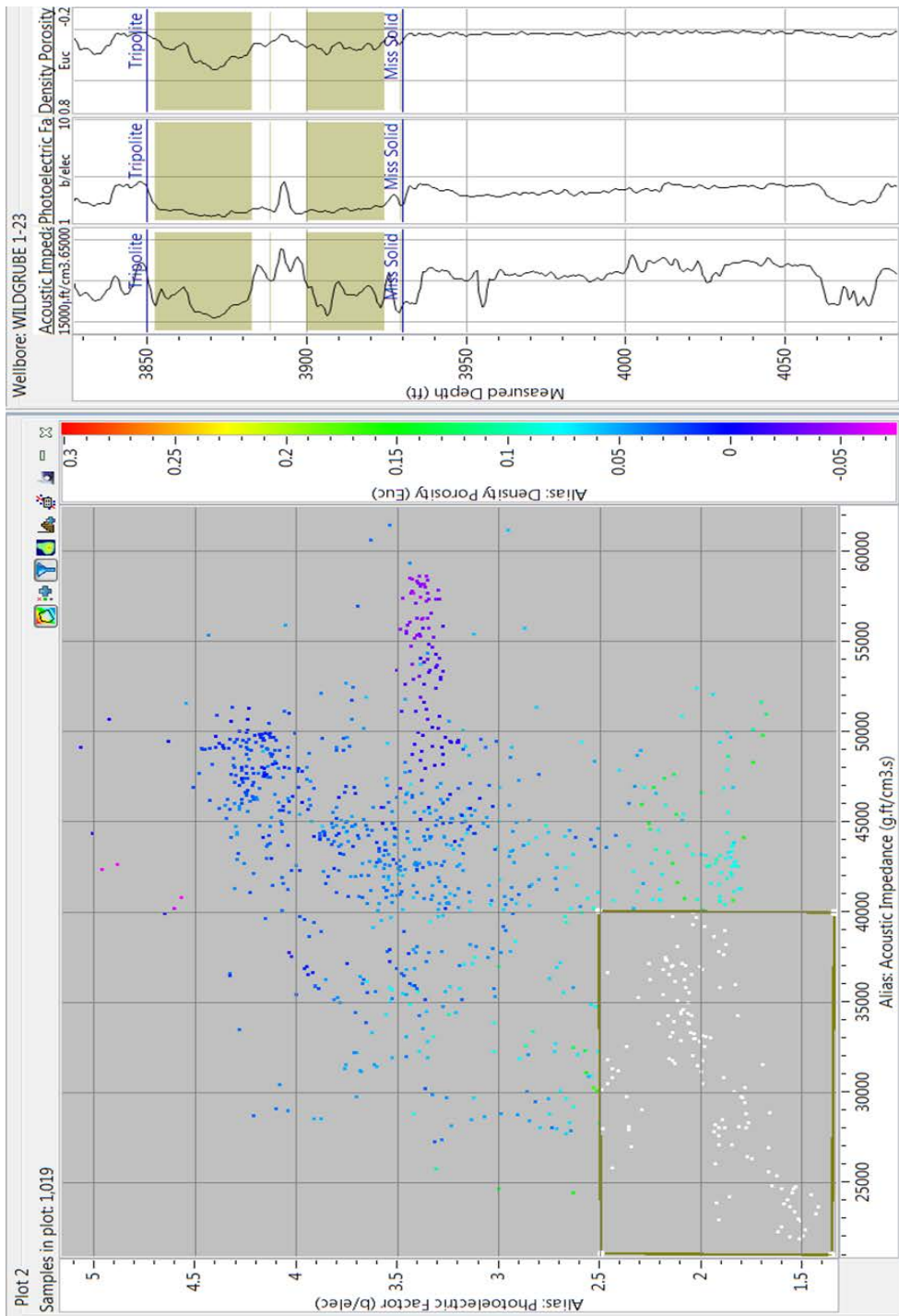


Figure 41. Post-stack acoustic impedance plotted against photoelectric factor colored by density porosity for the zone 3850-4050 ft shown on the well logs at the right. Logs show that photoelectric factor can be an effective lithology discriminator with respect to acoustic impedance. Isolated data population corresponding to highlighted tripolite as shown in the well logs appears as white in crossplot.

It is also important to consider, in a visual sense, what the seismic data is representing at the well bore. This is important for two reasons. First, it is a good way to quality control the data to make sure the data volume is representing the same thing you are observing at the well log level. Secondly, this allows an interpreter the ability to extrapolate through the data both positive and negative characteristics. Figure 42 is an example of the visual representation of the post-stack acoustic impedance co-rendered with grayscale amplitude at one of the well bores found within the survey limits. This image shows the well bore as it penetrates through the Mississippi Lime. The wellbore is in the shape of the corresponding calculated acoustic impedance from well logs. The Mississippi horizon is also delineated as a gray line. You can see from this image that there is a strong visual correlation from the low impedance values calculated from the well logs for the tripolite at the well bore, and the low acoustic impedance values calculated in the post-stack seismic data set. This particular well produced about 25,000 barrels of oil from the tripolitic chert member of the Mississippi Lime. With this in mind, a correlation can be drawn between the oil production from the tripolite and post-stack acoustic impedance. Lower values of acoustic impedance can be associated with higher values of oil production from the tripolitic chert member of the Mississippi Lime. Figure 43 demonstrates this relationship across the 3D seismic survey. This shows the surface of the post-stack acoustic impedance extracted 40 ms below the Mississippi horizon. The well bores from the Mississippi tested wells are shown as the black lines, while the cumulative production from the Mississippian is exhibited in relative terms as

the green production bubble posted on top of the well bores. The size of the production bubble is relative to the amount of oil production from the Mississippi. Most of the Mississippi productive wells intersect this Mississippi surface in places with lower acoustic impedance values. Figures 44-46 also show phantom horizon slices of post-stack acoustic impedance from the Mississippi Lime horizon extracted at 20 ms intervals with production values plotted at the wellbore. Production magnitudes are coded by color in the legends. Figure 44 is extracted 0-20 ms below the Mississippi horizon, Figure 45 is extracted 20-40 ms below the Mississippi horizon, and Figure 46 is extracted 40-60 ms below the Mississippi horizon. In observing these figures, you can clearly see that the majority of the production correlates with values of low impedance, even moving down in time throughout the Mississippi section. Figure 47 provides a statistical representation of this relationship. This is a cross plot of cumulative oil production with RMS post-stack acoustic impedance extracted at the Mississippi horizon and 50 ms below. While the statistical correlation between the two is not the best, having an R squared value of 0.0664, you can clearly see in the cross plot that the higher values of production come from moderate to lower values of post-stack acoustic impedance.

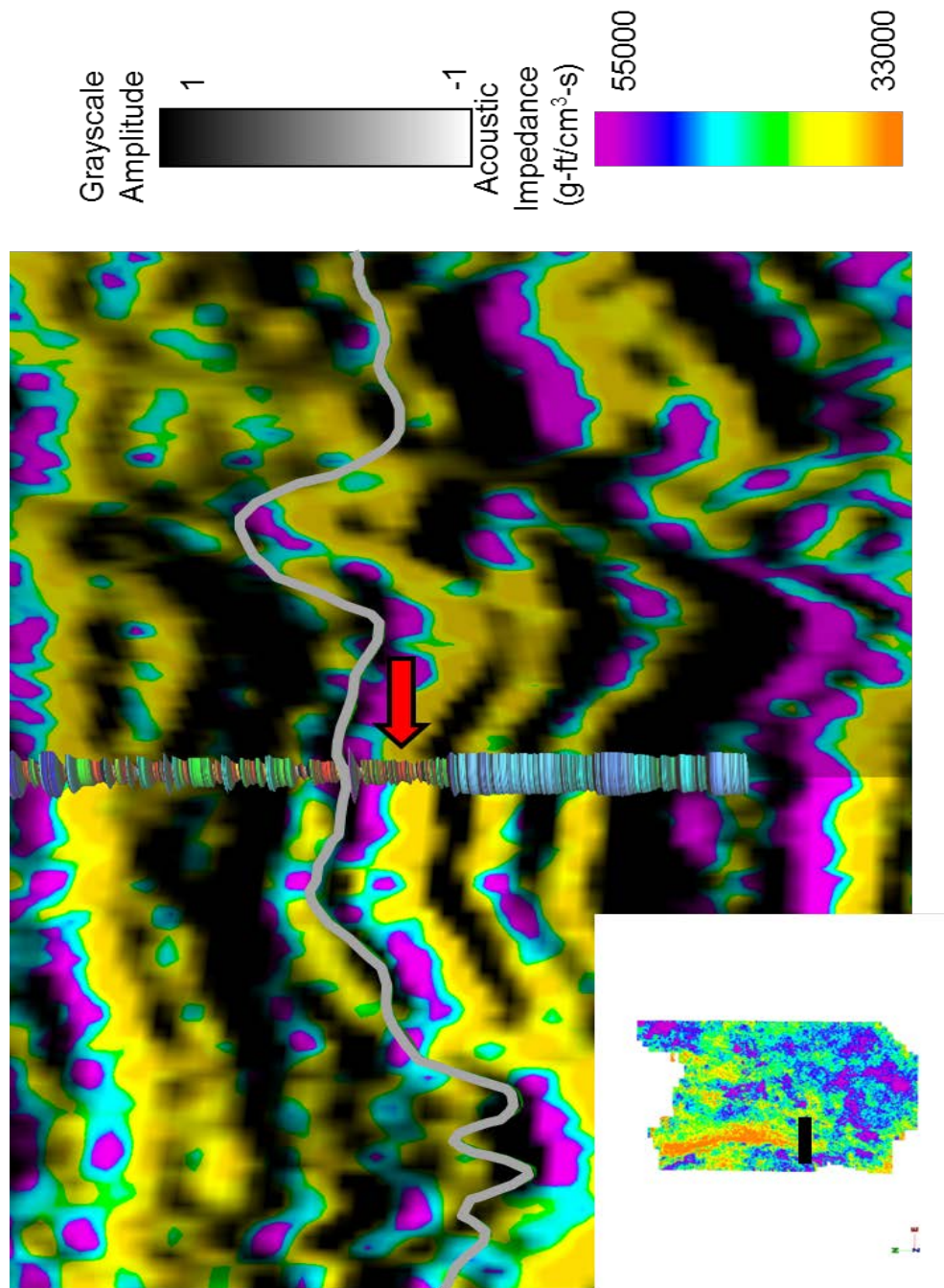


Figure 42. Well tie with post-stack acoustic impedance at the Mississippi horizon. Light gray line indicates the Mississippi Horizon. Red arrow points to low acoustic impedance values characteristic of production from the Mississippi Lime and tripolitic chert. Radial log at the well bore is calculated acoustic impedance from logs. Radial AI log displays low acoustic impedance values in correlation with the seismic data. Inset map shows location of seismic section with black line.

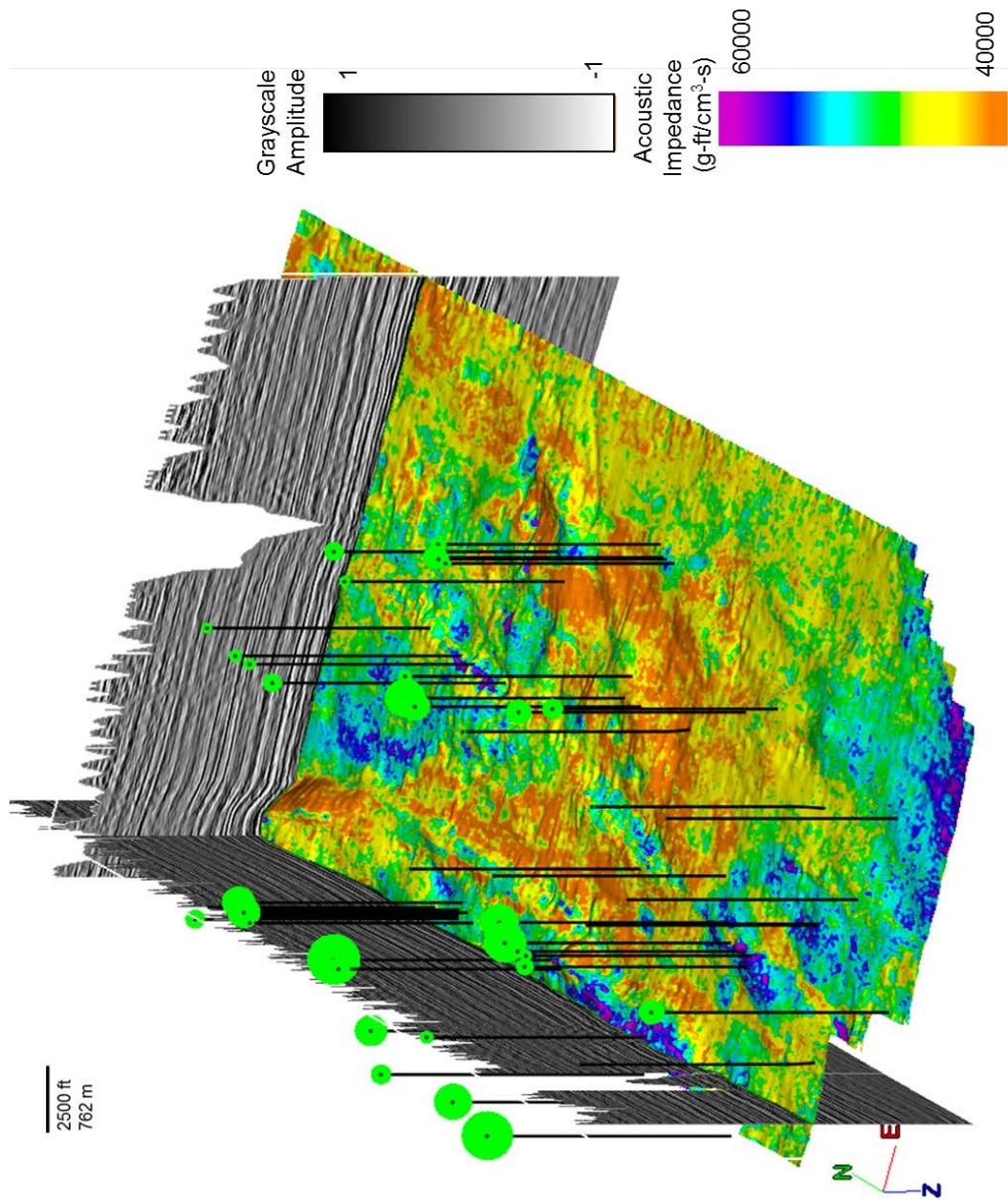


Figure 43. Post-Stack impedance along Mississippi horizon shown with well bores and cumulative oil production from the Mississippi Lime posted as green circles at the top of the well bore. Amplitude (grayscale) shown in cross-line and inline. Magnitude of oil production is directly related to the size of the circle.

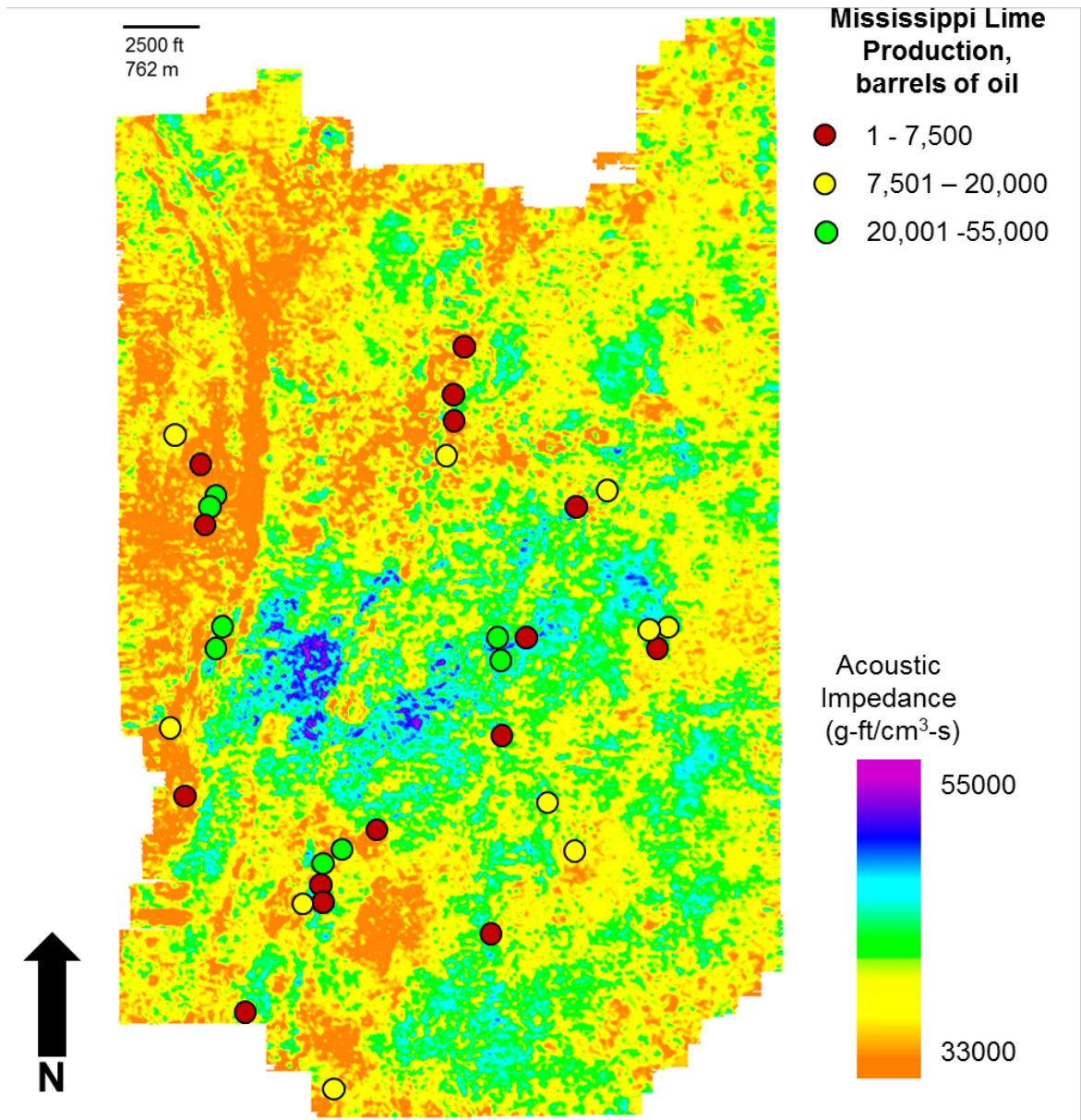


Figure 44. Phantom horizon slice 0-20 ms below the top Mississippi horizon through post-stack acoustic impedance volume. Cumulative oil production from Mississippi Lime indicated by red, yellow, and green circles. Magnitude of production indicated in legend.

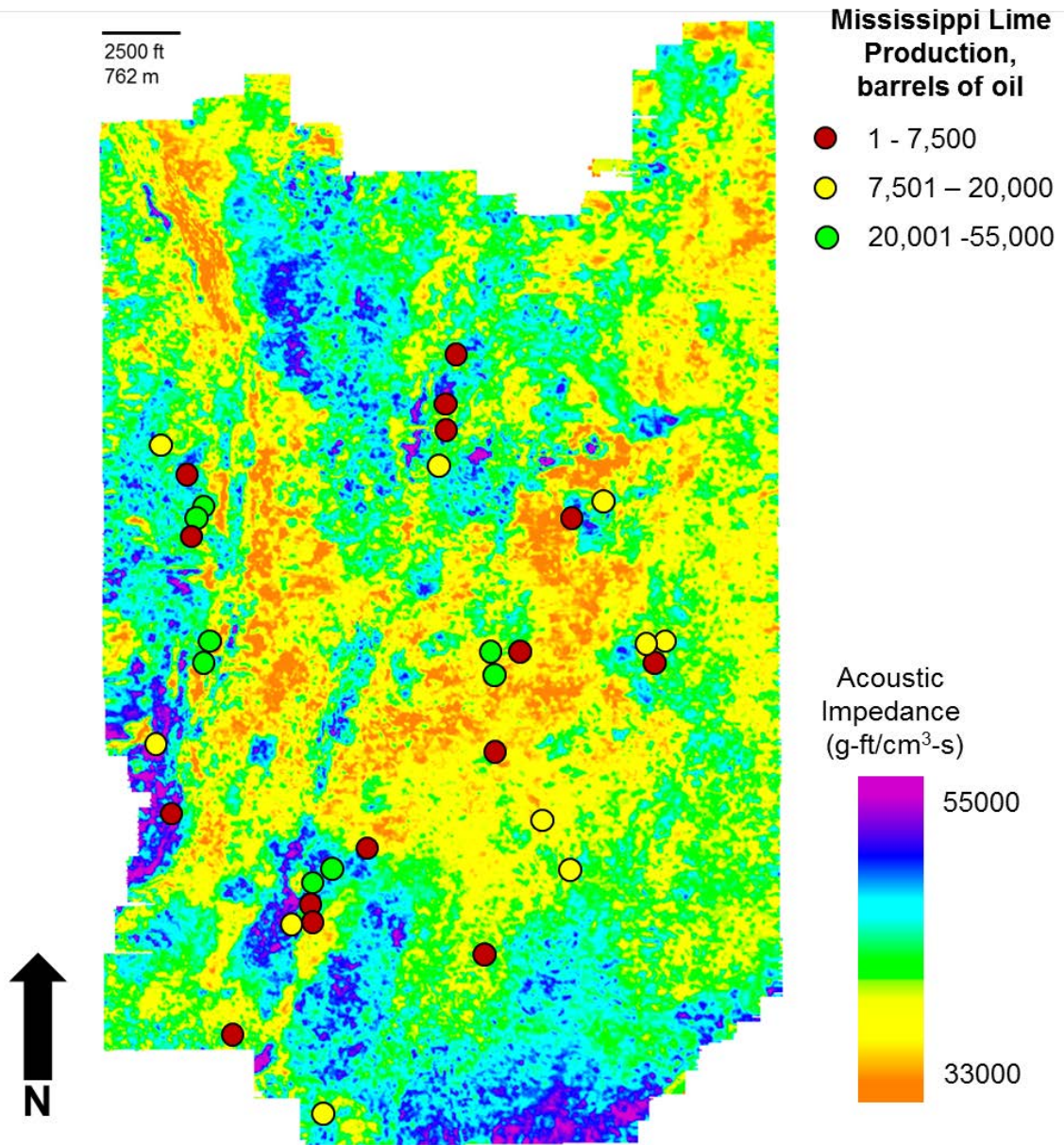


Figure 45. Phantom horizon slice 20-40 ms below the top Mississippi horizon through post-stack acoustic impedance volume. Cumulative oil production from Mississippi Lime indicated by red, yellow, and green circles. Magnitude of production indicated in legend.

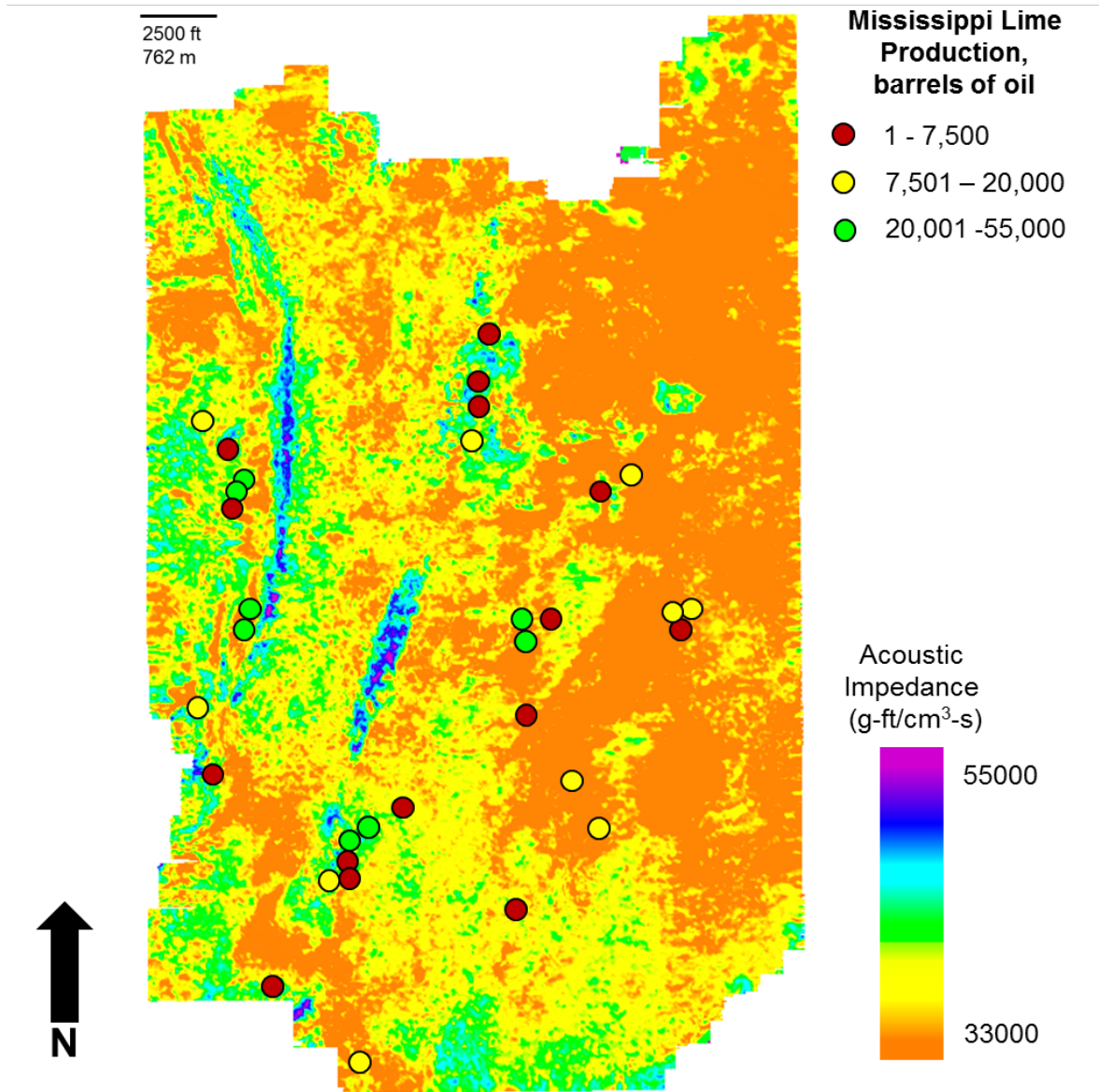


Figure 46. Phantom horizon slice 40-60 ms below the top Mississippi horizon through post-stack acoustic impedance volume. Cumulative oil production from Mississippi Lime indicated by red, yellow, and green circles. Magnitude of production indicated in legend.

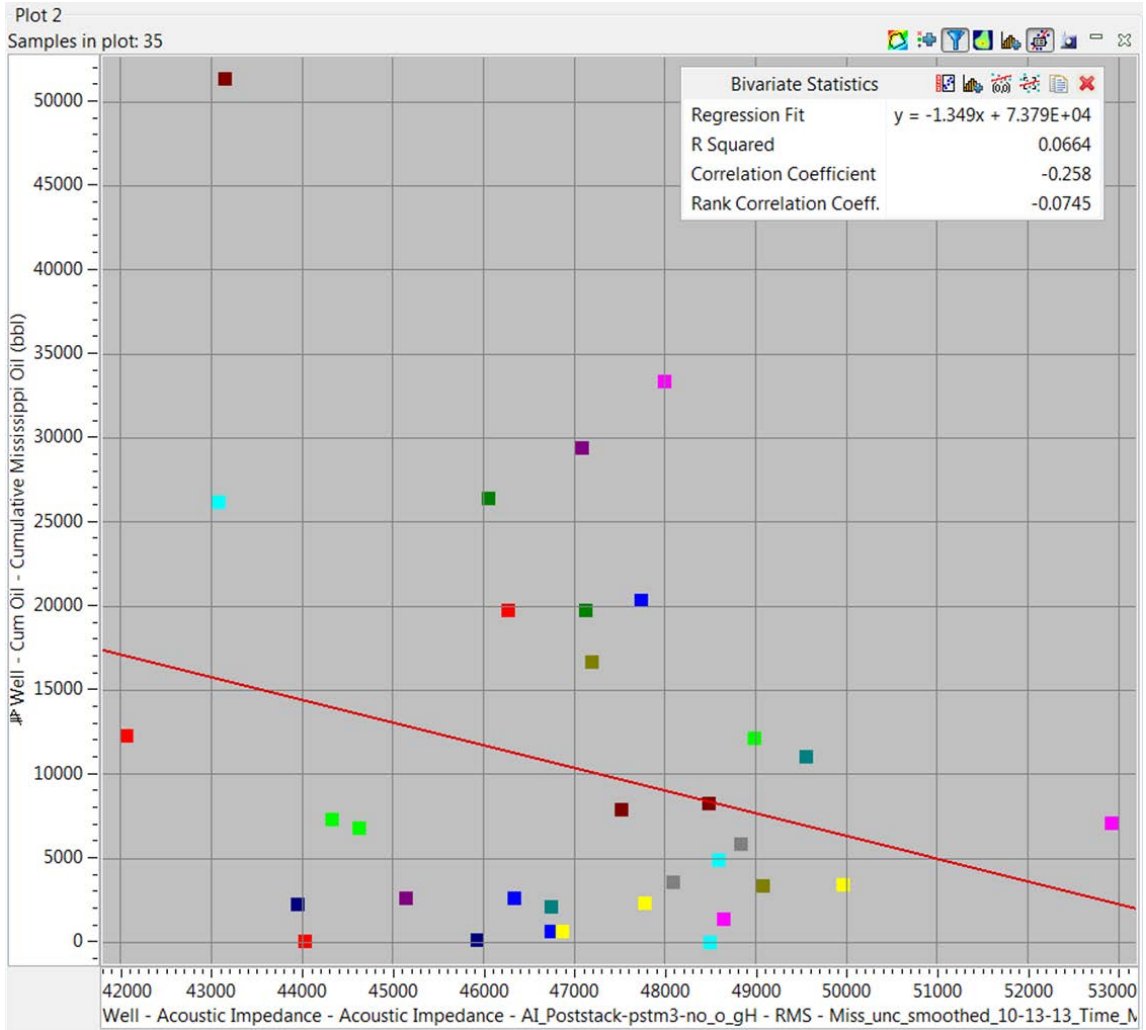


Figure 47. RMS post stack acoustic impedance extracted on the Mississippi horizon and 50 ms below, extracted from the horizon to the well location plotted against cumulative oil production from the Mississippi Lime.

CORRELATION OF PRE-STACK ACOUSTIC IMPEDANCE INVERSION ATTRIBUTES TO PRODUCTION

While having a post-stack acoustic inversion model is helpful in attempting to predict reservoir properties and production, pre-stack inversion models can offer more insight into the reservoir characteristics that may be contributors to production. The goal of pre-stack acoustic impedance is to use seismic gathers to obtain reliable estimates of P-wave velocity, S-wave velocity, and density to predict fluid and lithologic properties of the Earth (Hampson and Russel, 2005). This description of pre-stack acoustic impedance by Hampson and Russel sounds similar to the objective of performing post-stack acoustic impedance analysis, however the introduction of shear wave velocity data allows for further reservoir characteristics to be considered. Shear wave velocity data allows the interpreter to consider Lamé's parameters as they relate to rock properties observed through 3D seismic data. Dowdell 2012 uses lambda and mu Lamé parameters to parameterize elasticity. The first parameter, lambda, is often called the incompressibility and is sensitive to pore pressure. The second parameter, mu, is often called the rigidity of the rock and is unaffected by any present fluids as shear stress is not supported by fluids or gasses. P-Impedance, Z_P , is the product of density and p-wave velocity, while S-Impedance, Z_S , is the product of density and s-wave velocity. While both Z_P and Z_S are sensitive to changes within lithology, Z_S is not sensitive to changes in pore fluid. Because Z_S is not sensitive to pore fluid, it is often used as a lithology discriminator. Goodway et al. (1997) computes lambda and mu from Z_P and Z_S ,

extracted from well logs and pre-stack seismic data. For moderate offset data we can obtain good estimates of lambda-rho and mu-rho, but not of density (rho). These attributes allow us to better extract rock properties from 3D seismic data using elastic parameters directly linked to the rock's bulk and shear moduli (Goodway et al. 1997). The lambda-rho and mu-rho attributes are commonly used together to define brittleness of shale resource plays. At present, little microseismic has been published for Mississippi Lime Plays.

In order to observe the elastic impedance properties provided by pre-stack acoustic impedance volumes, you must begin in the same fashion as you would when observing post-stack impedance inversion attribute, at the well log level. The one critical difference between modeling pre-stack and post-stack acoustic impedance volumes is the introduction of shear wave sonic data to the pre-stack impedance volumes. One of the issues encountered in this particular evaluation of the Mississippi Lime is that while there is a plethora of compressional sonic data within the limits of the subject 3D seismic data volume, there is not a single piece of shear wave sonic data available within the limits of the survey. In order to remedy this short coming of the evaluation, well data from a borehole in near proximity to the seismic survey that contains shear wave sonic data is incorporated into the evaluation. While this is not the ideal protocol for performing an evaluation of pre-stack seismic attributes, the shear wave sonic well log that was selected to be incorporated exhibits many of the same rock characteristics that the Mississippi Lime possesses when observed within the limits of the seismic survey. With this in mind, the evaluation of the pre-stack

acoustic impedance attribute volumes of the subject seismic data set should be a close approximation to the expected result of the same evaluation that would be performed if shear wave sonic well log data existed within the limits of the 3D seismic survey.

Figure 48 shows acoustic impedance cross plotted by shear impedance and colored by density. The characteristics highlighted in the well logs are low acoustic impedance and low shear impedance. This shows that seismic inversion by itself cannot differentiate all porosity zones from each other. The inversion data will be able to get you 'in the ballpark' of identifying desired lithologies and porosities, but you must know something about the rock type in order to fully capture the desirable rock properties related to production. Figure 49 shows acoustic impedance cross plotted with density porosity colored by PE. This relationship shows that as density porosity increases, acoustic impedance decreases. It also shows that PE is a good indicator of the high density porosity tripolite. The relationship between acoustic impedance and density porosity shown in Figure 49 is the same relationship observed in the post-stack acoustic impedance. Even though this well log that contains shear wave sonic data is located in near proximity to, but outside of the subject seismic survey, the fact that the same relationship exists in the pre-stack acoustic impedance data with this foreign sonic log that exists in the post-stack acoustic impedance data with local sonic log data, validates the creation of the pre-stack acoustic impedance data with a log that contains like characteristics of well logs in the limits of the seismic survey, but does not fall within the limits of the survey itself. Figure 50

shows lambda-rho cross plotted with acoustic impedance and colored by density porosity. The tripolite is characterized by low lambda-rho values and low acoustic impedance values. The low lambda-rho values suggest a low fluid incompressibility, while the low values of acoustic impedance suggest the possibility of fluid filled porosity. This relationship is further validated because of the known high water production that is associated with well completions in the tripolite. Figure 51 shows mu-rho cross plotted with lambda-rho colored by density porosity. This relationship shows that the high porosity tripolite is characterized by both low mu-rho values and low lambda-rho values. The low lambda-rho values again suggest low fluid incompressibility while the low mu-rho values suggest low rigidity. Mu-rho values would likely be high in relation to shale characterization, so the mu-rho data is likely a good indicator of lithology as well as rigidity.

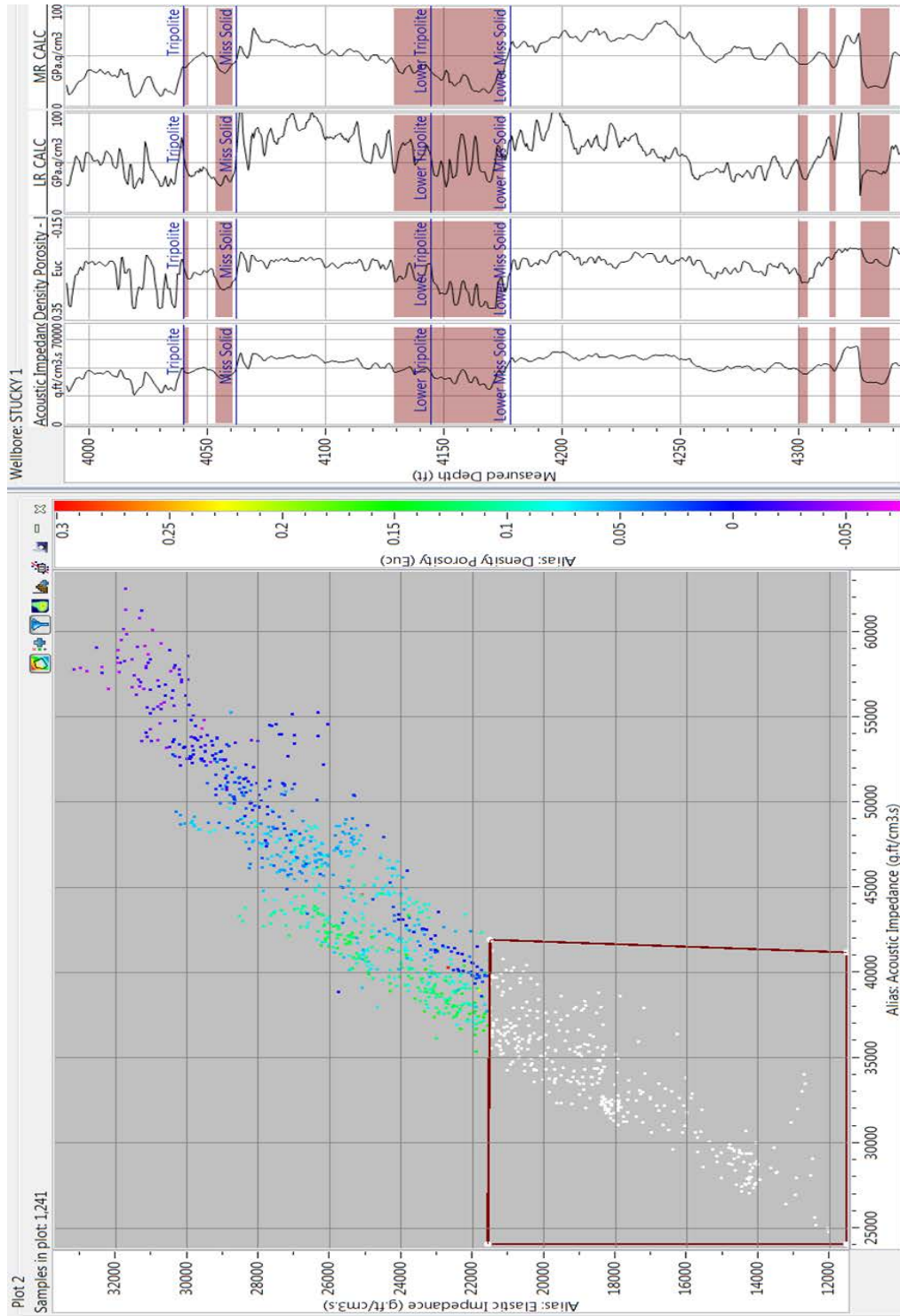


Figure 48. Acoustic impedance plotted against shear impedance colored by density porosity for the zone 4020-4350 ft shown on the well logs at the right. Data from shear sonic well log data in neighboring Sumner County, Ks.

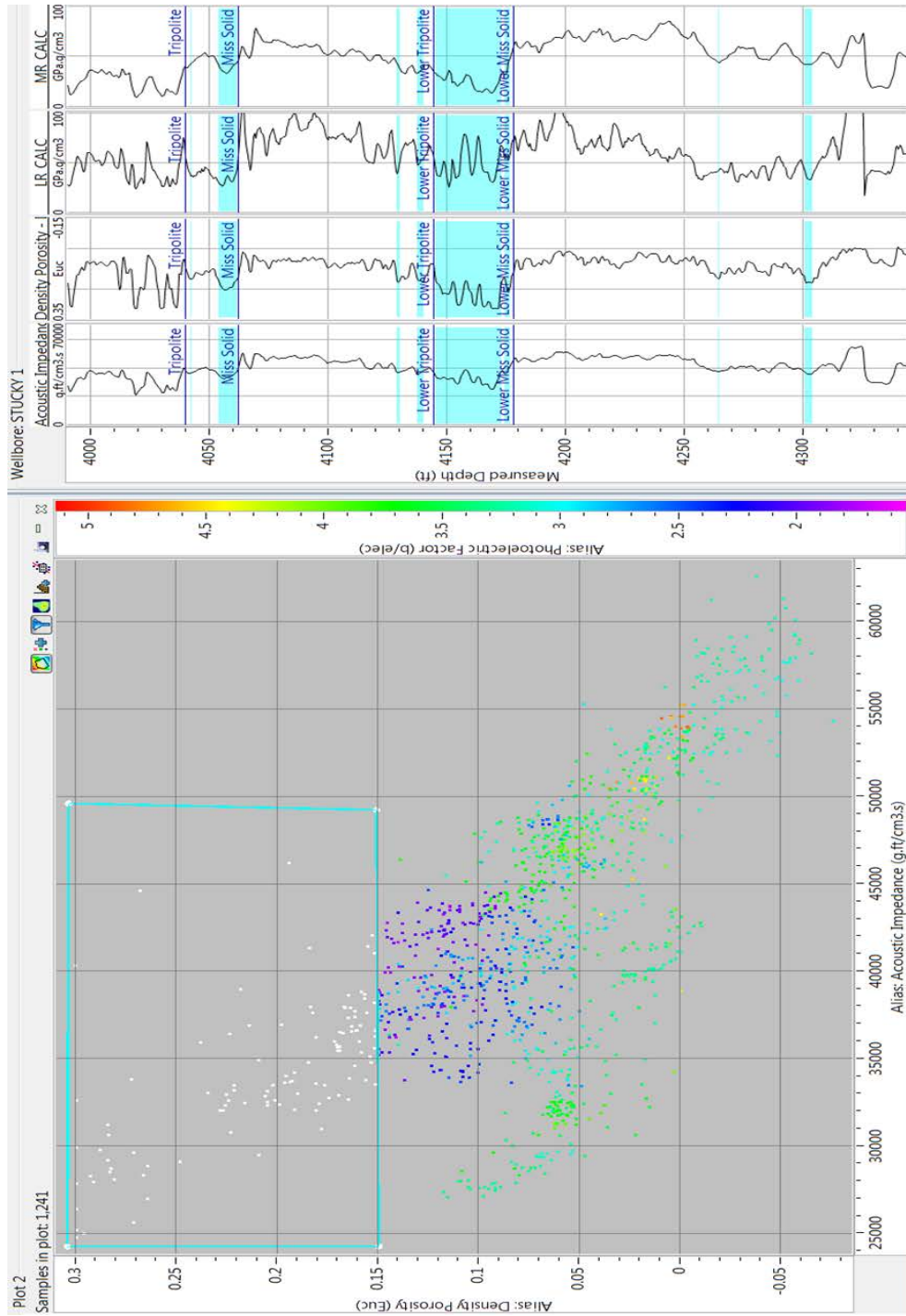


Figure 49. Acoustic impedance plotted against density porosity colored by photoelectric factor for the zone 3850-4050 ft shown on the well logs at the right. Data from shear sonic well log in neighboring Sumner County, Ks. Tripolite exhibits characteristics of high porosity and low acoustic impedance shown by highlighted portion of well logs to the right and white data points within the cyan polygon in the crossplot.

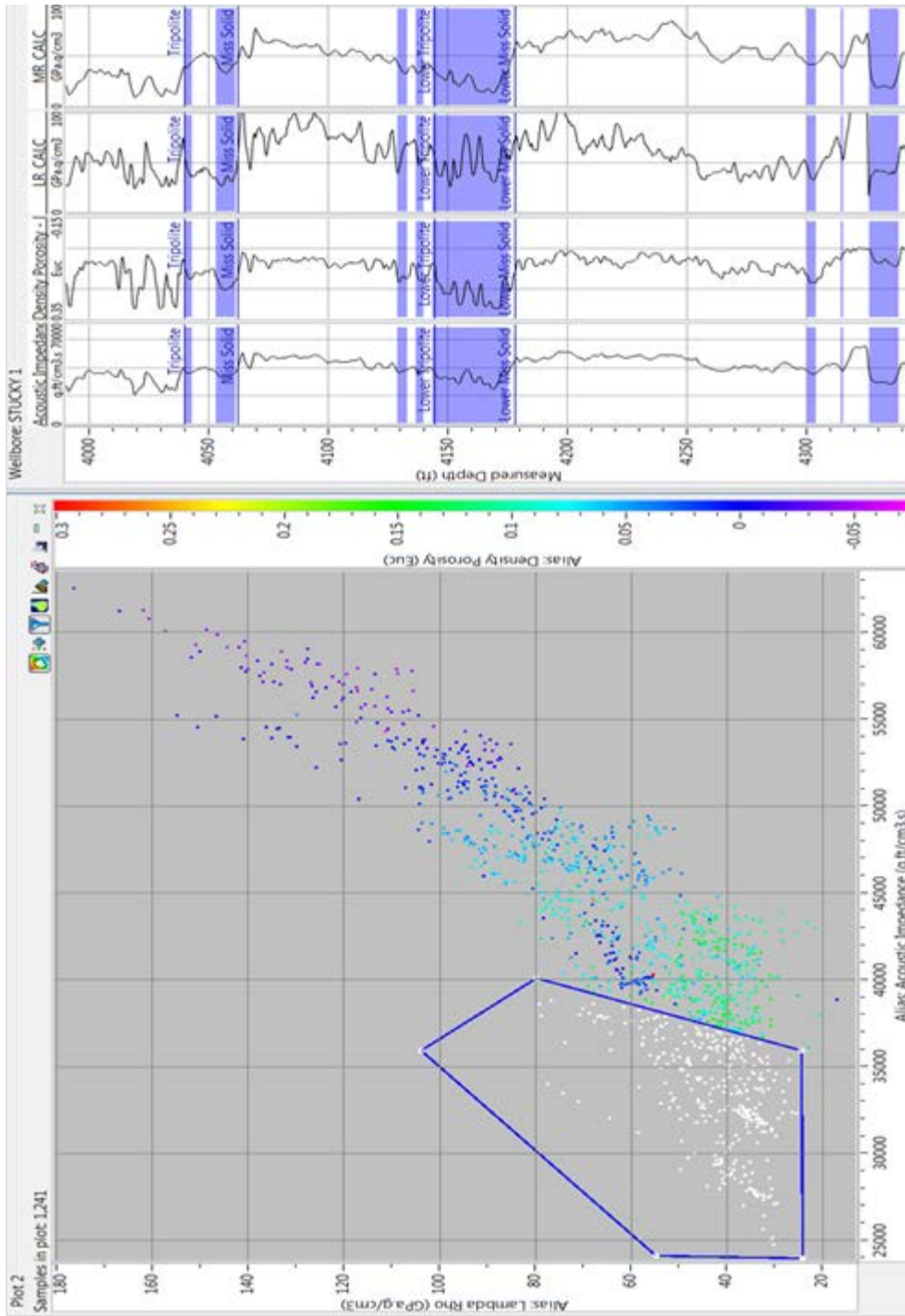


Figure 50. Acoustic impedance plotted against lambda-rho colored by density porosity for the zone 3850-4050 ft shown on the well logs at the right. Data from shear sonic well log in neighboring Sumner County, Ks. Tripolite has the characteristics of low acoustic impedance and low lambda-rho shown by highlighted portion of well logs to the right and white data points within the blue polygon in the crossplot.

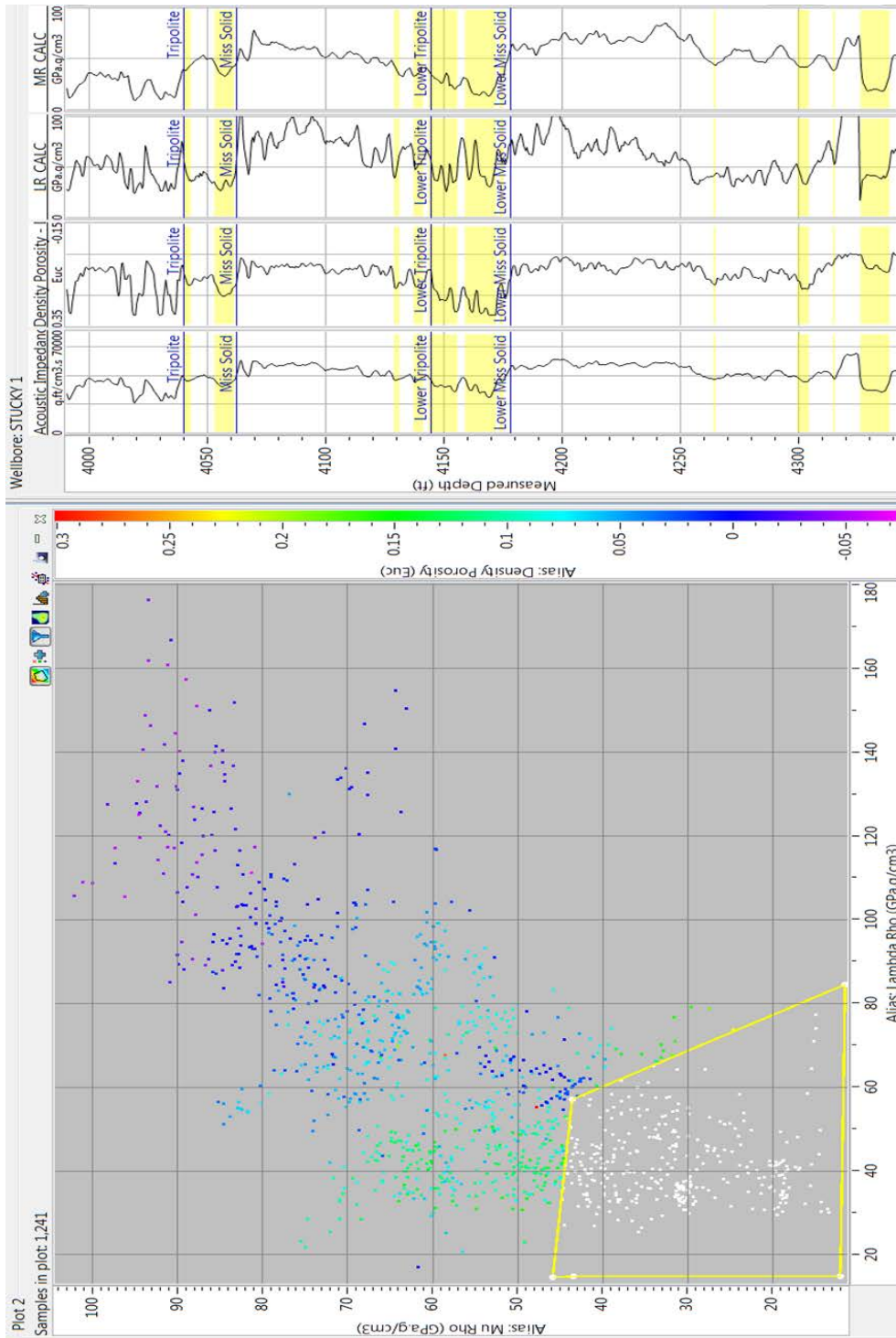


Figure 51. Lambda-rho plotted against mu-rho colored by density porosity for the zone 3850-4050 ft shown on the well logs at the right. Data from shear sonic well log in neighboring Sumner County, Ks. Tripolite has the characteristics of low lambda-rho as well as low mu-rho shown by highlighted portion of well logs to the right and white data points within the yellow polygon in the crossplot.

Now that the pre-stack acoustic impedance inversion characteristics of the tripolite have been demonstrated at the well log level, I can translate these findings to the pre-stack seismic volumes. In order to calibrate the individual wells I extracted the inversion products as well logs. This allows me to cross plot the seismic data in the same fashion I was able to cross plot the well log data. From the well log cross plot data, I found that the best discriminators of the tripolitic chert member of the Mississippi Lime are low lambda-rho and low acoustic impedance. Figures 52-54 show this relationship on the seismic scale. In these figures, lambda-rho is cross plotted with acoustic impedance (Z_P) and colored by density porosity. You can observe that the tripolite is characterized by low acoustic impedance values and low lambda-rho values as expressed by the seismic data. The wells represented in Figures 52-54 in this cross plot analysis are representative of the entire pre-stack seismic data, as they are scattered throughout the seismic survey. The wells in Figures 52-54 were all productive from the tripolitic chert member of the Mississippi Lime in the seismic survey. Figure 50 shows the same relationship described in Figures 52-54. Figure 55 is different from the previously mentioned figures. In Figure 55, the tripolite is characterized by high values of acoustic impedance and high values of lambda-rho. Subsequently, the well represented by Figure 55 was tested in the tripolitic chert member of the Mississippi Lime and deemed to be a dry hole. This provides support to the desirable productive characteristics of the tripolite being those of low acoustic impedance values and low lambda-rho values in the seismic data set.

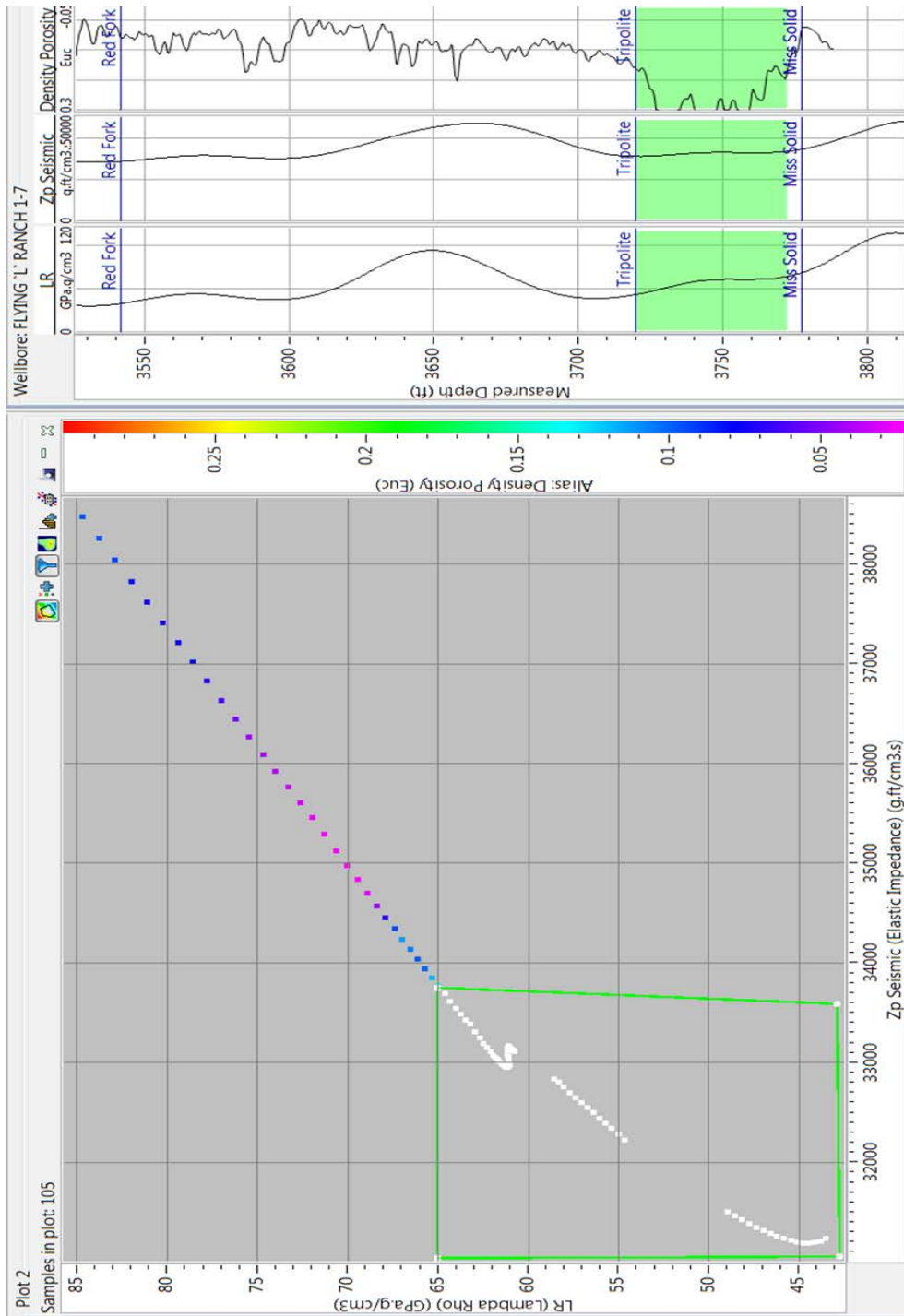


Figure 52. Pre-stack acoustic impedance (Z_P) plotted against lambda-rho colored by density porosity for the zone 3530-3800 ft shown on the well logs at the right. Plot shows that the low acoustic impedance and low lambda-rho characteristics of the tripolite can be discriminated within the seismic data as shown by highlighted portion of well logs to the right and white data points within the green polygon in the cross plot.

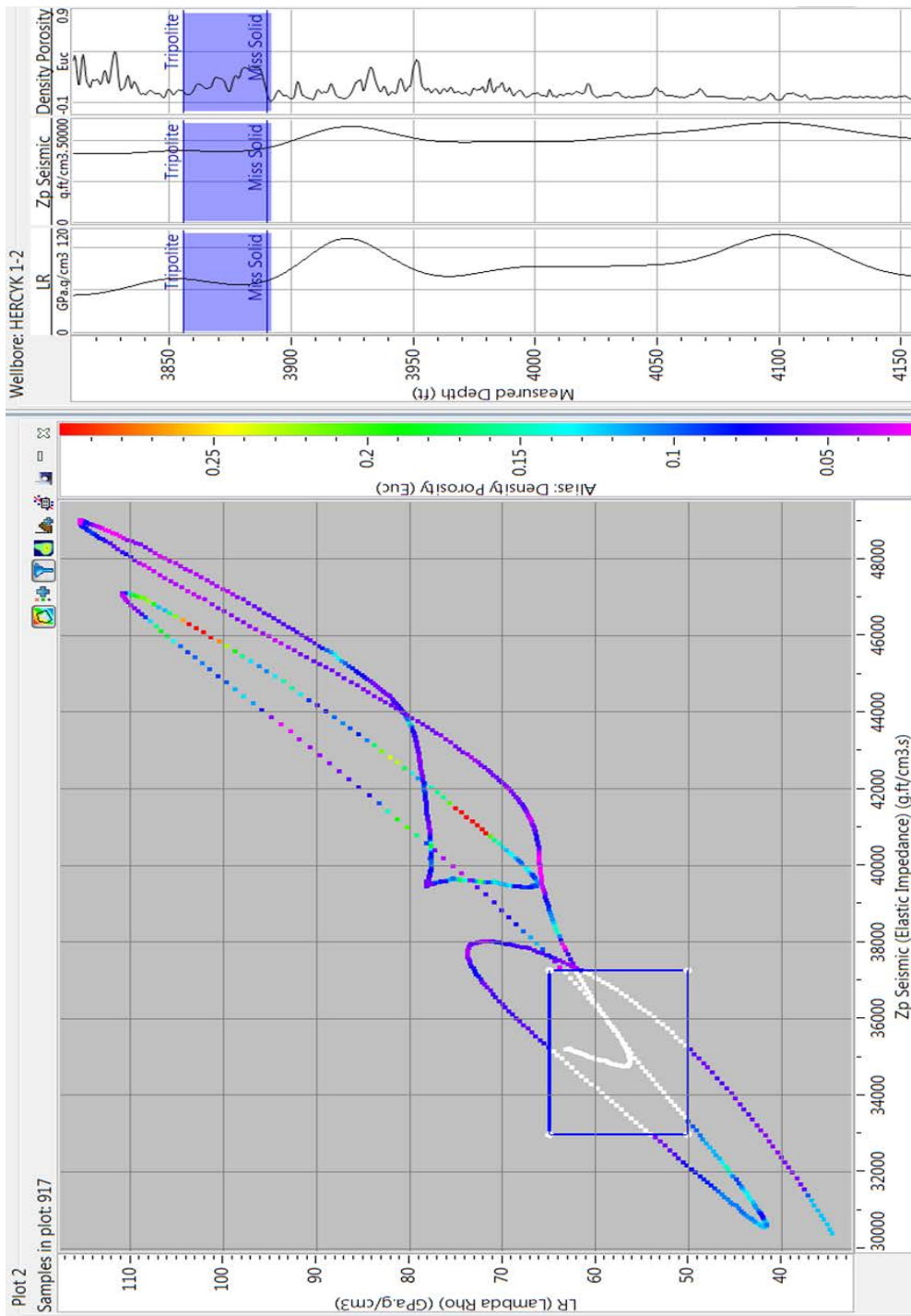


Figure 53. Pre-stack acoustic impedance (Z_P) plotted against lambda-rho colored by density porosity for the zone 3820-4150 ft shown on the well logs at the right. Plot shows that the low acoustic impedance and low lambda-rho characteristics of the tripolite can be discriminated within the seismic data as shown by highlighted portion of well logs to the right and white data points within the purple polygon in the cross plot.

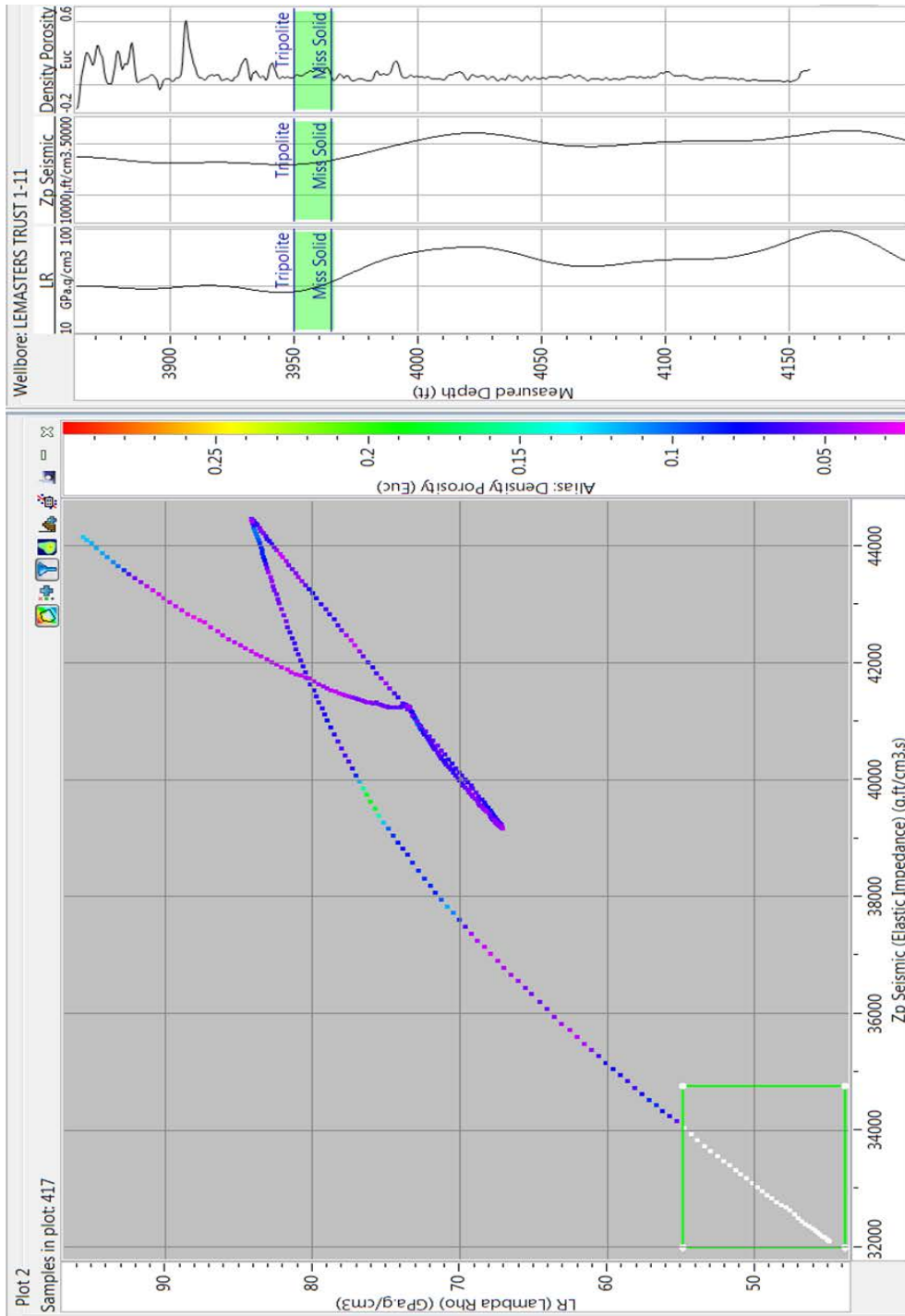


Figure 54. Pre-stack acoustic impedance (Z_P) plotted against lambda-rho colored by density porosity for the zone 3870-4190 ft shown on the well logs at the right. Plot shows that the low acoustic impedance and low lambda-rho characteristics of the tripolite can be discriminated within the seismic data as shown by highlighted portion of well logs to the right and white data points within the green polygon in the cross plot.

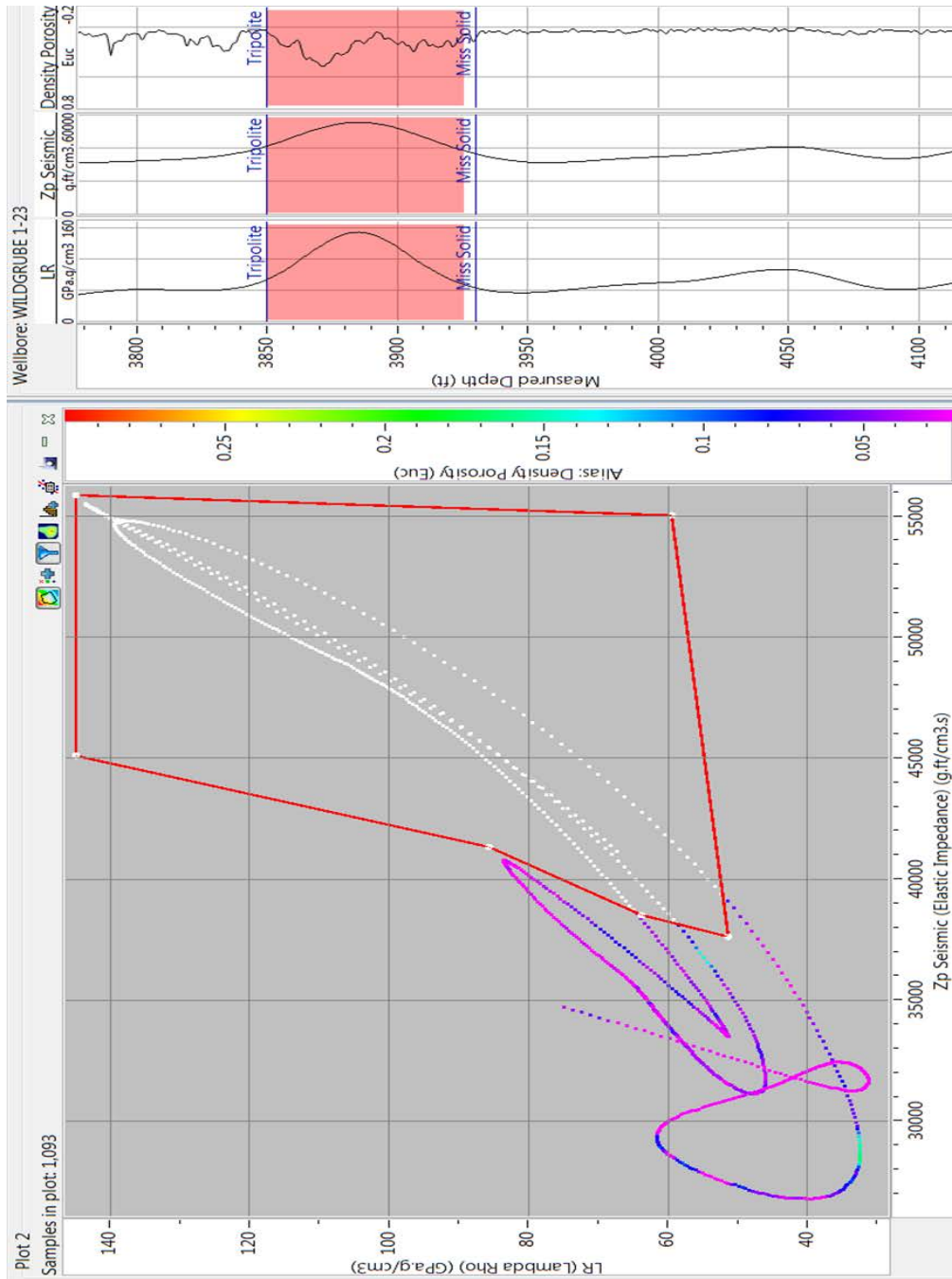


Figure 55. Pre-stack acoustic impedance (Z_P) plotted against lambda-rho colored by density porosity for the zone 3780-4110 ft shown on the well logs at the right. Plot shows that the low acoustic impedance and low lambda-rho characteristics of the tripolite can be discriminated within the seismic data as shown by highlighted portion of well logs to the right and white data points within the red polygon in the crossplot. This particular well does not exhibit the same seismic characteristics in the Mississippi Lime as the previously mentioned wells. This particular well was deemed a dry hole after testing the tripolite.

Visual correlation is very important to the seismic interpretation process. I have demonstrated quantitatively that a correlation exists between the geologic data available and the pre-stack acoustic impedance inversion attributes as they relate to the tripolitic chert member of the Mississippi Lime. The following figures represent a more qualitative relationship between the pre-stack acoustic impedance inversion attributes as they relate to production from the tripolitic chert member of the Mississippi Lime.

Figure 56 is an image of pre-stack P-impedance phantom slice extracted 40 ms below the Mississippi horizon within the subject seismic data set. Cumulative oil production from the Mississippi Lime is represented by the green circles, with the magnitude of oil production directly relating to the size of the circles. As you can see in Figure 56, most of the production exists from lower values of pre-stack P-impedance values. There is one exception to this, however. On the up-thrown side of the main fault located in the western portion of the survey, there is a cluster of production that occurs in an area of high impedance values. This could be due to a change of depositional conditions in proximity to the fault. Figures 57-59 also show phantom horizon slices of post-stack acoustic impedance from the Mississippi Lime horizon extracted at 20 ms intervals with production values plotted at the wellbore. Production magnitudes are coded by color in the legends. Figure 57 is extracted 0-20 ms below the Mississippi horizon, Figure 58 is extracted 20-40 ms below the Mississippi horizon, and Figure 59 is extracted 40-60 ms below the Mississippi horizon. These figures also demonstrate that the production from within the Mississippi

Lime occurs in correlation with lower impedance values. Figure 58, however, shows something unique. I believe that extracting impedance values at this time interval represents the presence of tripolite in the same way the geologic data represents the tripolite. Referring back to Figure 16, the tripolite thins out as you move southeast in the survey area. Figure 59 represents the same image in a seismic sense. The higher impedance values represent a lack of presence of the tripolite. Figure 60 is pre-stack acoustic impedance extracted 20-40 ms below the Mississippi horizon showing the cross section C-C'. The main faults are indicated by red arrows in Figure 60. Figure 61 shows a vertical slice of grayscale amplitude along the cross section C-C' with pre-stack acoustic impedance extracted 20-40 ms below the Mississippi horizon. The main faults are indicated with red arrows. The important thing to note in Figure 61 is highlighted by the light blue oval. There is a dimming of the negative amplitude in this oval that correlates with the higher impedance values. This shows that pre-stack acoustic impedance, when extracted at the right times, can be a good predictor of the presence of tripolite. Figure 62 is pre-stack acoustic impedance extracted 20-40 ms below the Mississippi horizon showing the cross section D-D'. The main faults are indicated by red arrows in Figure 62. Figure 63 shows a vertical slice of grayscale amplitude along the cross section D-D' with pre-stack acoustic impedance extracted 20-40 ms below the Mississippi horizon. The main faults are indicated with red arrows. The main thing to note in Figure 63 is indicated by the magenta arrow. At this location in the figure exists a structural high. At this location, the impedance values are higher than the surrounding

area. This indicates that the tripolite was not deposited on structural highs in the excess that it is in surrounding area. Figure 64 is nearly an exact replica of Figure 43. The only difference between the figures is that Figure 64 shows pre-stack impedance (Z_P) instead of post stack impedance. Here you can see that the productive wells from within the Mississippi Lime correspond mostly with low impedance values. It also shows that there is almost no production from the Mississippi Lime in the southeastern portion of the survey, where there is less tripolite. Figure 65 is an image of a horizon slice of lambda-rho values extracted 40 ms below the Mississippi horizon within the subject seismic data set. Cumulative oil production for the Mississippi Lime is represented by the red, yellow, and green circles, with the magnitude of oil production dictated in the legend. Observed here is that the majority of the production is clustered around or in near proximity to portions of the seismic survey that exhibit low values of lambda-rho data. This is a visual representation of the quantitative interpretation previously discussed. Figure 66 is an image of the same lambda-rho values found in Figure 65. Here, these lambda-rho values are co-rendered with incoherence with cumulative oil production from the Mississippi Lime shown by the red, yellow, and green circles. Again, the magnitude of the oil production is dictated in the legend. This image allows you to observe the production values as they relate to lambda-rho, as well as the other main constraint of production, geologic structure. This image demonstrates how the production from the Mississippi Lime in this area is influenced by more than just rock properties observed at the well bore. The existence of the Nemaha fault complex within the

bounds of this seismic survey is obviously a controlling factor on the production from the Mississippi Lime. It is difficult to quantitatively assess how this type of geologic circumstance could affect the production. However, this image clearly represents two influential factors on production. One factor being production from areas of low lambda-rho values, and the other factor being production along the structural lineaments found on or in near proximity to the faults present in the area of study. Figure 67 is an image of pre-stack S-impedance values extracted 40 ms below the Mississippi horizon. Again, cumulative oil production from the Mississippi Lime is indicated by the red, yellow, and green circles, and the magnitude of production is dictated in the legend. Here you can observe that the majority of the production is related to low values of pre-stack S-impedance. S-impedance can be a fluid discriminator. In this case, it is well known that the Mississippi Lime will produce large quantities of water. Perhaps the areas of lower pre-stack S-impedance indicate portions of the seismic survey where there is a greater presence of hydrocarbons. As was the case with the pre-stack P-impedance, there is a cluster of production on the up-thrown side of the large fault located in the western part of the seismic survey. This cluster of production falls in an area that reads high S-impedance values. This could be due to a change in depositional conditions of the Mississippi Lime caused by the fault, or as the S-impedance would suggest, a change of fluid content in that particular area of the seismic survey. Figures 68-70 show phantom horizon slices of pre-stack S-impedance (Z_S) from the Mississippi Lime horizon extracted at 20 ms intervals with production values plotted at the wellbore. Figure 68 is extracted 0-

20 ms below the Mississippi horizon, Figure 69 is extracted 20-40 ms below the Mississippi horizon, and Figure 70 is extracted 40-60 ms below the Mississippi horizon. These figures also demonstrate that the production from within the Mississippi Lime occurs in correlation with lower pre-stack shear impedance values. Figure 69 demonstrates the same characteristics observed in Figure 58. Referring back to Figure 16, the tripolite thins out as you move southeast in the survey area. Figure 69 represents the same thinning of the tripolite in a seismic sense. The higher impedance values represent a lack of presence of the tripolite. This also says that shear impedance extracted at the correct values is also a good predictor of the presence of tripolite. Figure 70 shows that production is still mostly correlated with low values of Z_S 40-60 ms below the Mississippi horizon. Since μ -rho is a good predictor of lithology, this could be an indicator of the presence of thicker areas of productive tripolite. Figure 72 shows a phantom horizon slice of μ -rho extracted 40 ms below the top Mississippi Horizon. Production is shown at the wellbores by green, yellow, and red circle. Magnitude of production is shown in the legend. This figure shows that production is mostly correlated with low values of μ -rho. Figure 72 is an image of a cross plot of λ -rho, μ -rho, and cumulative oil production from the Mississippi Lime. Here, λ -rho and μ -rho values are extracted on the Mississippi horizon at the well locations. The plot shows λ -rho plotted against μ -rho colored by cumulative production. As you can observe in this figure the majority of production from the Mississippi Lime in this seismic survey occurs in locations that exhibit both low λ -rho values and low μ -rho

values. Statistically speaking, this is an average correlation of data, with the R-squared value being 0.653. While some of the production is not economical by the industry standards of today (or even yesterday), the important thing to note in this case is that the majority of the production from the Mississippi Lime in this portion of Kay County comes from locations that exhibit the characteristics of low values of lambda-rho and low values of lambda-rho.

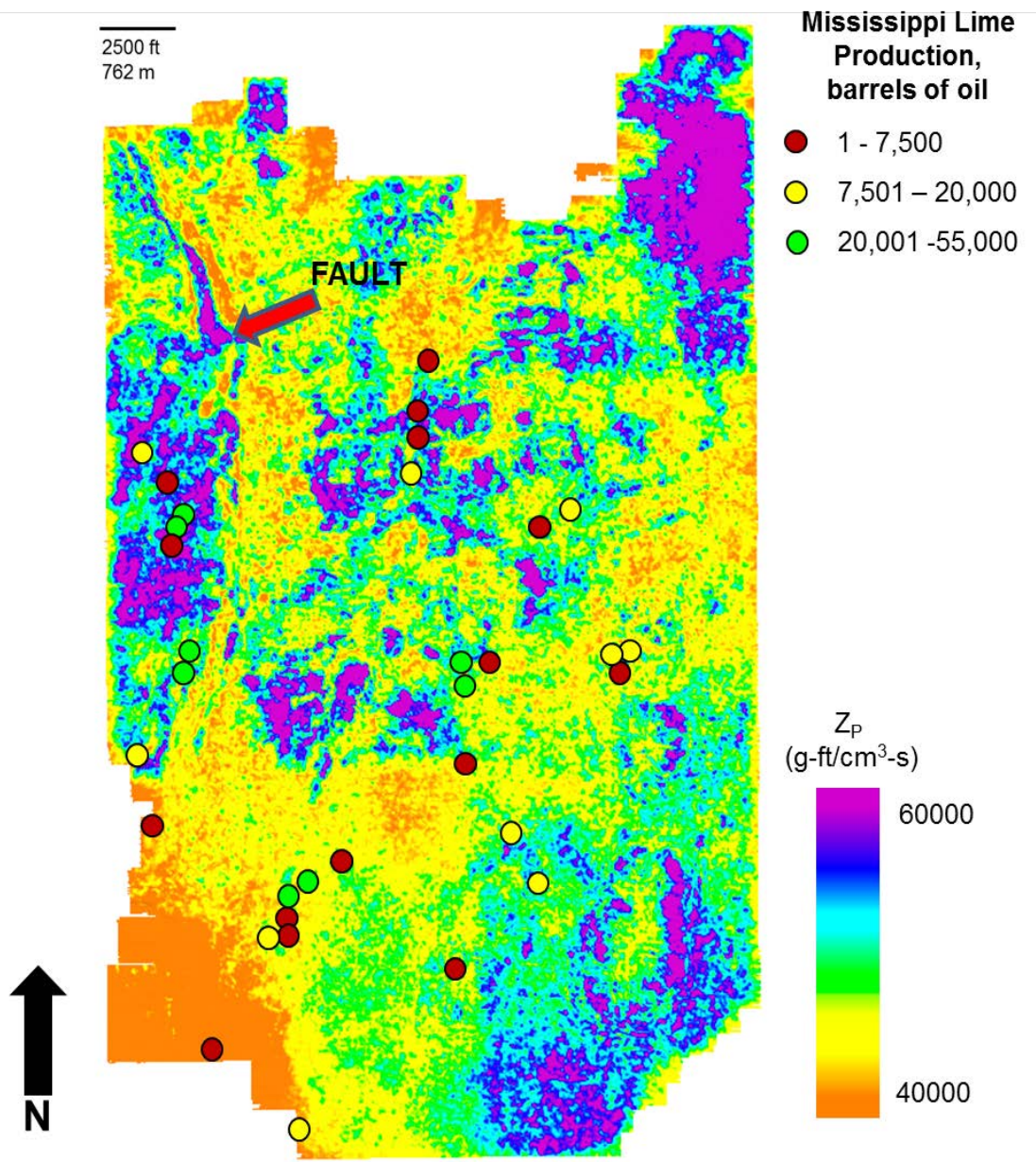


Figure 56. Phantom horizon slice 40 ms below the Mississippi horizon through prestack P-impedance (Z_P) volume. Cumulative oil production from Mississippi Lime indicated by red, yellow, and green circles. Magnitude of production indicated in legend.

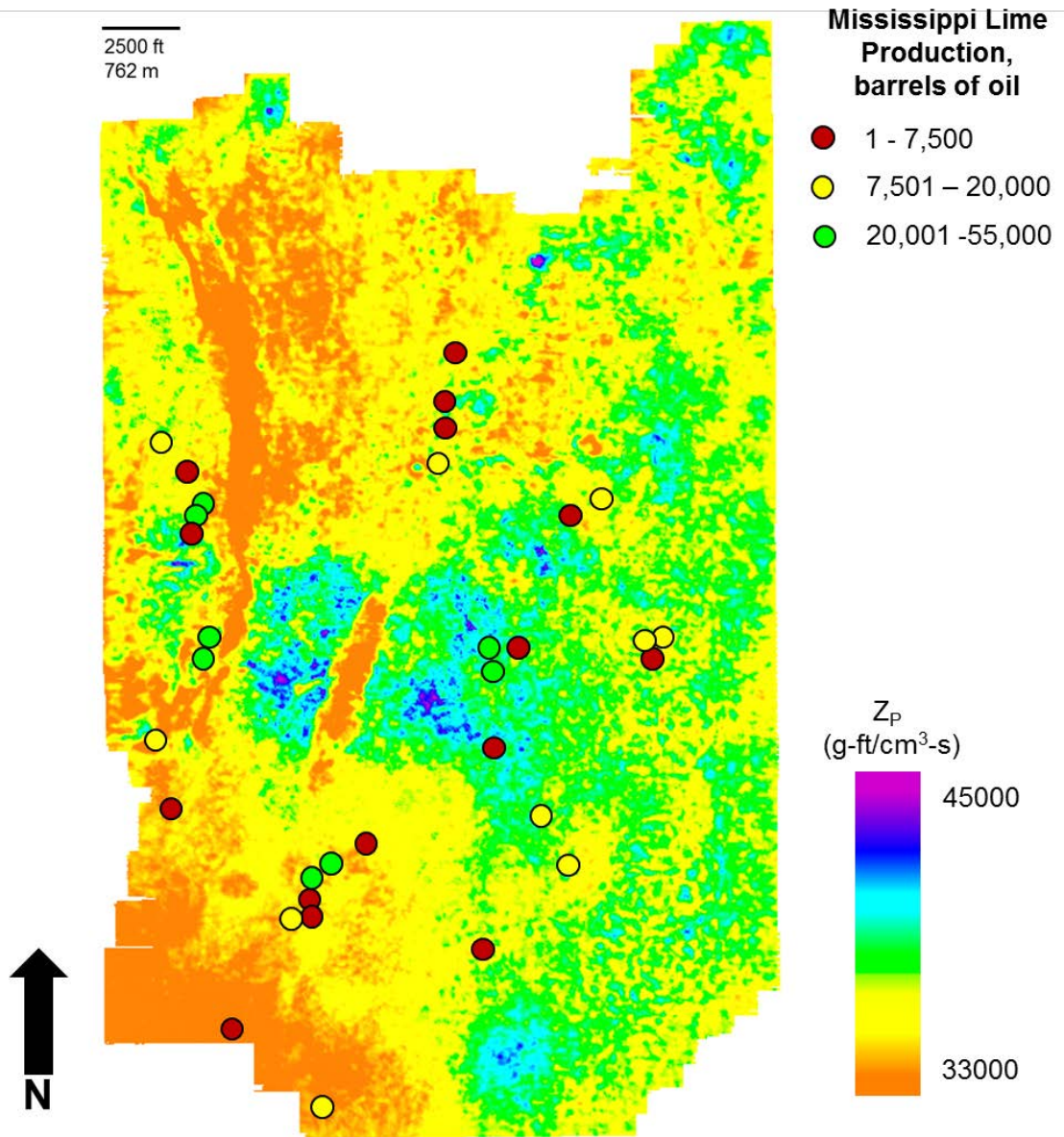


Figure 57. Phantom horizon slice 0-20 ms below the top Mississippi horizon through prestack Z_P volume. Cumulative oil production from Mississippi Lime indicated by red, yellow, and green circles. Magnitude of production indicated in legend.

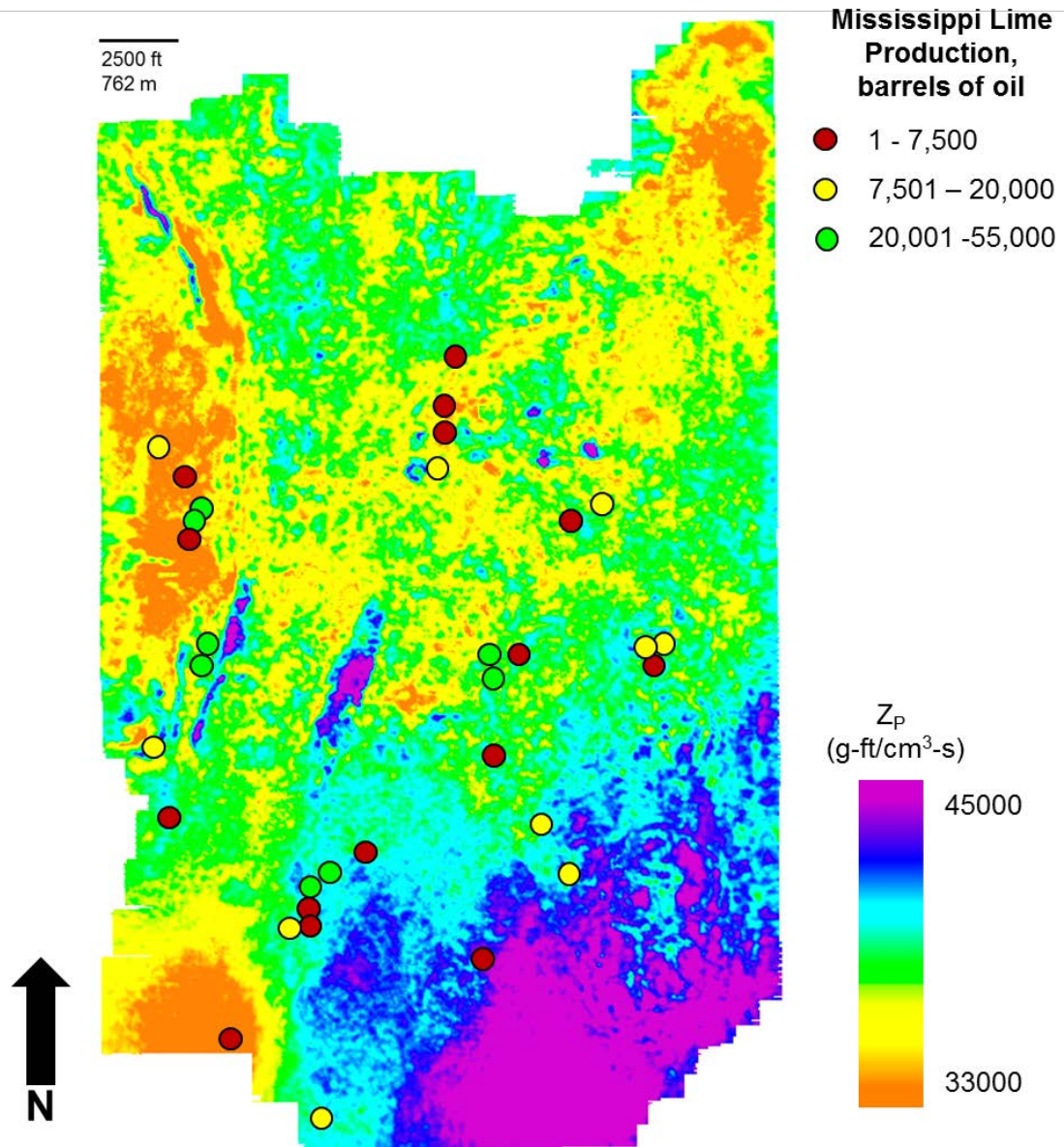


Figure 58. Phantom horizon slice 20-40 ms below the top Mississippi horizon through prestack Z_p volume. Cumulative oil production from Mississippi Lime indicated by red, yellow, and green circles. Magnitude of production indicated in legend.

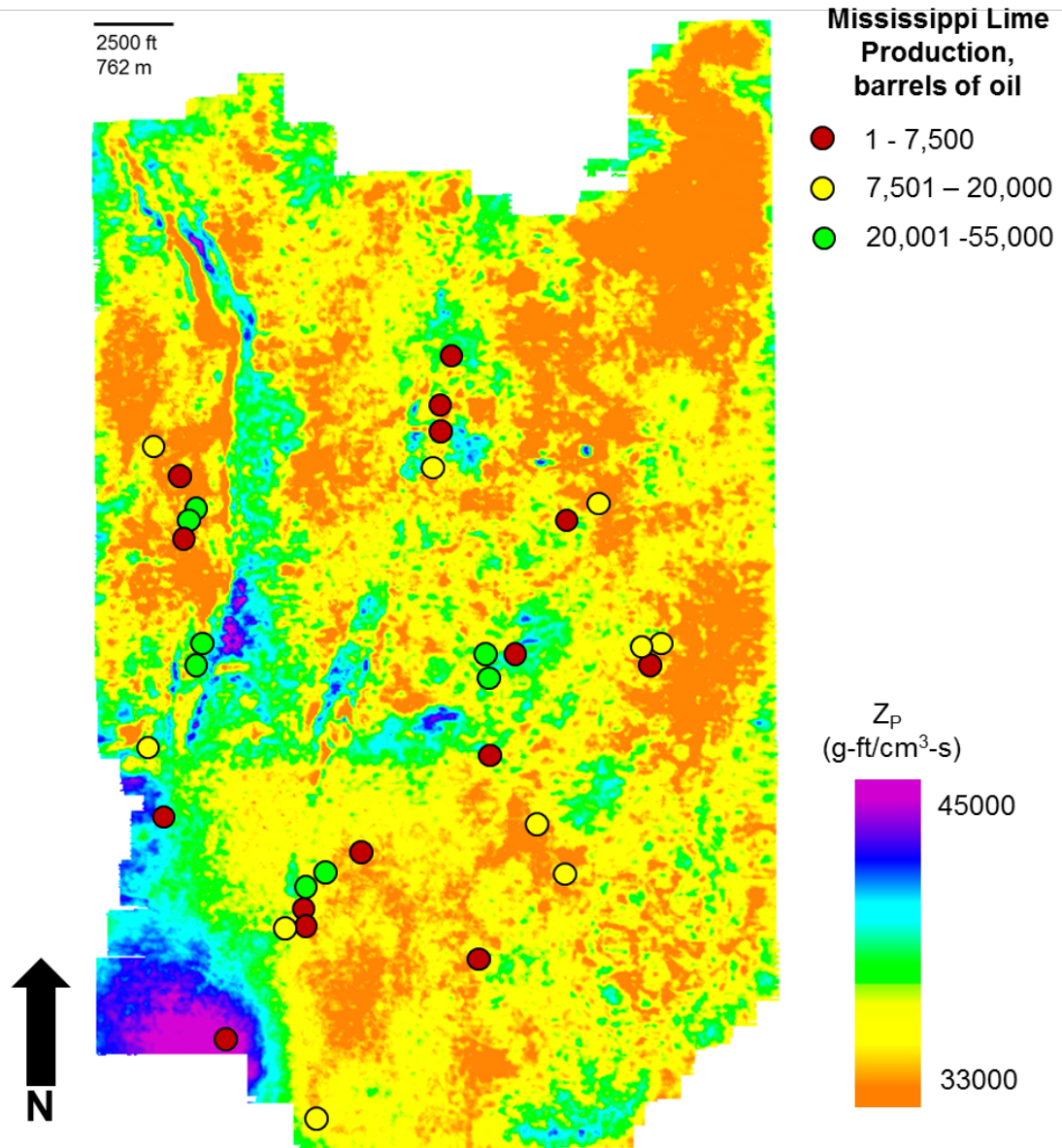


Figure 59. Phantom horizon slice 40-60 ms below the top Mississippi horizon through prestack Z_p volume. Cumulative oil production from Mississippi Lime indicated by red, yellow, and green circles. Magnitude of production indicated in legend.

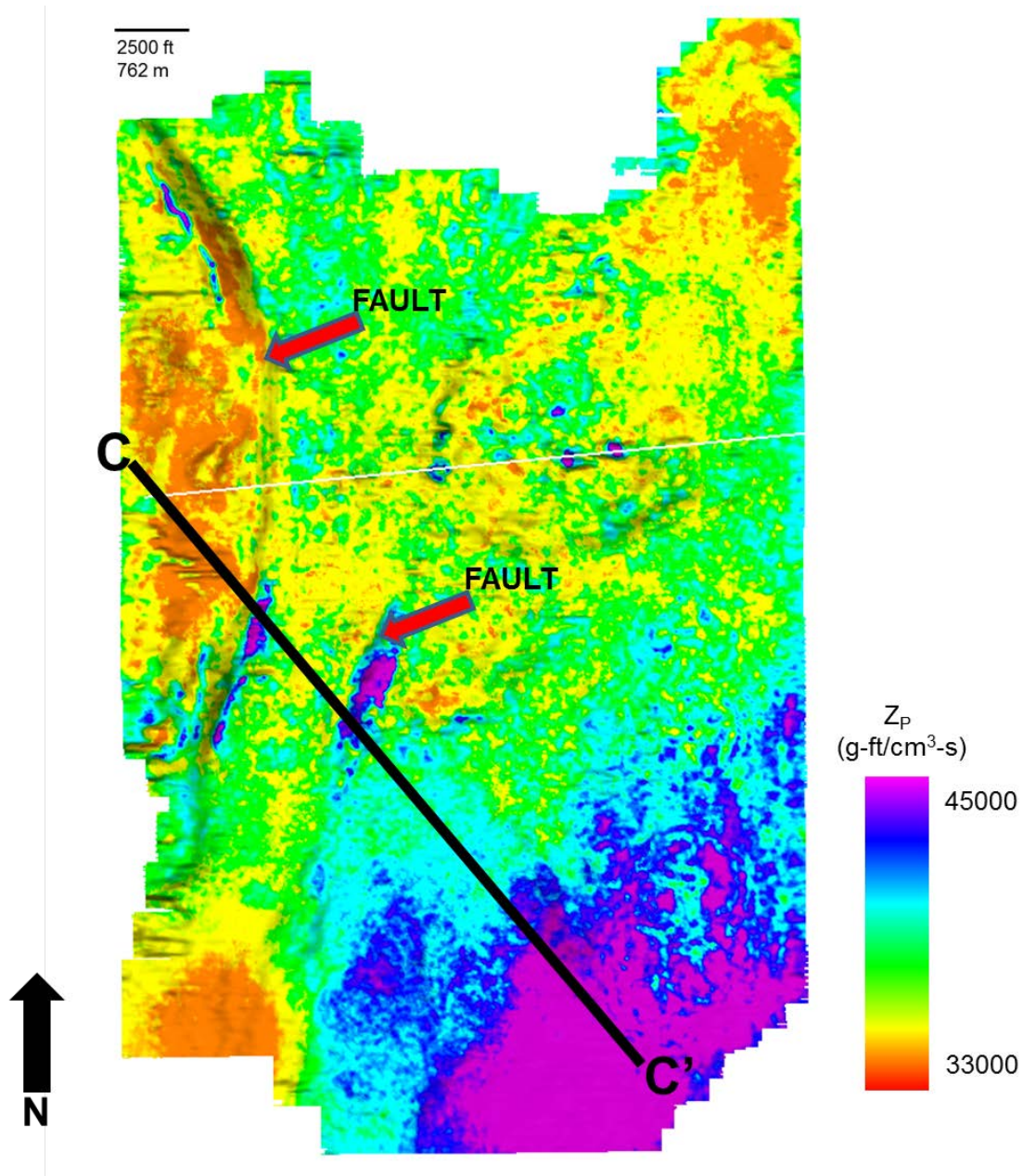


Figure 60. Prestack Z_p impedance extracted along the Mississippi horizon. Faults are indicated by red arrows. Cross section C-C' through the seismic data indicated by black line.

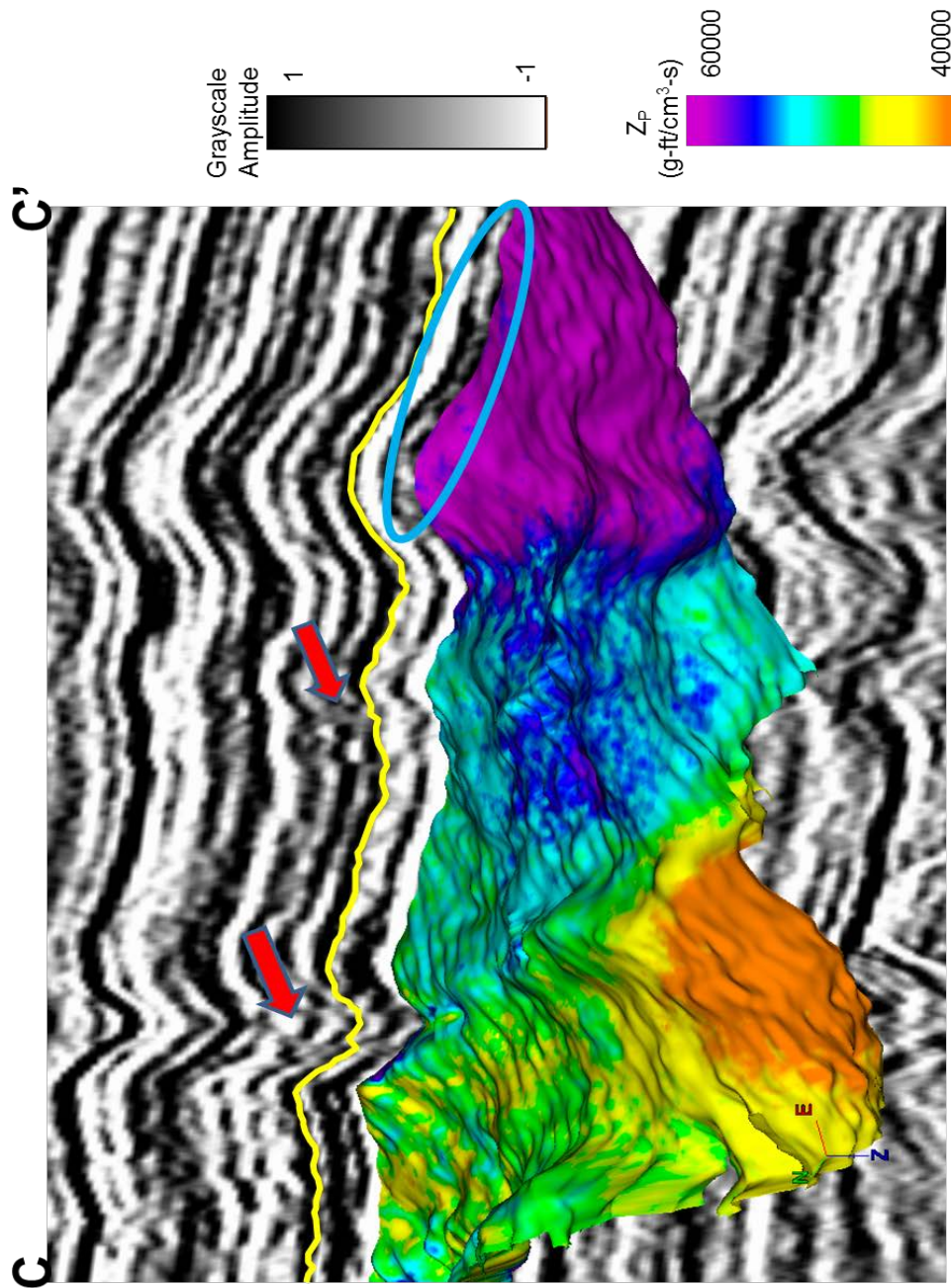


Figure 61. Prestack Z_P impedance extracted 20-40 ms below the Mississippi horizon shown with amplitude (grayscale) along cross section C-C'. Mississippi horizon indicated by yellow line. Faults indicated by red arrows. Blue oval indicates the dimming of a low amplitude trough as impedance values become higher. This dimming of the trough indicates a lack of presence of the tripolite as demonstrated in Figure 18. High values of impedance coincide with structural high, suggesting that the deposition of the tripolite is structurally controlled.

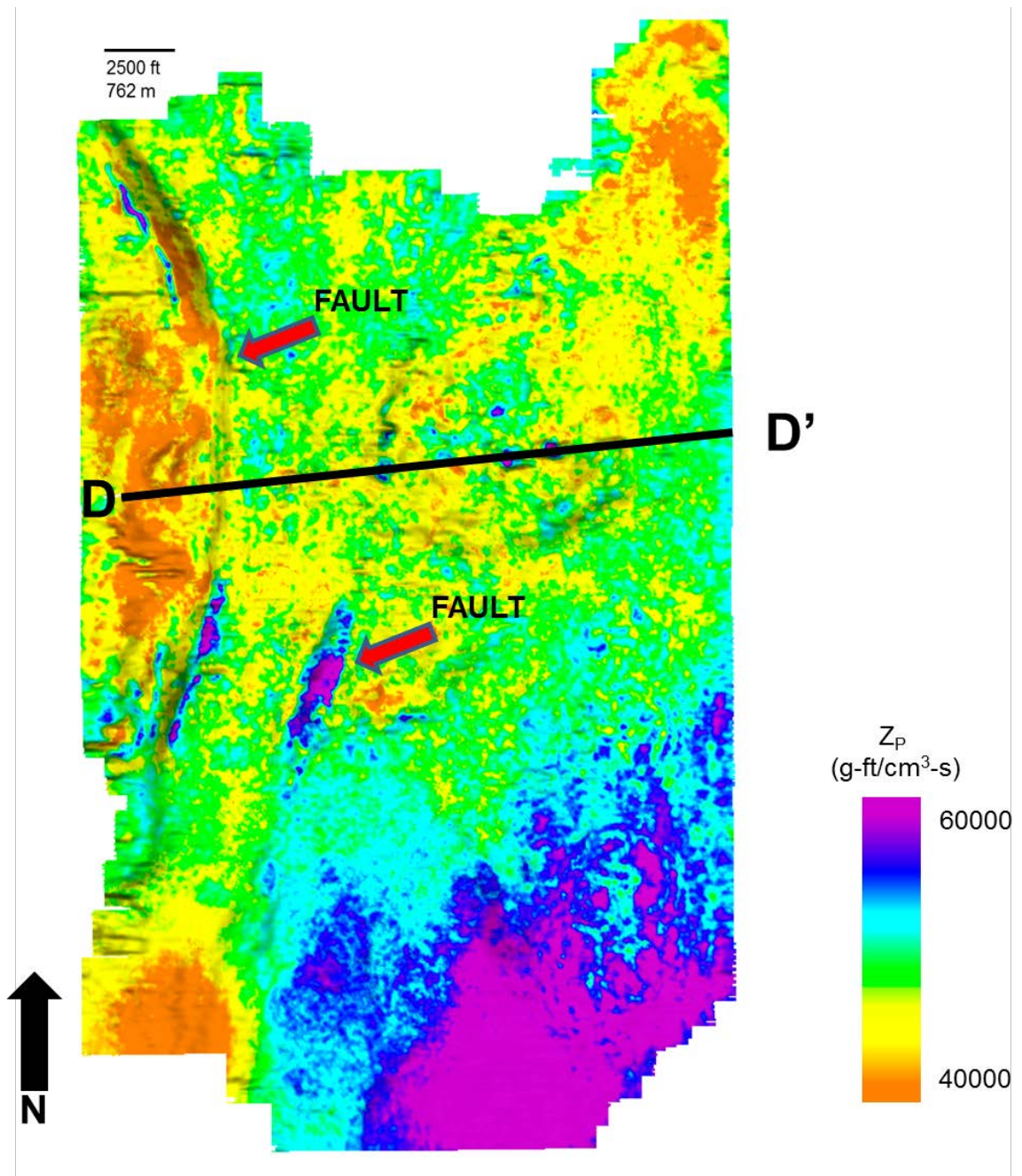


Figure 62. Prestack Z_p impedance extracted along the Mississippi horizon. Faults are indicated by red arrows. Cross section D-D' through the seismic data indicated by black line.

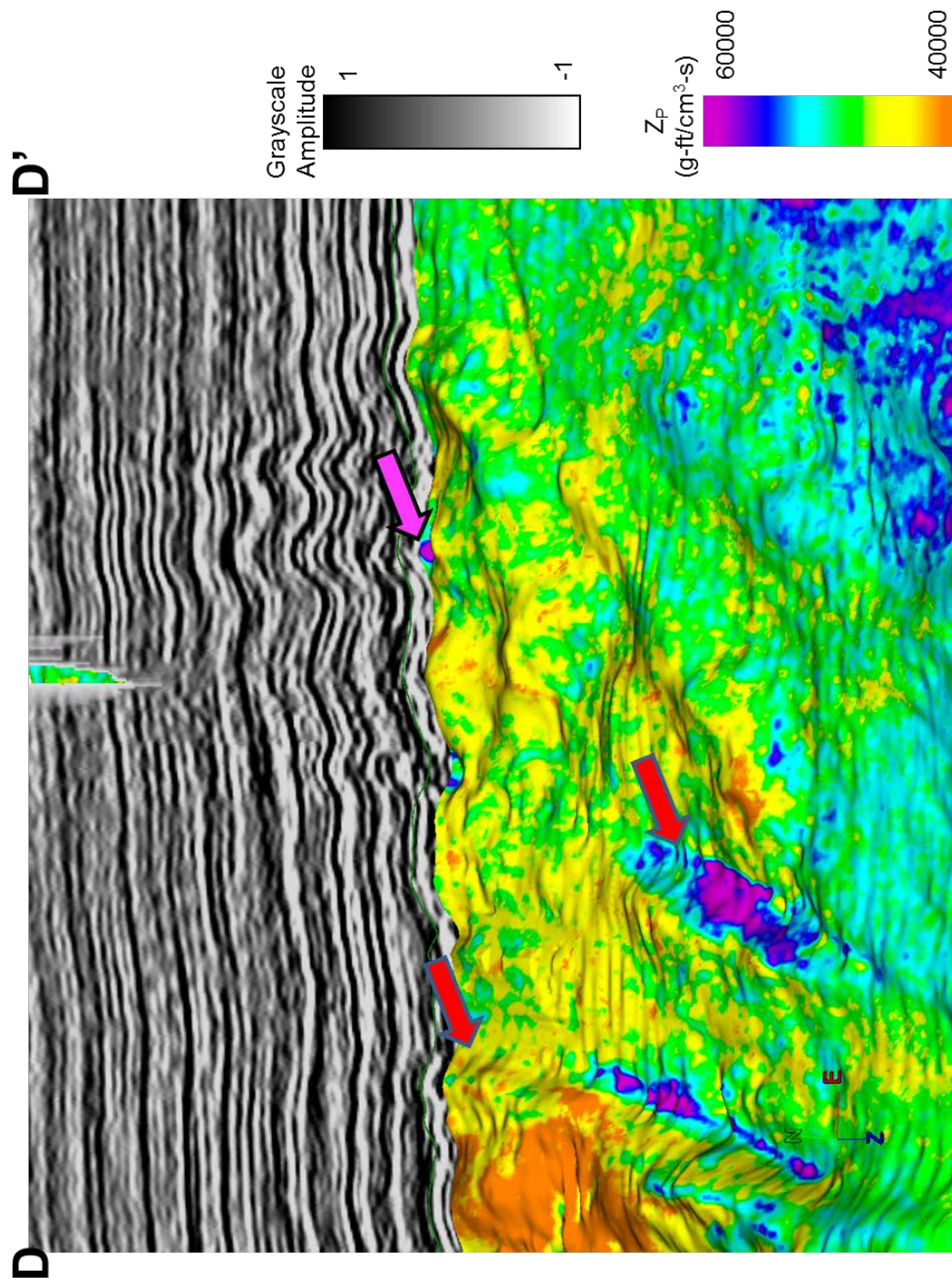


Figure 63. Pre-stack Z_P impedance extracted along Mississippi horizon shown with amplitude (grayscale). Faults are indicated by red arrows. Magenta arrow shows high impedance value on a localized structural high, likely as a result of thinning tripolite deposition onto structural high.

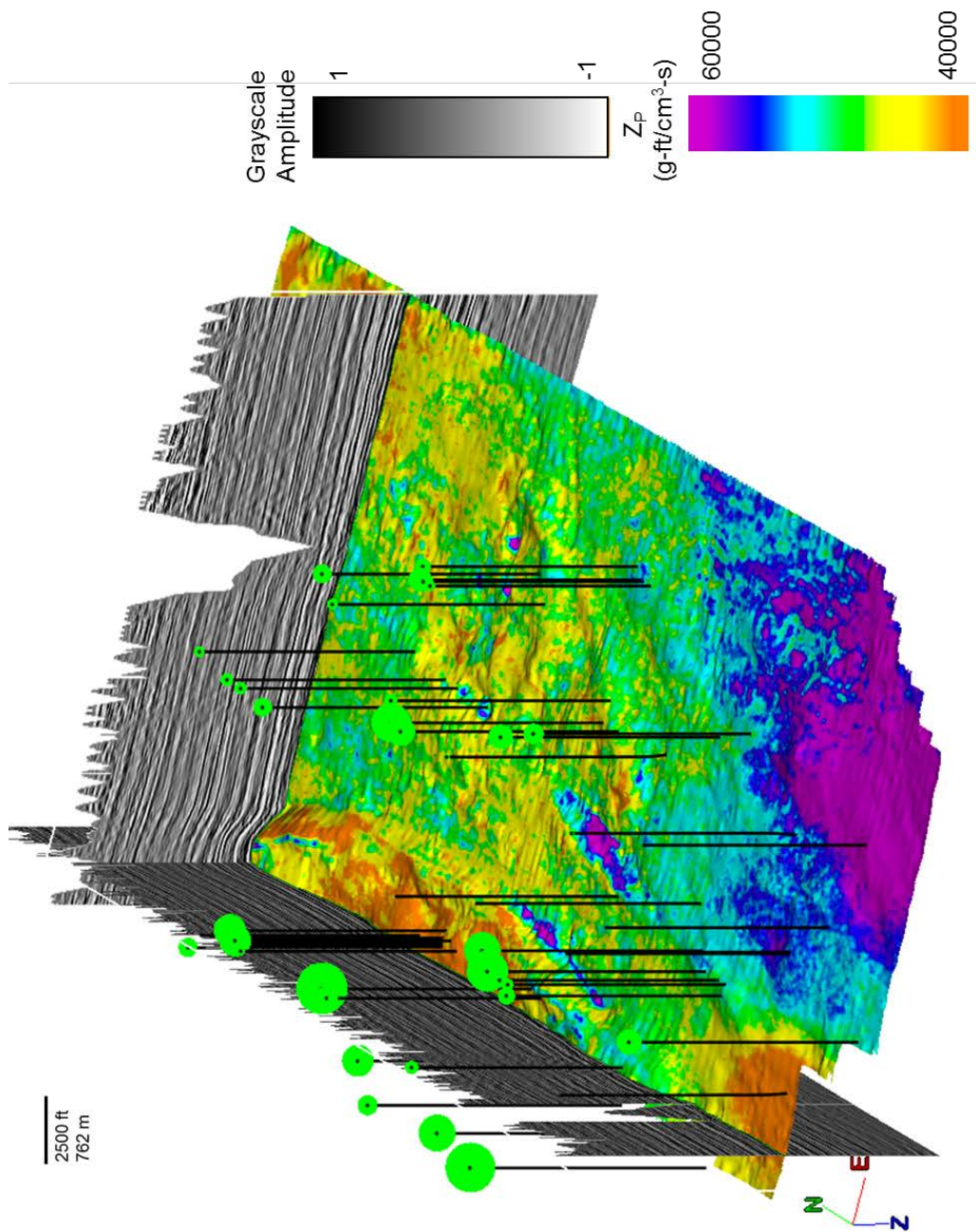


Figure 64. Pre-stack Z_P impedance along Mississippi horizon shown with well bores and cumulative oil production from the Mississippi Lime posted as green circles at the top of the well bore. Amplitude (grayscale) shown in cross-line and inline. Magnitude of oil production is directly related to the size of the circle.

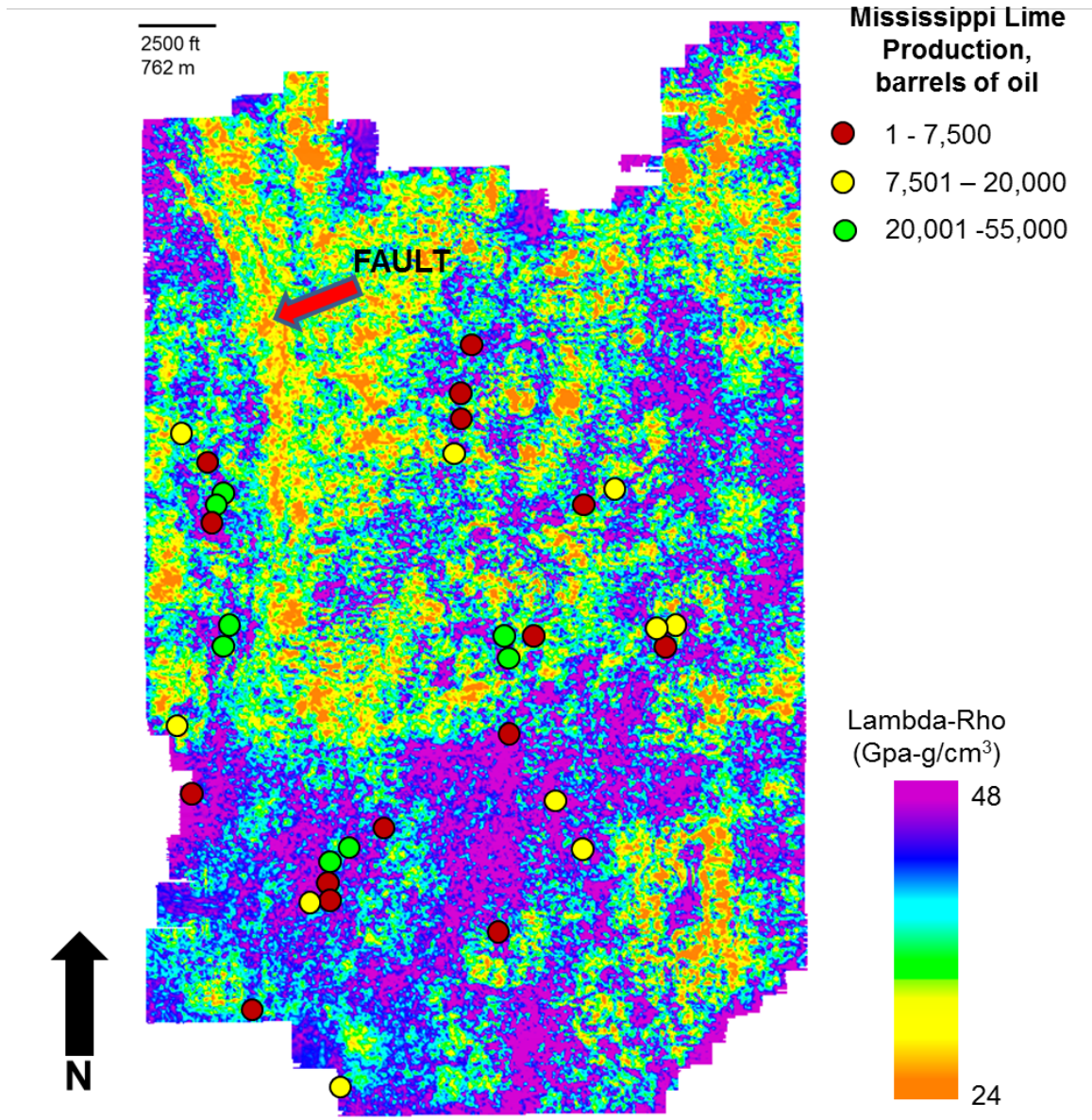


Figure 65. Phantom horizon slice 40 ms below the top Mississippi horizon through lambda-rho volume. Cumulative oil production from Mississippi Lime indicated by red, yellow, and green circles. Magnitude of production indicated in legend.

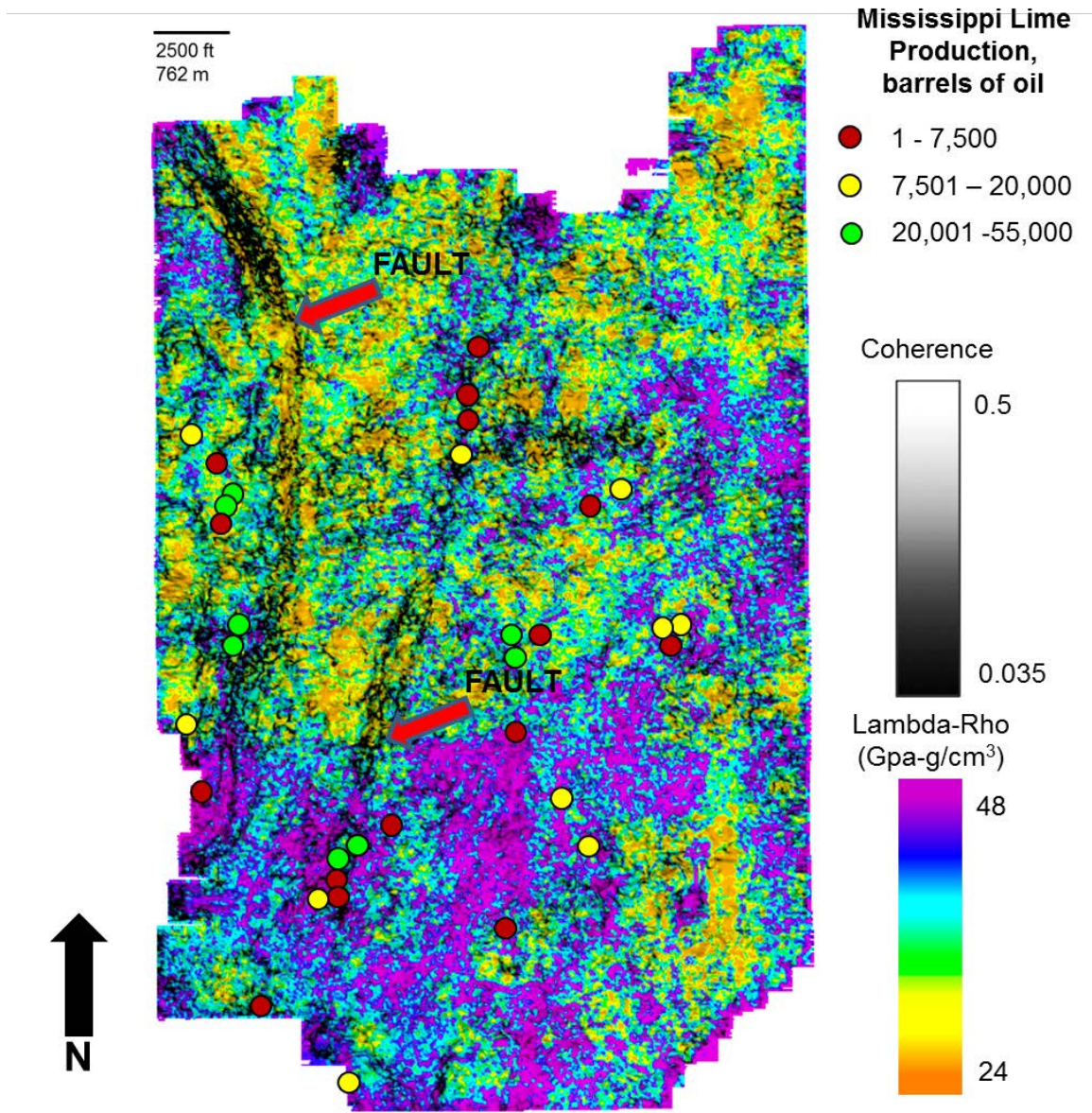


Figure 66. Phantom horizon slice 40 ms below the top Mississippi horizon through lambda-rho co-rendered with coherence. Cumulative oil production from Mississippi Lime indicated by red, yellow, and green circles. Magnitude of production indicated in legend.

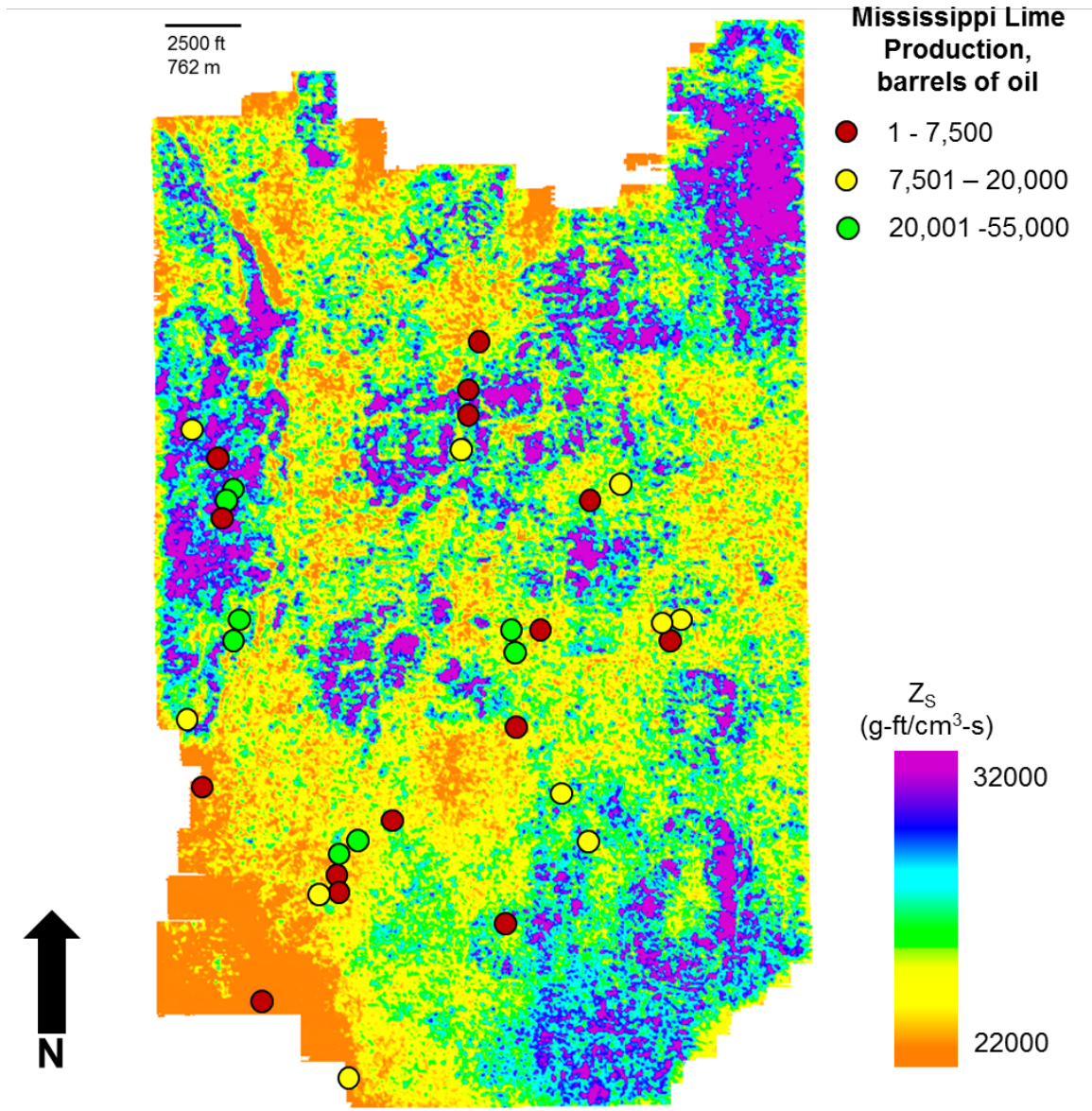


Figure 67. Phantom horizon slice 40 ms below the top Mississippi horizon through prestack S-impedance (Z_s) volume. Cumulative oil production from Mississippi Lime indicated by red, yellow, and green circles. Magnitude of production indicated in legend.

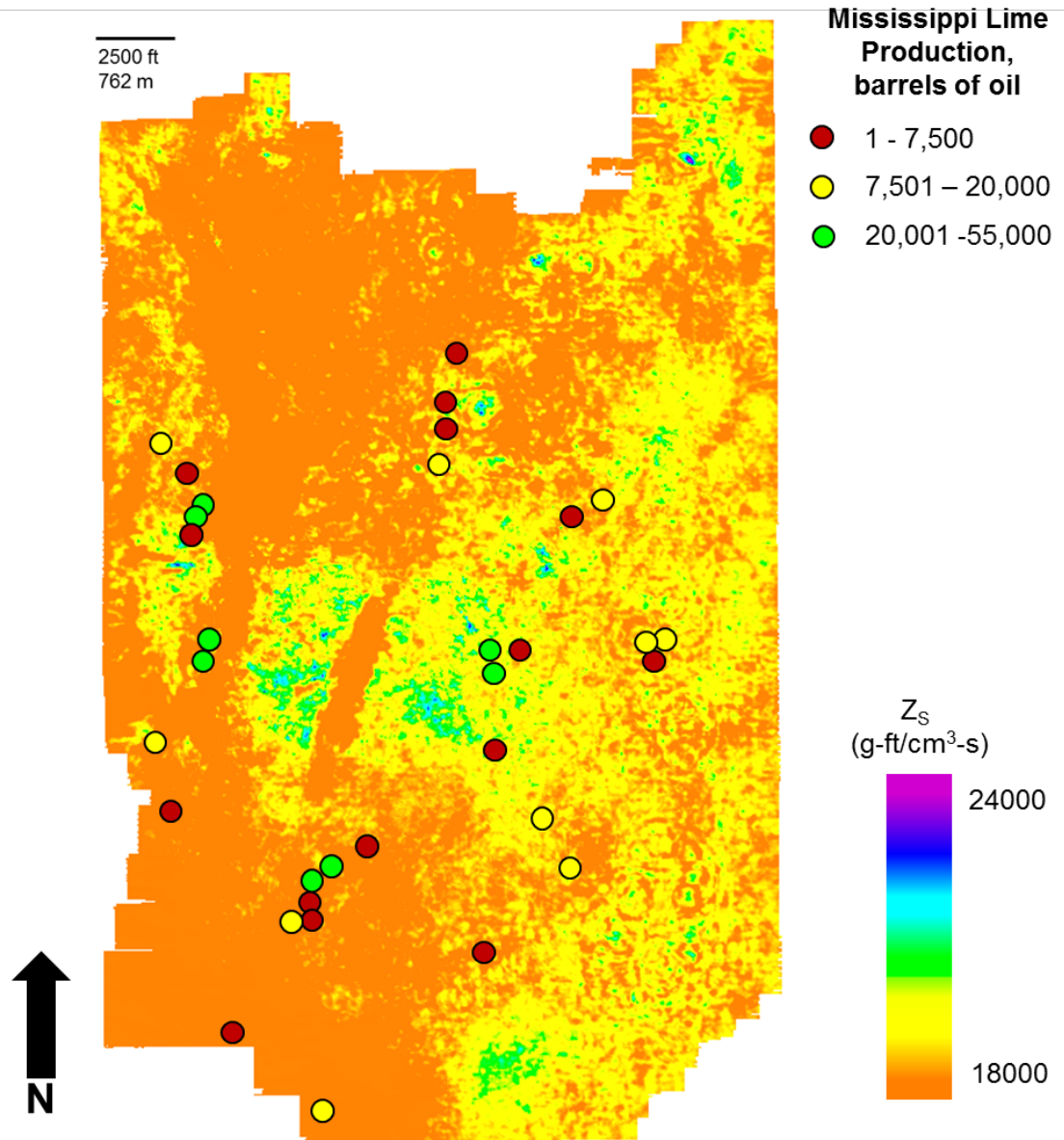


Figure 68. Phantom horizon slice 0-20 ms below the top Mississippi horizon through prestack (Z_s) volume. Cumulative oil production from Mississippi Lime indicated by red, yellow, and green circles. Magnitude of production indicated in legend.

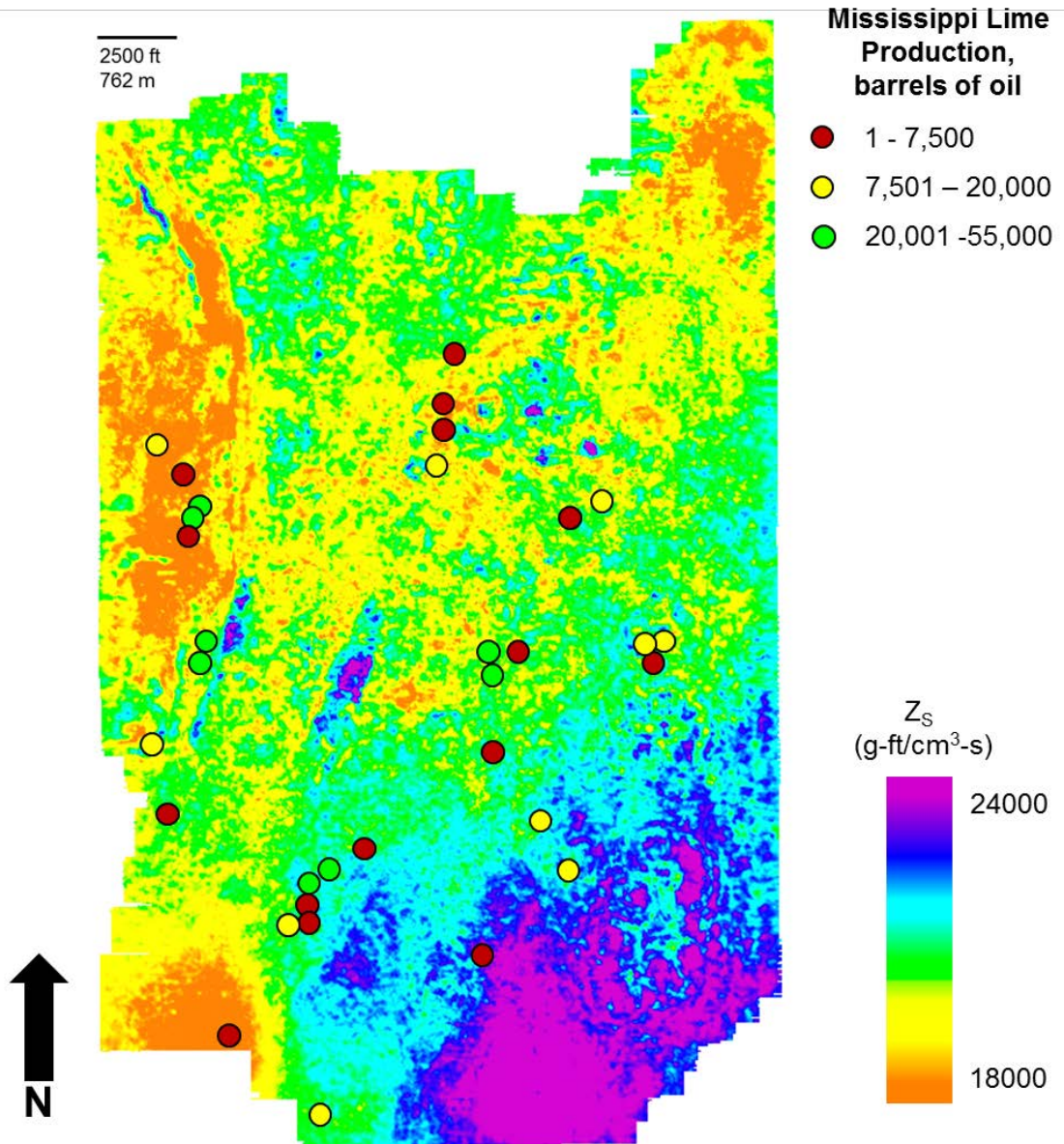


Figure 69. Phantom horizon slice 20-40 ms below the top Mississippi horizon through prestack (Z_s) volume. Cumulative oil production from Mississippi Lime indicated by red, yellow, and green circles. Magnitude of production indicated in legend.

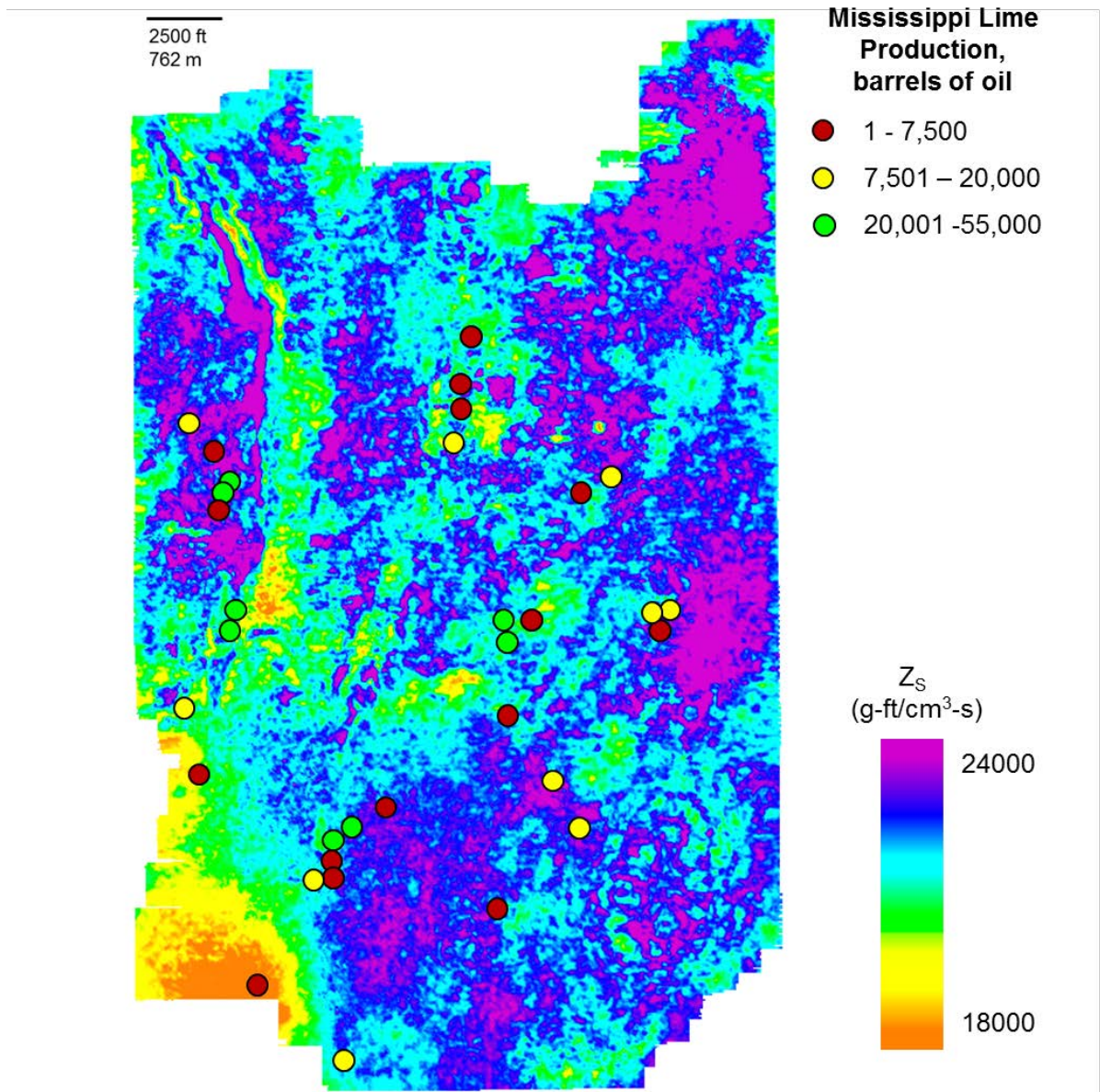


Figure 70. Phantom horizon slice 40-60 ms below the top Mississippi horizon through prestack (Z_s) volume. Cumulative oil production from Mississippi Lime indicated by red, yellow, and green circles. Magnitude of production indicated in legend. Production still mostly correlates with lower Z_s values. This may indicate the presence of thicker more productive tripolite as you move below the Mississippi horizon in time since Z_s is a good lithologic indicator.

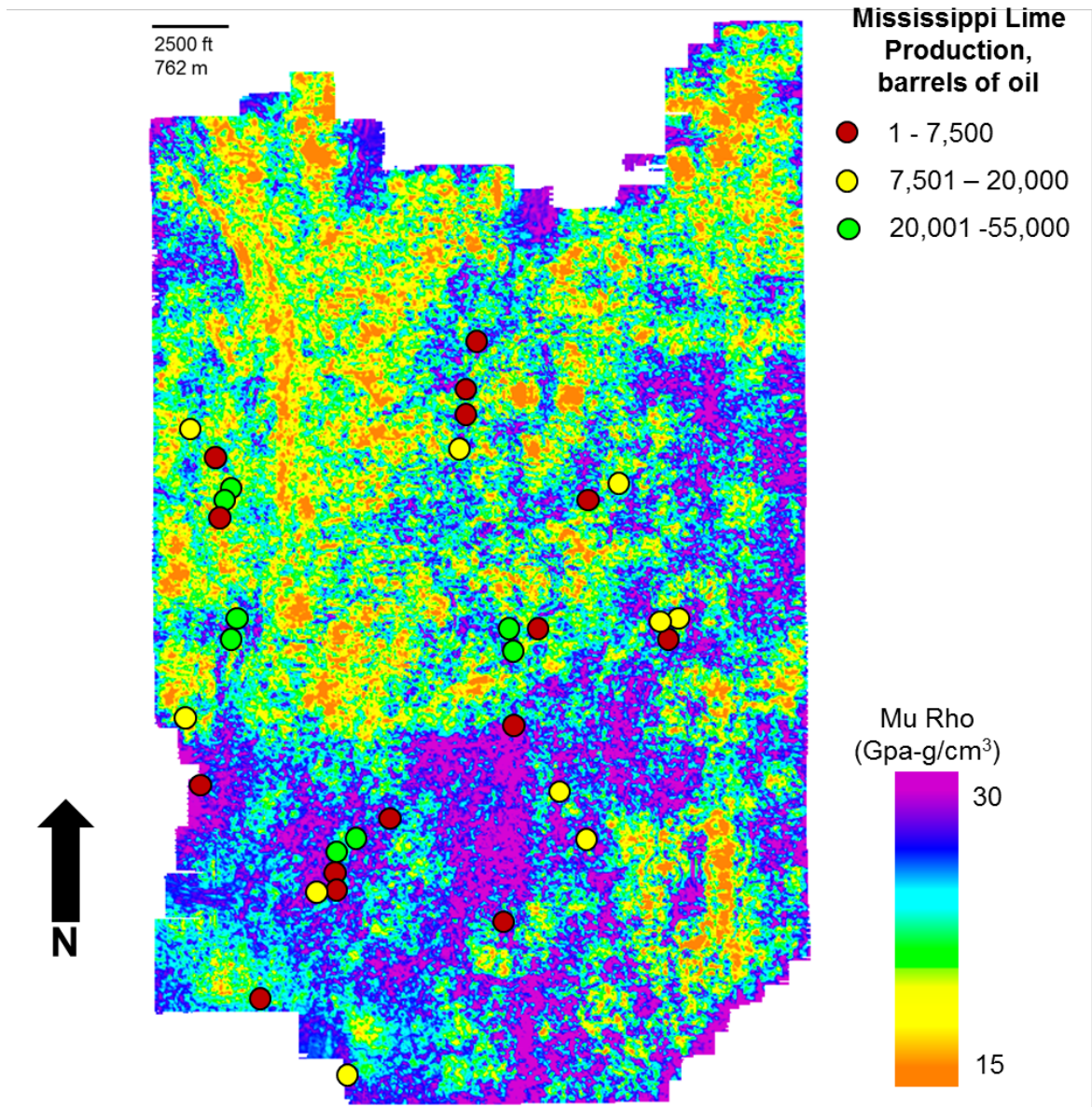


Figure 71. Phantom horizon slice 40 ms below the top Mississippi horizon through prestack mu-rho volume. Cumulative oil production from Mississippi Lime indicated by red, yellow, and green circles. Magnitude of production indicated in legend.

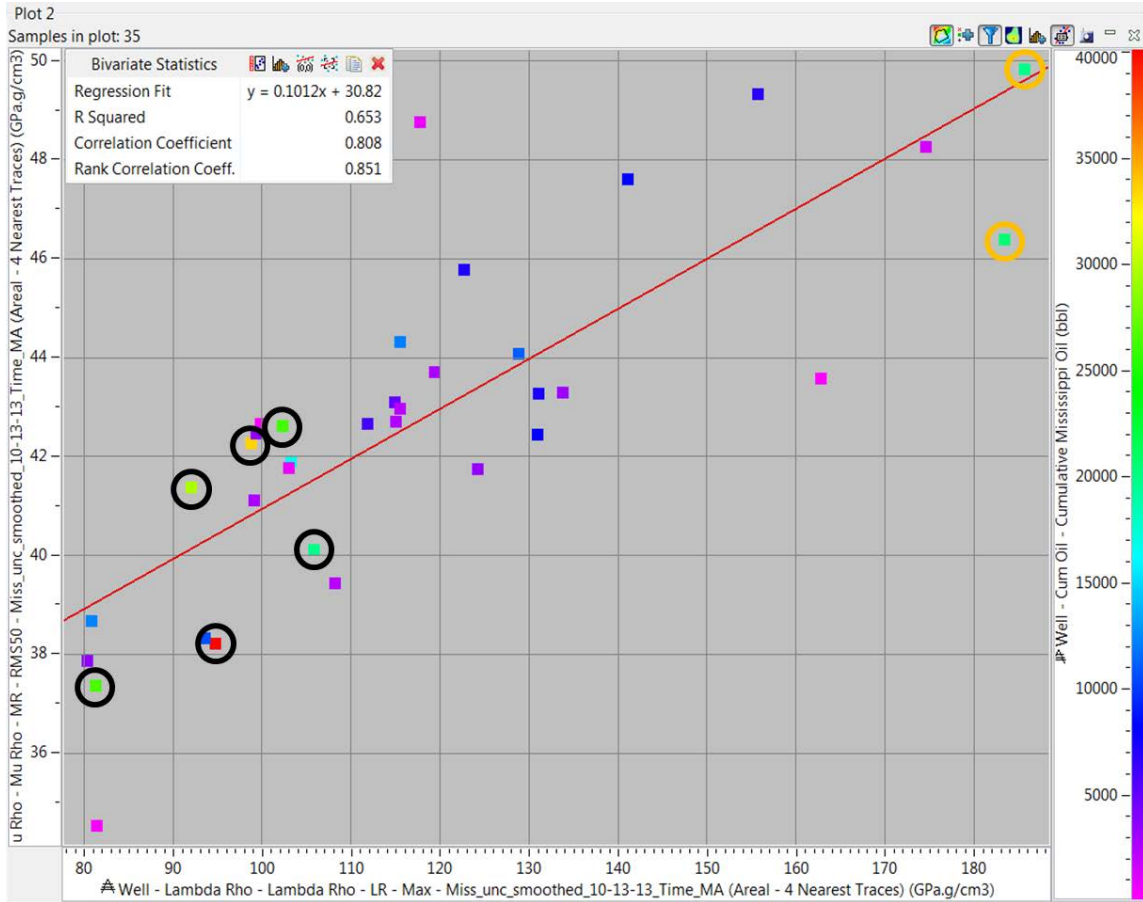


Figure 72. Lambda-rho and Mu-rho values extracted on the Mississippi horizon at the well locations. Lambda-rho plotted against mu-rho colored by cumulative production from the Mississippi Lime. Six of the eight best producing wells, highlighted by black circles, correlate with lower lambda-rho values and low mu-rho values, suggesting thicker tripolite. If the two other of the better oil producing wells, highlighted by orange circles, are located near a fault, I hypothesize that those two wells may have produced larger amounts of water as compared to the others, and we abandoned earlier.

Chapter 5

CONCLUSIONS AND LIMITATIONS

The Mississippi Lime is a complex oil and gas reservoir that has many variations both laterally and vertically. In Kay County, Oklahoma production from the Mississippi Lime has occurred for nearly 100 years. It was not until recently that technology allowed for a more accurate assessment of the characteristics that contribute to the known deposition and production from the Mississippi Lime. The Mississippi is made up of two end members in Kay County, the tripolitic chert (tripolite) and the Mississippi solid (Saint Joe Limestone). The traditional target for exploration in the subject area is the tripolitic chert with fracture porosity and plumbing in the Mississippi solid holding secondary potential. The tripolite in the area of study was depositionally controlled by the Nemaha Ridge fault complex that occurred in Pennsylvanian time. The silica rich Mississippi Lime was uplifted by this fault complex, and subsequently eroded and deposited as tripolite on an unconformity surface at the beginning of Pennsylvanian time. Tripolite thickness is structurally controlled, with thicker portions of the tripolite occurring in structurally higher areas closer in proximity to the Nemaha Ridge and thinner to no thickness of tripolite present in the structurally deeper portions of the survey. Figure 73 shows a schematic illustration of the deposition of the tripolite within the study area.

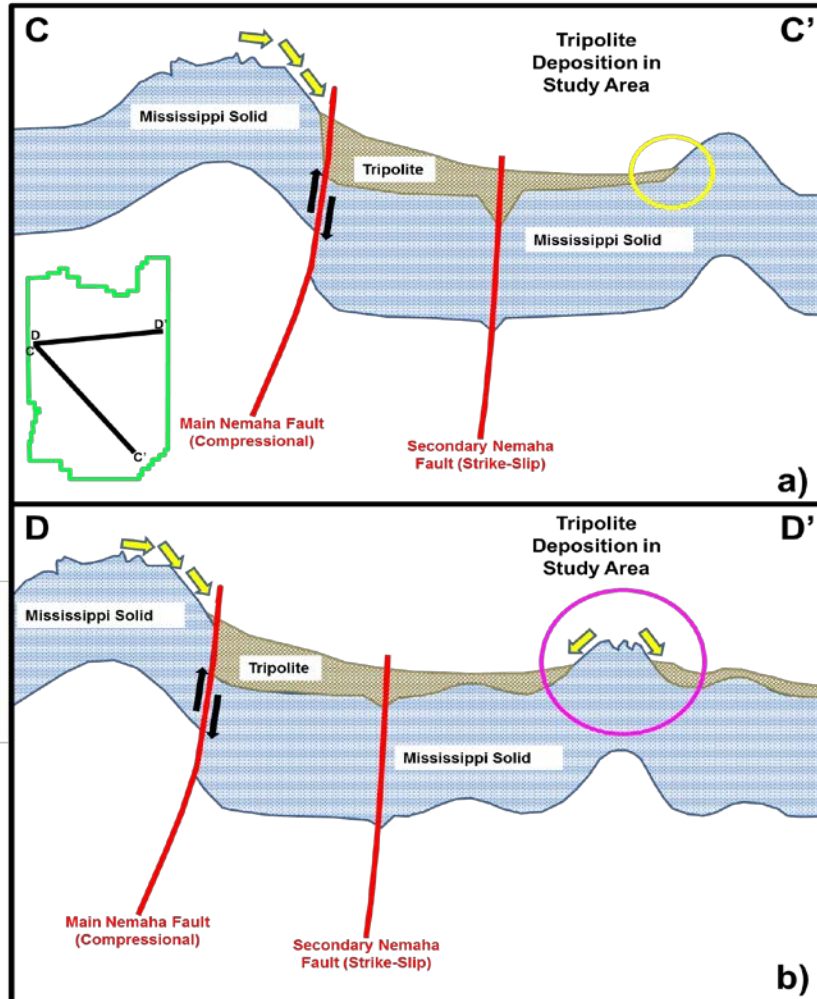


Figure 73. Schematic illustrating the deposition of Tripolite corresponding to figures 61 and 63 (cross sections C-C' and D-D') within the study area, integrating seismic data, well control, and Rogers (2001) model shown in figure 11. The Mississippi Solid was uplifted by the main Nemaha fault in early Pennsylvanian times. Subsequent to this uplift, the silica rich Mississippi Solid was eroded into areas adjacent to the main fault. This deposition is indicated by the yellow arrows in portion a) of the figure. Aerial extent of the deposition of the eroded Mississippi Solid was controlled by localized structural highs, as illustrated by the yellow circle. Portion b) of the figure highlights the same erosional deposition of the Mississippi Solid, but this time from a localized structural high seen in cross section D-D' highlighted by the magenta circle. This particular structural high corresponds with values of high Z_P seen in cross section D-D' suggesting the presence of little to no tripolite. Post deposition of the silica rich Mississippi Solid, diagenesis helped to form the tripolite in place. The two main faults are shown with red lines. Movement along the main fault shown with black arrows. Inset green outline of the seismic survey shows location of cross sections.

There appears to be a very strong correlation of production to structural lineaments, including the large faults of the Nemaha Ridge as discussed, as well as localized structural highs found within the limits of the seismic survey. While it is difficult to quantify exactly how these structural features may have had an effect on the production from the Mississippi Lime, the visual correlation between the historical production and proximity to these structural features is extremely high. In addition to a strong correlation of production to structural lineaments, correlating existing and historical production from vertical wells to low seismic impedance values correlate to thicker zones of high porosity tripolite. Using this motivation, the potential for identifying bypassed pay exists. The correlation to oil production is good, but somewhat disappointing. Low values of lambda-rho correlate to a majority of the productive Mississippi Lime wells within the seismic survey.

A major limitation with this legacy data volume is that most of the water production has not been recorded. I speculate that high porosity (low lambda-rho) zones adjacent to faults that produce small amounts of oil may have produced large amounts of water. Indeed, average water production in today's Mississippi Lime wells is 95%. If correlation of high water volumes could be made, the real value of 3D seismic may be in deciding where *not* to drill your wells.

In addition to the lack of water production records, there are a few other limitations to this study. The first limitation is the lack of shear sonic data available within the seismic survey necessary for creating prestack acoustic

impedance attribute volumes. Incorporating shear wave sonic data from a well bore in very near proximity (Sumner County, Kansas) to the study area that possesses nearly identical rock properties to the Mississippi Lime found within the seismic survey provided an approximate measurement. The second limitation to consider from this study is the use of cumulative production data as opposed to a more modern 3 or 9-month EUR measure used in resource plays. The potential issue here is that the length of time some of these wells have produced may have been dictated by low oil prices in the past. The third limitation to this study is the inability to quantify the structural effects on production from the Mississippi Lime. I make the claim that production from the Mississippi Lime is strongly controlled by structural lineaments. This assertion comes largely from a visual correlation without image logs or production logs to quantify the relationship between structural lineaments and natural fractures. The fourth and final limitation to consider in this study is one of a shift in industry technology and development. This study relates rock characteristics of the Mississippi Lime to production in an existing mature field. This characterization of the Mississippi Lime only reflects the historical exploration and production using vertical well bores. Given the contribution of fractures to production, horizontal wells would provide a statistically more accurate evaluation of the subsurface and hence to the value of 3D seismic data. The industry, at this point in time, strongly favors development using horizontal wells. I predict that the production from Mississippi Lime horizontals will tell a much more complete story than I have documented in this thesis.

REFERENCES

- Aisenberg, M., 2013, The value of reprocessing legacy data: A case study of Bois D'Arc, a Mississippi play in Northeastern Oklahoma, M.S. Thesis, The University of Oklahoma, Norman.
- Blakey, R., 2011, Colorado Plateau stratigraphy and geology and global and regional paleogeography: Northern Arizona University of Geology, <http://www2.nau.edu/rcb7/RCB.html>, accessed 11/13/2013.
- Chopra, S. and K.J. Marfurt, 2007, Seismic attributes for prospect identification and reservoir characterization: Tulsa, Oklahoma, Society of Exploration Geophysicists, 464 p.
- Craig, L.C., and K.L. Varnes, 1979, History of the Mississippian system, an interpretive summary, in L.C. Craig, et al., (ed.), Paleotectonic Investigations of the Mississippi System in the United States: U.S. Geological Survey Professional Paper, **1010**, 371-406.
- Dowdell, B.L., 2013, Prestack seismic analysis of a Mississippi Lime resource play in the Midcontinent, U.S.A. Master's Thesis, The University of Oklahoma, Norman.
- Elebiju, O.O., S. Matson, G.R. Keller, and K.J. Marfurt, 2011, Integrated geophysical studies of the basement structures, the Mississippi chert, and the Arbuckle group of Osage County region, Oklahoma: AAPG Bulletin, **95**, 371-393.

- Gay Jr., S.P., 2003, The Nemaha Trend – A system of compressional thrust-fold, strike-slip structural features in Kansas and Oklahoma, Parts 1 and 2: The Shale Shaker, **54**, 9-17, and 39-49.
- Goodway, B., T. Chen, and J. Downton, 1997, Improved AVO fluid detection and lithology discrimination using Lamé petrophysical parameters; “lr”, “mr”, & “l/m fluid stack”, from P and S inversions: 67th Annual International Meeting, SEG, Expanded Abstracts, 6-51.
- Hampson, D., B.H. Russell, and B. Bankhead, 2005, Simultaneous inversion of pre-stack seismic data: SEG Expanded Abstract.
- Johnson, K.S., 2008, Geologic history of Oklahoma: Oklahoma Geologic Survey Educational Publication **9**.
- Johnson, K.S., and B.J. Cardott, 1992, Geologic framework and hydrocarbon source rocks of Oklahoma, in K.S. Johnson, and B.J. Cardott, (eds.), Source Rocks in the Southern Midcontinent, 1990 Symposium: Oklahoma Geological Survey Circular, **93**, 21-37.
- Kansas Geological Survey, 2003, Reading the rocks from wireline logs tutorial: Kansas Geological Survey Website, Oil and Gas Information, [HTTP://www.kgs.ku.edu/PRS/ReadRocks/PEScale.html](http://www.kgs.ku.edu/PRS/ReadRocks/PEScale.html), accessed 11/15/2013.
- Mazzullo, S.J., B.W. Wilhite, and I.W. Woolsey, 2009, Petroleum reservoirs within a spiculite-dominated depositional sequence: Cowley Formation (Mississippian: Lower Carboniferous), South-Central Kansas: AAPG Bulletin, **93**, 1649-1689.

- Mazzullo, S.J., and B.W. Wilhite, 2010, Chert, tripolite, chat – What’s in a name?
: Kansas Geological Society Bulletin, **85**, 21-25.
- Mazzullo S.J., 2011, Mississippian oil reservoirs in the Southern Midcontinent:
New exploration concepts for a mature reservoir objective: Search and
Discovery Article #10373.
- Mazzullo S.J., and B.W. Wilhite, 2010, Outcrop analog of Mississippian
(Osagean) tripolite reservoirs in South-Central Kansas: Kansas Geological
Society Bulletin, **85**, 25-28.
- Northcutt, R.A., K.S. Johnson, and G.C. Hinshaw, 2001, Geology and petroleum
reservoirs in Silurian, Devonian, and Mississippian rocks in Oklahoma, in
K.S. Johnson, (ed.), Silurian, Devonian, and Mississippian Geology and
Petroleum in the Southern Midcontinent, 1999 Symposium: Oklahoma
Geological Survey Circular, **105**, 1-15.
- Partyka, G., J. Gridley, and J. Lopez, 1999, Interpretational applications of
spectral decomposition in reservoir characterization: The Leading Edge,
18, 353-360.
- Rogers, S.M., 2001, Deposition and diagenesis of Mississippian chat reservoirs,
North-Central Oklahoma: AAPG Bulletin, **85**, 115-129.
- Rottman, K., 2011, Field examples of Osagean/Meramacian reservoir systems:
Slides from Oklahoma Geological Survey Mississippian Play Workshop,
May 18 and August 2, 2011.
- Selley, R.C., 1998, Elements of petroleum geology, Second edition, San Diego,
California, Academic Press, 470 p.

- Snyder, R., R. Carter, R. Haveman, D. Jacobs, and W. Spitzer, 2013, A case history of the East Hardy Unit Mississippian Highway 60 Trend, Osage County, Oklahoma: AAPG Mississippian Lime Forum.
- Society of Petroleum Engineers PetroWiki, 2014, Density Logging, [http://petrowiki.org/Density_logging#Photoelectric .28PE.29_absorption](http://petrowiki.org/Density_logging#Photoelectric_.28PE.29_absorption), accessed 2/15/2014.
- Taner, M. T., 2000, Attributes revisited: http://www.rocksolidimages.com/pdf/attrib_revisited.htm, Accessed 2/10/2014.
- Wagner, C., A. Gonzalez, V. Agarwal, A. Koesoemadinata, D. Ng, S. Trares, and N. Biles, 2012, Quantitative application of poststack acoustic impedance inversion to subsalt reservoir development: The Leading Edge, **31**, 528-537.
- Watney, W.L., W.J. Guy, and A.P. Byrnes, 2001, Characterization of the Mississippian chat in South-Central Kansas: AAPG Bulletin, **85**, 85-113.
- White, H., B. Dowdell, K.J. Marfurt, and Z. Reches, 2012, Calibration of surface seismic attributes to natural fractures using horizontal image logs, Mississippian Lime, Osage County, Oklahoma: SEG Technical Program Expanded Abstracts, 1-6.

APPENDIX: Legacy Seismic Data Quality and Reprocessing Techniques

In January 2001, Crawley Petroleum Corporation acquired a 64 square mile proprietary 3D seismic data over the study area in Kay County, Oklahoma. Generally speaking, the P-wave seismic data are of high quality with frequencies approaching 100 Hz. Table 1 summarizes the acquisition parameters. Offsets equal to or greater than the target depth are acquired giving incident angles exceeding thirty degrees.

This particular 3D seismic survey was acquired with the intent of being able to image Red Fork formations resulting in a smaller than normal bin size used in the acquisition. Otherwise, the data went through the standard processing and analysis flow with a focus on processing to maximize bandwidth. The sweep range acquired in the shoot is a little high for the purposes of running an inversion, but at the time of the shoot running an inversion was not considered.

Subsequent to the processing and interpretation of this data set, Crawley drilled six wells into the Ordovician Arbuckle formation in an attempt to find commercial quantities of oil and gas. All of the well locations were selected based off of the interpretation from the 3D data set. The primary targets of these wells were the Pennsylvanian Red Fork sand and Mississippi Lime, with the secondary target being the Ordovician Wilcox sand. Crawley experienced mixed results on these wells. Two of the wells were deemed to be dry holes. Three of the remaining four wells were tested in the Mississippi Lime, with only one well proving economic in the interval, making roughly 25,000 barrels of oil. One well

was productive from the Ordovician Wilcox. The remaining production from these wells came from the Pennsylvanian Red Fork sand. The lack of production from the tested intervals in these wells was frustrating for Crawley to say the least.

My colleague Mark Aisenberg published his thesis titled 'The Value of Reprocessing Legacy Data : A Case Study of Bois D'Arc , A Mississippi Play in Northeastern Oklahoma' in the Fall of 2013. With permission from Crawley Petroleum, Aisenberg used this same data set as his topic for his thesis. The goal of Aisenberg's thesis was to show that by employing increased computing power coupled with new processing technologies, there was still value to be placed in legacy 3D seismic data sets.

Aisenberg was able to accomplish this by doing a number of things. He was able to improve the signal to noise ratio by using improved processing techniques. This improved signal to noise ratio suppressed the acquisition footprint contained in the original data set by an enormous amount. He was also able to improve both the vertical and lateral resolution by employing re-processing techniques that allowed for the frequency spectrum of the data to increase to 120 Hz from 96 Hz. This increased frequency bandwidth provided for an easier interpretation of the data, as this re-processing enhanced the characteristics of the seismic data from the original.

With this improved data, Aisenberg was then able to show how beneficial this newly conditioned data could be to interpretation. By performing both pre-stack and post-stack acoustic impedance inversion processes on the data, he

was able to effectively delineate the characteristics found within the Mississippi
Lime as it exists in Kay County, Oklahoma.